Report No. UM-HSRI-BI-74-2-2

THORACIC MODEL IMPROVEMENTS
(EXPERIMENTAL TISSUE PROPERTIES)

J. W. Melvin
A. S. Wineman

Highway Safety Research Institute
The University of Michigan
Huron Parkway and Baxter Road
Ann Arbor, Michigan 48105

August 12, 1974

Final Report for Period July 1, 1973 - July 31, 1974

Prepared for: National Highway
Traffic Safety Administration
U.S. Department of Transportation
Nassif Building
7th and E Street, S.W.
Washington, D.C. 20590

TECHNICAL REPORT STANDARD TITLE PAGE

1. Report No.	2. Government Accession No.	3. Recipient's Catalog No.
UM-HSRI-BI-74-2-2		

4. Title and Subtitle	5. Report Date
Thoracic Model Improvements (Experimental Tissue Properties) Volume II Technical Report	12 August 1974
	6. Performing Organization Code
7. Author(s)	8. Performing Organization Report No
J. W. Melvin and A. S. Wineman	UM-HSRI-BI-74-2-2
9. Performing Organization Name and Address Highway Safety Research Institute The University of Michigan Huron Parkway and Baxter Road Ann Arbor, Michigan 48105	10. Work Unit No 11. Contract or Grant No. DOT-HS-031-3-763
12. Sponsoring Agency Name and Address National Highway Traffic Safety Administration U. S. Department of Transportation Nassif Building, 7th and E Streets, S.W. Washington, D.C. 20590	13. Type of Report and Period Covered Final Report 1 July 1973-31 July 1974 14. Sponsoring Agency Code

15. Supplementary Notes

16. Abstract

The general objective of this research program was to obtain mechanical properties, both stress, strain, and rupture strength, for various human tissues that are directly applicable to the thoracic injury problem as defined in the finite element model of the human thorax that is being developed by the Franklin Institute Research Laboratory (FIRL) under NHTSA Contract No. DOT-HS-243-2-424, "Thoracic Impact Injury Mechanism." The properties were determined at strain rates that can occur during fatal automobile accidents. The properties of Rhesus monkey tissues are also of interest in the modelling effort, and consideration was given to providing experimental data on selected Rhesus tissues [illegible] human tissues.

17. Key Words	18. Distribution Statement
Dynamic Mechanical Properties Thoracic Tissues High Strain Rate Tests	Document is available to the public through the National Technical Information Service, Springfield, Virginia 22151.

19. Security Classif. (of this report)	20. Security Classif. (of this page)	21. No. of Pages	22. Price
Unclassified	Unclassified		

Form DOT F 1700.7 (8-69)

ACKNOWLEDGMENTS

The authors of this report would like to express their appreciation and gratitude for the efforts of the many people who made this project possible. In particular, Dr. Lee Ovenshire, contract technical Manager; Dr. M. M. Reddi, FIRL representative; Dr. L. Weatherbee, pathologist; Mr. H. Overstreet, pathology technician; Mr. J. Benson, test engineer; Ms. K. Saucier, manuscript and report preparation; Ms. C. Dunn, Mr. G. Myers, Mr. K. Gyr, bibliography preparation; Mr. J. Brindamour, photography technician; Mr. S. Fisher and Mr. J. Embach, drafting and Mr. M. Zaremba, data reduction. A special word of appreciation is due to Mr. D. Mohan for his tireless efforts in all phases of this project.

CONTENTS

1.0 INTRODUCTION

The general objective of this research program was to obtain mechanical properties, both stress, strain, and rupture strength, for various human tissues that are directly applicable to the thoracic injury problem as defined in the finite element model of the human thorax that is being developed by the Franklin Institute Research Laboratory (FIRL) under NHTSA Contract No. DOT-HS-243-2-424, "Thoracic Impact Injury Mechanism." The properties were to be determined at strain rates that can occur during fatal automobile accidents. The properties of Rhesus monkey tissues are also of interest in the modelling effort, and consideration was given to providing experimental data on selected Rhesus tissues as well as on human tissues.

The general approach to achieving the goals of the program were to:

1. Perform a detailed literature survey concentrating on soft tissue test techniques and mechanical properties data on the tissues of primary interest.
2. Develop basic test techniques, fixture design and test analysis methods.
3. Implement the test program with tissue priorities based on the needs of the modelling effort.
4. Analyze and synthesize the test data with respect to developing constitutive relations to describe the behavior of the tissues tested within the scope of the test program.

The following sections of this report detail the methodology used in the conduct of this project and the results obtained.

1.1 BACKGROUND

Many investigators have performed mechanical tests on various biological tissues which exhibit the general characteristics of markedly non-linear

behavior accompanied by finite deformations. The use of principles of solid mechanics to assist in the description of the mechanical properties and behavior of biological materials requires consideration of questions of isotropy, homogeneity, compressibility, elasticity and viscoelasticity, and universality. Soft tissues such as muscle and ligaments are clearly composite materials, preferentially structured and, microscopically, far from isotropic and homogeneous. However, in some tissues effective homogeneity may exist on a macroscopic scale. Soft tissues are generally accepted to be incompressible (1), although in some states of compression, a volume decrease can occur due to exudation of fluid (2). It is also recognized that soft tissues in general are viscoelastic (3), however, under certain conditions it is useful to consider the elastic behavior of some tissues only (1). The question of universal representation of the behavior of soft tissues poses a complex experimental problem. In cases where consideration is of elastic behavior only, the application of experimental and analytical techniques developed in the study of elastomeric polymers can be applied to soft tissue characterization. This approach utilizes the concepts developed in finite elasticity (4) and involves determination of a strain energy function W which will allow a description of the behavior of the material specifically through the parameters $\partial W/\partial I_1$, $\partial W/\partial I_2$ and $\partial W/\partial I_3$, where I_1, I_2 and I_3 are the strain invariants. These parameters are functions of the state of deformation in the material and require measurement of stress resultants and finite strains for a sufficiently large array of states of strain. For an incompressible material the principal strains are interrelated so that W becomes independent of I_3 thereby reducing the experimental work somewhat. Suitable use of thin membranes of material also allows further simplification of experimental procedure. Nevertheless it is necessary to conduct tests under at least three deformation states

to describe an isotropic incompressible material. Experimentally, the three states usually chosen are: simple elongation, pure shear and two dimensional extension (or uniaxial compression for incompressible materials). Very few studies have utilized anything other than the uniaxial tensile test to describe the elastic behavior of soft tissues. A variety of forms for the strain energy function have been proposed and evaluated for rabbit mesentery (3, 5) and cat's skin (6) based on uniaxial tensile data. Fung (7) last year reviewed current efforts along these lines and has indicated that "the greatest need lies in the direction of collecting data in multiaxial loading conditions and formulating a theory for the general rheological behavior of living tissues when stresses and strains vary with time in an arbitrary manner. Virtually no experimental data exist on the viscoelastic behavior of living tissues in multiaxial loading conditions. None of the numerous theoretical proposals has received extensive experimental support." Lanir and Fung (8) have just recently published the preliminary experimental results on the two dimensional mechanical properties of rabbit skin.

Typical soft tissues are not elastic and their viscoelastic nature must be accounted for as there is considerable difference in stress response to loading and unloading and to rate loading (3). Many soft tissues have been studied using simple states of strain such as uniaxial tension, simple shear and uniaxial compression to obtain viscoelastic data. These tests are usually either creep, relaxation or steady state small oscillation tests and the results are usually discussed in terms of the framework of linear viscoelastic theory relating stress and strain on the basis of the Voigt, Maxwell and Kelvin models (9, 10, 11). A nonlinear theory of the Kelvin type has been proposed for tendons and ligaments (12) on the basis of a sequence of springs of different natural length, with the number of partipating springs increasing with increasing strain.

For finite deformations, the nonlinear stress-strain characteristics of soft tissues must be accounted for. An alternative to the development of a constitutive equation by gradual specialization of a general formulation has been put forward by Fung (3). Utilizing special hypotheses, the history of the stress response in a material subjected to a uniaxial step elongation is called the relaxation function $K(\lambda,t)$ and is assumed to have the form

$$K(\lambda,t) = G(t)\, T^{(e)}(\lambda), \quad G(0) = 1$$

in which a normalized function of time, is called the reduced relaxation function, and $T^{(e)}(\lambda)$, a function of λ alone is called the elastic response. This formulation allows the function $T^{(e)}(\lambda)$ to play the role assumed by the strain in the conventional theory of viscoelasticity, thereby extending the machinery of the theory of linear viscoelasticity to use in characterization of nonlinear materials. In cases where the stress response to a loading process is insensitive to the rate of loading $T^{(e)}(\lambda)$ may be approximated by the uniaxial tensile stress response in a loading experiment with a sufficiently high rate of loading. Recent results suggest that the characteristic relaxation term may also depend on the strain level. This would result in $G(t)$ depending on λ.

Much of the experimental work on determining the mechanical behavior of soft tissues has not been cast in the framework of a complete solid mechanics description, thus it is possible to obtain only a partial characterization of tissue behavior from the existing literature. The most extensive summary of work on the simple loading behavior of biological tissue is that of Yamada (13). The basic tests reported include uniaxial tension, biaxial membrane inflation and burst, tubular inflation, torsion and direct compression on a very wide range of human and animal tissues. The data presented in this extraordinary work provides no information of real use to a continuum mechanics

characterization of the tissue behaviors. A survey of the existing literature on soft tissue properties reveals almost a complete lack of data on the stress-strain behavior to failure at anything other than quasi-static loading rates.

The main emphasis in this program was upon impact type high strain rate behavior of biological tissues and as such the main form of data acquisition was in terms of high strain rate stress-strain curves to failure. The experimental results obtained in this program were analyzed to provide the most useful data in terms of failure criteria and numerical parameters in forms most suitable for the FIRL finite element modelling effort. The details of the experiments performed on the various tissues, the test parameters measured, and the form of data analysis were coordinated to the extent possible with both FIRL and the CTM during the test technique development phases of the program. The limited scope and duration of the program (10 man months equivalent) was not sufficient to allow a complete continuum mechanics description of all the tissues of interest. In fact, the overriding consideration of data generation for the finite element model strongly influenced the tests performed and the subsequent data analysis. However, wherever possible the test configurations, measured test parameters and subsequent analysis were couched within the framework of proper solid mechanics characterization so that the data developed, while at this point in time may be incomplete in the sense of a total description, will be applicable to future efforts.

2.0 LITERATURE SURVEY

A literature survey which concentrated on the areas of soft tissue testing and analytical representation of soft tissue mechanical behavior was implemented early in the program as an aid in guiding the experimental design and data analysis techniques. In addition, the literature survey was used to study mechanical properties data on thoracic tissues of primary interest to the project.

The list of journals that were surveyed includes the following:

American Journal of Physiology

Journal of Applied Physiology

Journal of General Physiology

Physiological Reviews

ASME Publications

SAE Publications

Applied Mechanics Reviews

Journal of Biomechanics

Biorheology

Medical and Biological Engineering

Biomedical Engineering

Experimental Mechanics

Advances in Bioengineering and Instrumentation

American Journal of Physical Medicine

U.S. 6570 Aerospace Medical Research Laboratories Reports (Med. Library RC1050 u.63)

NASA Scientific and Technical Aerospace Reports

Acta Orthopaedica Belgica

Acta Orthopaedica Scandinavica

Archives Physical Medicine

Clinical Orthopaedics

Journal of Bone and Joint Surgery

Rheumatology and Physical Medicine

Aerospace Medicine

Journal Sports Medicine/Physical Fitness

Journal of Trauma

Injury

Monatschrift Unfallheilkunde

Thoras

A bibliography based on the papers located by the literature survey was compiled in the following manner:

1. Obtain the paper.
2. Code it using the scheme shown on the master card shown in Figure 1.
3. Abstract the article.
4. Type the information on a Keysort card, an example of which is shown in Figure 2.
5. Punch the card according to the code.

Duplication of the Keysort card bibliography was done by Xeroxing the cards on a dark background at a slight reduction in order to allow attaching on the duplicate to a blank Keysort card for punching as indicated by the duplicate. The copies of these bibliography cards are contained in Volume III of this report. A total of over 500 cards were prepared during the project. In addition, selected articles of particular pertinence to the program have been microfilmed in their entirety and supplied in microjacket form to the CTM.

Figure 1. Literature Survey Keysort Master Cataloging Card

Specimen Origin

Man

Primates (apes, monkeys)

Rodents (rats, mice, guinea pigs)

Unguiculate (cats, dogs, rabbits)

Ungulate (horse, swine, cow, goat, deer, elephants)

Birds (chicken, ducks, fowls)

Cold Blooded Vertebrate (reptile, fish, amphibians)

Metals

Ionic Properties

Fibrous (wood)

Polymers

Other

Recorded Parameters

Age of Source

Time after Death

Specimen Geometry

Temperature

Moisture Content

Density

Viscosity

Elasticity

Hardness

Ductility, extensibility

Inhomogeneity

Anisotropy

Energy Absorption

Strength

Frequency

Amplitude

Rate of Variable Change

Stress

Strain

Strain Rate

Failure

Other

Radiation

Wounds and Healing

Velocity

Electrical Properties

Specimen Condition

Other

Dried

Solution

Embalmed

Frozen and Thawed

Refrigerated (unfrozen)

Fresh

Living Tissue (in vivo)

Body Fluids (CSF, synovial, serum)

Microstructural Compo- Blood
nents (osteons, collagen, hair)

Cardiovascular System & Lungs

Nerves & Nervous Tissue

Integument (skin and subcuta- Bone
neous tissue

Anatomy

Ligaments & Tendon

Muscle

Cartilage

Joints

Viscera

Torso (ribs, spine, pelvis, Skull
shoulder

Upper Extremeties

Lower Extremeties

Author

A N

B O

C P

D Q

E R

F S

G T

H U

I V

J W

K X

L Y

M Z

Index

Rate

Creep-Stress Relaxation

Quasi-static

Impact

High-Speed

Cyclic

Pulse

Mode of Analysis

Electrical (Piezoresistance, etc.)

Acoustical

Optical (X-ray, photography, polaroid)

Chemical

Pressure

Combined Stress

Torsion, shear, tearing, puncture, penetration

Flexure

Compression

Tension

Type of Paper

On file, no punch for R20 indicates comment.

Statistical Validity

Property Correlation

Apparatus Description

Technique Description

Review

Pathological

Histological

Experimental Work

Theoretical Work

Figure 2. Example of Literature Survey Abstract Card

Hildebrandt,J.
Extension of Small-Strain Theory to Finite Deformation of Cylindrical Vessels by Internal Over-Pressure
Angiologica 7: 257-272, 1970.

Abstract: Calculations of the pressure distention of closed cylindrical vessels using classical infinitesimal-strain theory predict that, for isotropic materials the length remains fixed while the diameter increases linearly with pressure. These predictions can be verified experimentally only if the radial deformation is less than 2-3%. This paper develops formulae applicable to deformations up to approximately 10 times the above , based on a modification of infinitesimal theory. The results predict significant lengthening of isotropic vessels, and ballooning or 'blow-out' above a certain pressure. It is shown that the classical stresses contain a common hydrostatic component which must be subtracted before the stresses can be integrated across the wall thickness to yield wall tensions. When the hydrostatic component is taken into account, Laplace's law is found to hold for thick-walled vessels as well as for thin-walled vessels.
key words: pressure distention; Elastic cylinders; infinitesimal theory; lengthening isotropic vessels

3.0 TEST TECHNIQUES

3.1 GENERAL

The effectiveness of a program in providing mechanical behavior data on varied tissues of the thorax depends on many factors. The test techniques and procedures must be kept as simple and efficient as possible in order to allow significant numbers of tests to be performed on each tissue with statistical validity. Additionally, the measurements made in the tests must provide sufficient information to allow the complete determination of the state of strain and state of stress for a proper analytical characterization of the behavior of the tissue. In addition to these basic requirements the test program must consider the questions of the effects of muscle tone, material storage, time after death, and in vivo configuration on the mechanical behavior of the tissues.

The test methods planned for use in the program can be classified into two types; basic mechanical properties tests and structural mechanical properties tests.

The basic mechanical properties tests consist of the following candidate loading states:

1. Uniaxial tension
2. Biaxial tension (membrane pressurization)
3. Uniaxial compression (equivalent to biaxial tension for incompressible materials)
4. Combined axial tension and internal pressurization (with suitable tubular vessel and organ samples).

The structural mechanics tests involve those tissue configurations where it was impossible to produce suitable samples of the tissue and therefore were tested as a structure.

Selection of which of the above test states was to be applied to each of the tissues of interest depended on many factors. The structural geometry of the tissue sample precluded certain testing modes. The degree of anisotropy that a particular tissue exhibits may limit the application of the more complex loading states. In addition to material considerations, the primary goal of providing data for use in the FIRL finite element model played a major role in the selection of test modes.

Due to limited supply of suitable material samples and the need for significant numbers of tests in any one test mode and tissue type, only uniaxial tension and biaxial tension tests were performed routinely to obtain basic mechanical properties.

3.1.1 Uniaxial Tension Test

The uniaxial tension test could be applied to virtually any tissue of interest. Three types of uniaxial tensile specimens were used in the program. The first two consisted of die cut specimens of the configurations shown in Figure 3. The smaller of the two die shapes (Type 2) was used in some human tissue where there was a limited amount of uniform tissue and in Rhesus monkey tissues. The third type of uniaxial tension specimen was the ring type specimen which can be formed by making two parallel transverse cuts across a tubular vessel. It was used in monkey tissue tests only. This type of specimen can be loaded with simple pin loading while the die cut specimens required a special low mass air grip design shown in Figure 4. The two test configurations are shown schematically in Figure 5 for the die cut specimen and Figure 6 for the ring type specimen.

The strains in the uniaxial tension test were determined photographically in the case of the die cut specimens and by pin displacement in the ring type specimens. The photographic strain measurement is shown schematically

Figure 3. Tensile Test Specimen Die Shapes

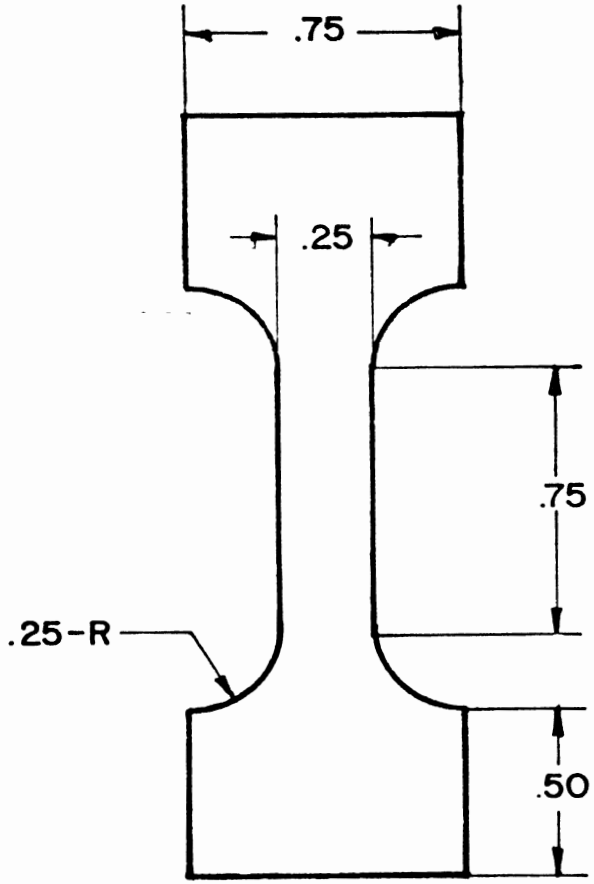

TYPE ONE: TENSILE
SPECIMEN SHAPE

DRAWN DOUBLE SIZE

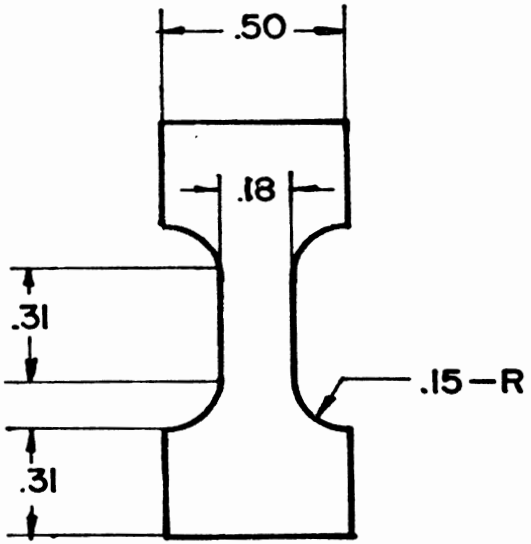

TYPE TWO: TENSILE
SPECIMEN SHAPE

DRAWN DOUBLE SIZE

Figure 4. Low Mass Air Grip Design for Tension Tests

TENSILE TEST AIR GRIP PARTS

DIMENSIONED IN INCHES
DRAWN FULL SCALE

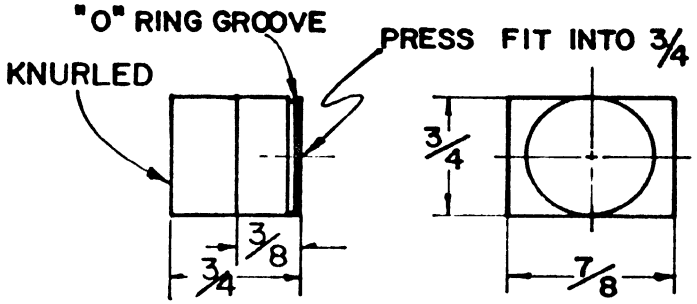

PISTON

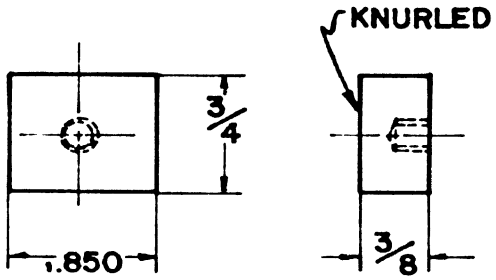

REACTION BLOCK

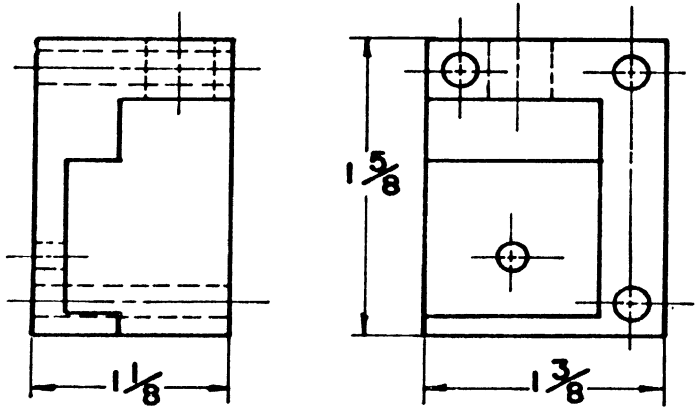

REACTION BLOCK HOUSING

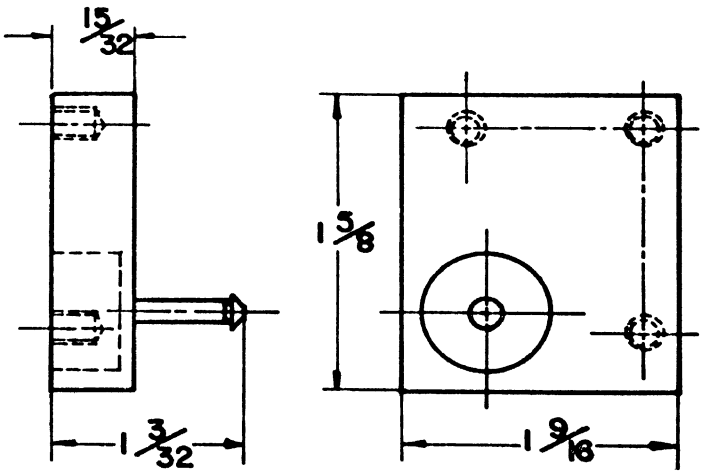

PISTON HOUSING

MATERIAL= MAGNESIUM

Figure 5. Schematic Representation of Tension Test with Die Cut Specimen

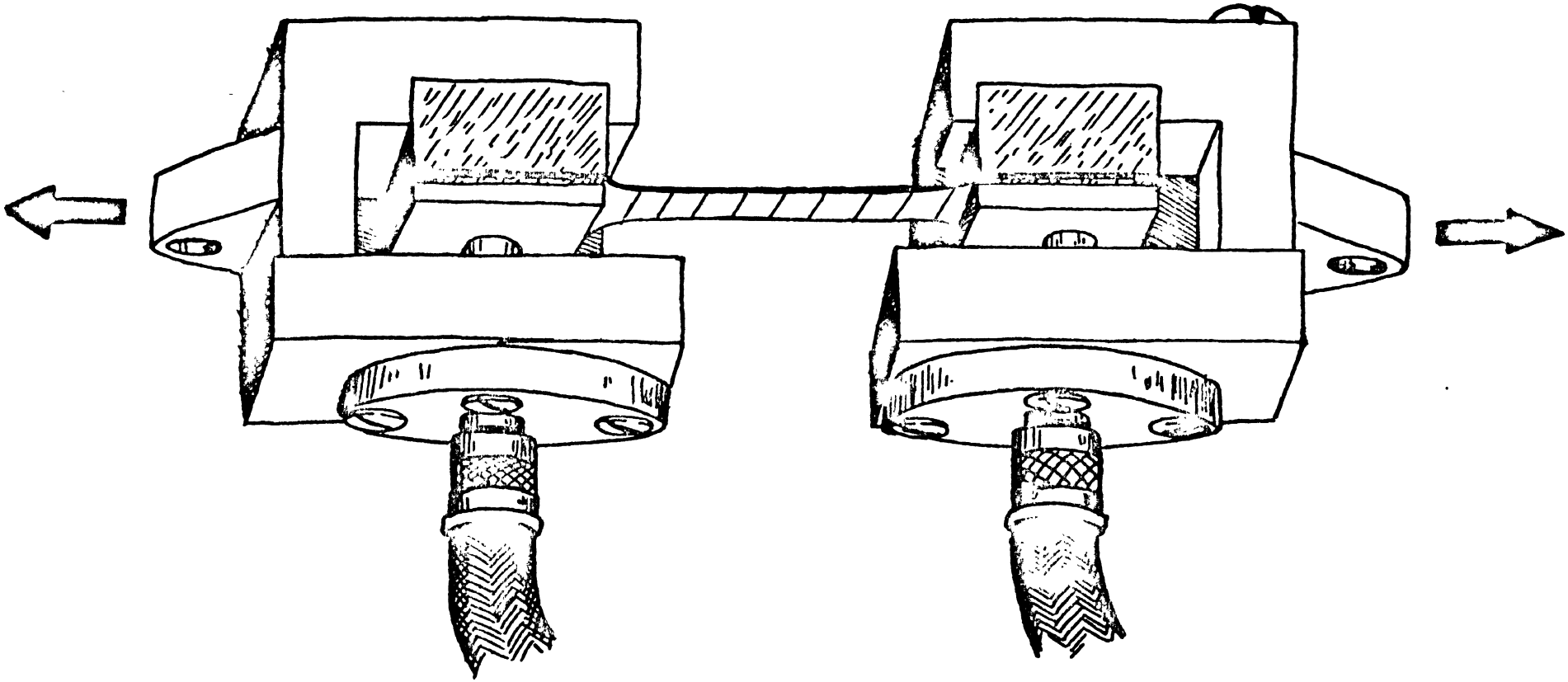

Figure 6. Schematic Representation of Tension Test with Ring Type Specimen

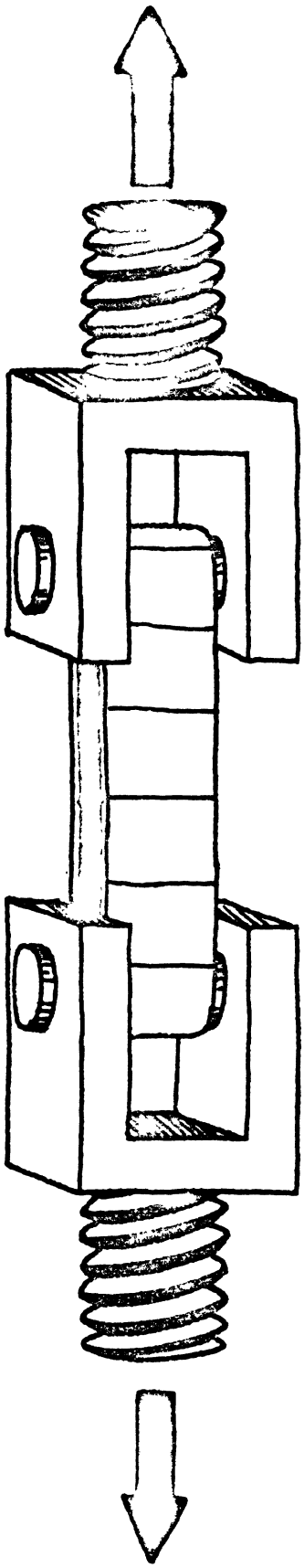

in Figure 7. Note the 45° angle mirror which allows recording of thickness changes on the same photograph as the width and length changes. The specimen is stamped with a grid of lines with a 0.25 inch spacing using conventional stamp pad ink. The stamp and holding fixture is shown in Figure 8 and a rubber trial specimen with the grid on it is shown in Figure 9. Also shown in Figure 9 is a specimen carrying frame for installing the more fragile specimens in the grips. Prior to testing, the thickness of the specimen was determined at three points along the specimen using an Ames 5642-1 thickness gauge. The camera used in static tests was a 35 mm Honeywell Pentax and in dynamic tests it was a 16 mm Photosonics 1B high speed (1000 pps) movie camera. Load measurement was done with an Instron strain gage load cell in the static tests and a Kistler 931A piezoelectric load cell in the dynamic tests. Synchronization of the strain analysis pictures with the load trace was achieved in the static tests by placing a photodiode in front of the strobe light used to illuminate the specimen. For each picture the resulting flash of light produced a voltage spike in the photodiode which was displayed on a separate channel along side of the load trace. In the dynamic tests a timing pulse generator was used which produced timing marks on the film and on the load trace. In both static and dynamic tests the load trace and the synchronization pulses were recorded on a Honeywell Visicorder light beam oscillograph. In the dynamic tests the grip displacement was also recorded.

The testing machines used in the tests are shown in Figures 10 and 11. The static tests were performed in a Instron TTC floor model universal testing machine at a crosshead speed of 0.5 inches/minute. The dynamic tests were performed in a Plastechon high speed universal testing machine at ram speeds of nominally 360 and 3600 inches/minute.

The analysis technique used in reducing the uniaxial tension test data is given in Appendix I.

Figure 7. Schematic Representation of Tension Test Strain Recording Technique

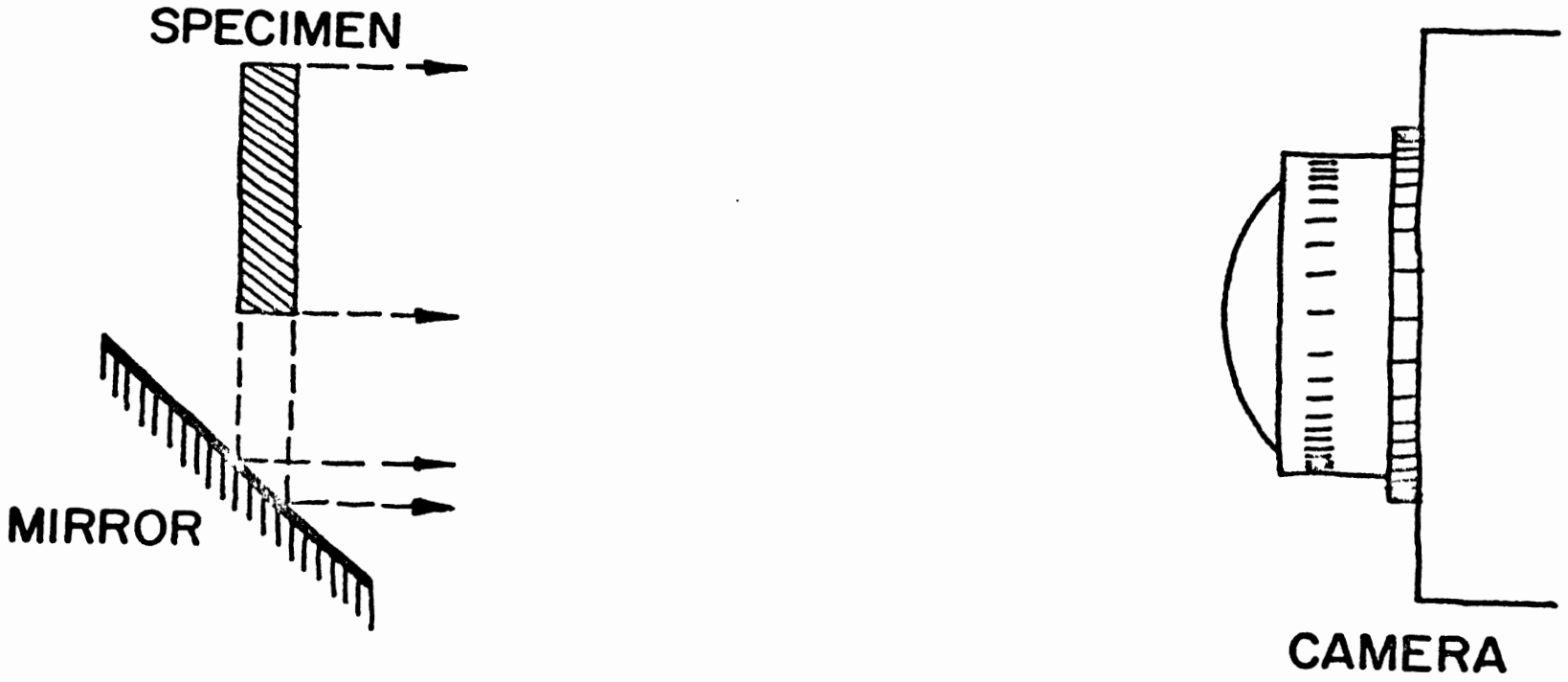
SPECIMEN
MIRROR
CAMERA

Figure 8. Tension Test Specimen Grid Stamp Apparatus

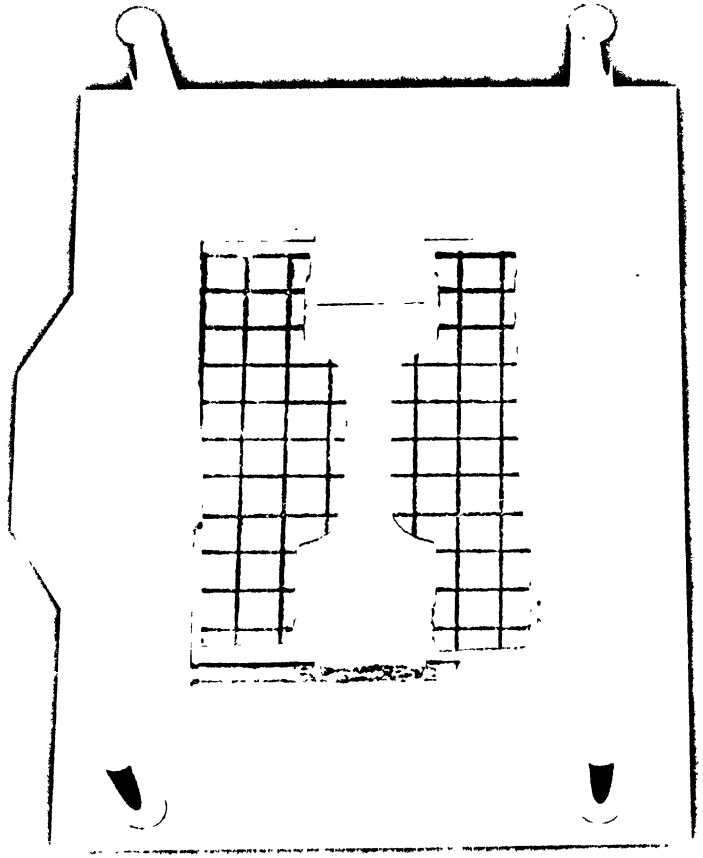

Figure 9. Tension Test Specimen and Holder
(Rubber Sample Shown)

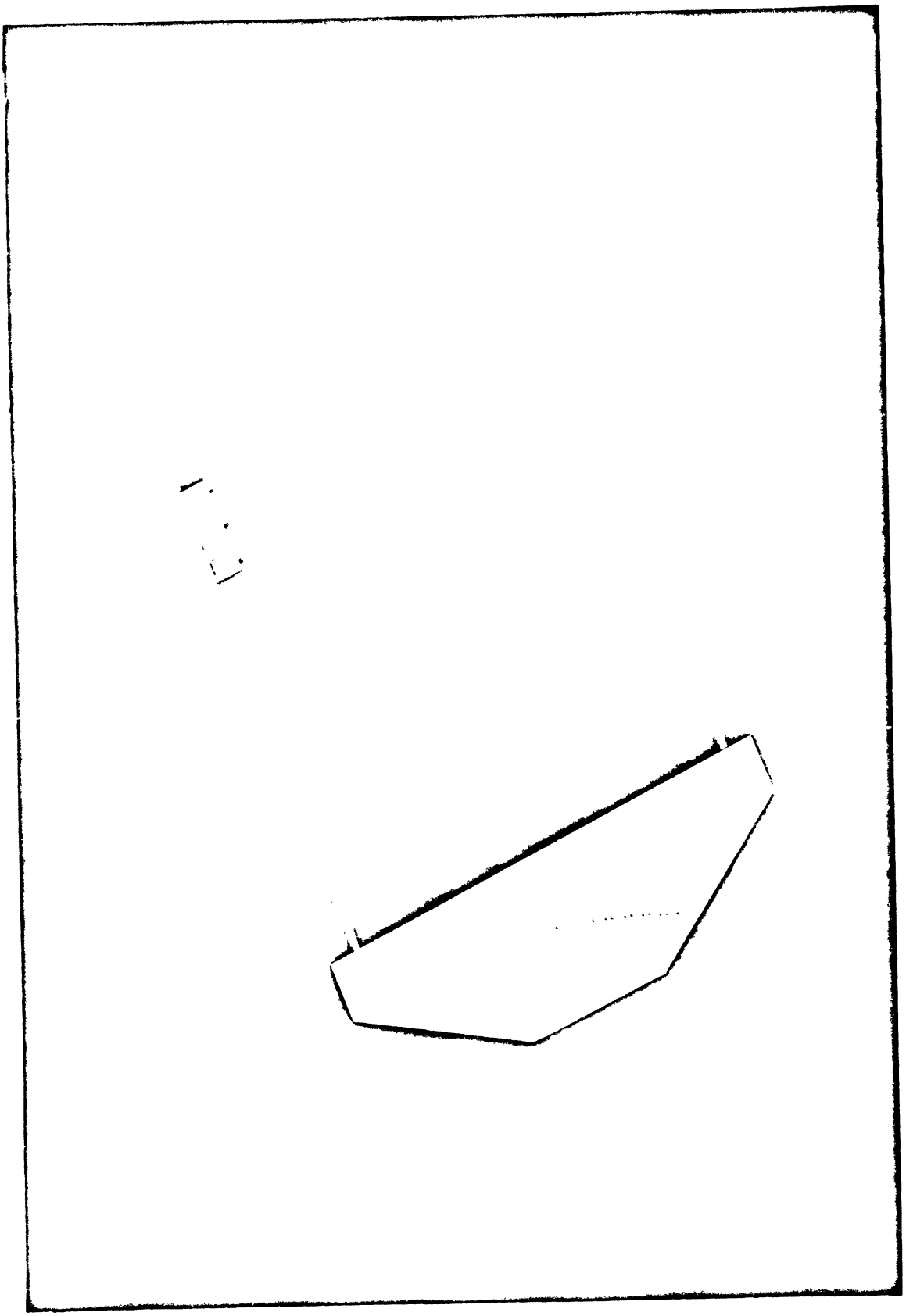

Figure 10. Static Tension Test Set-Up

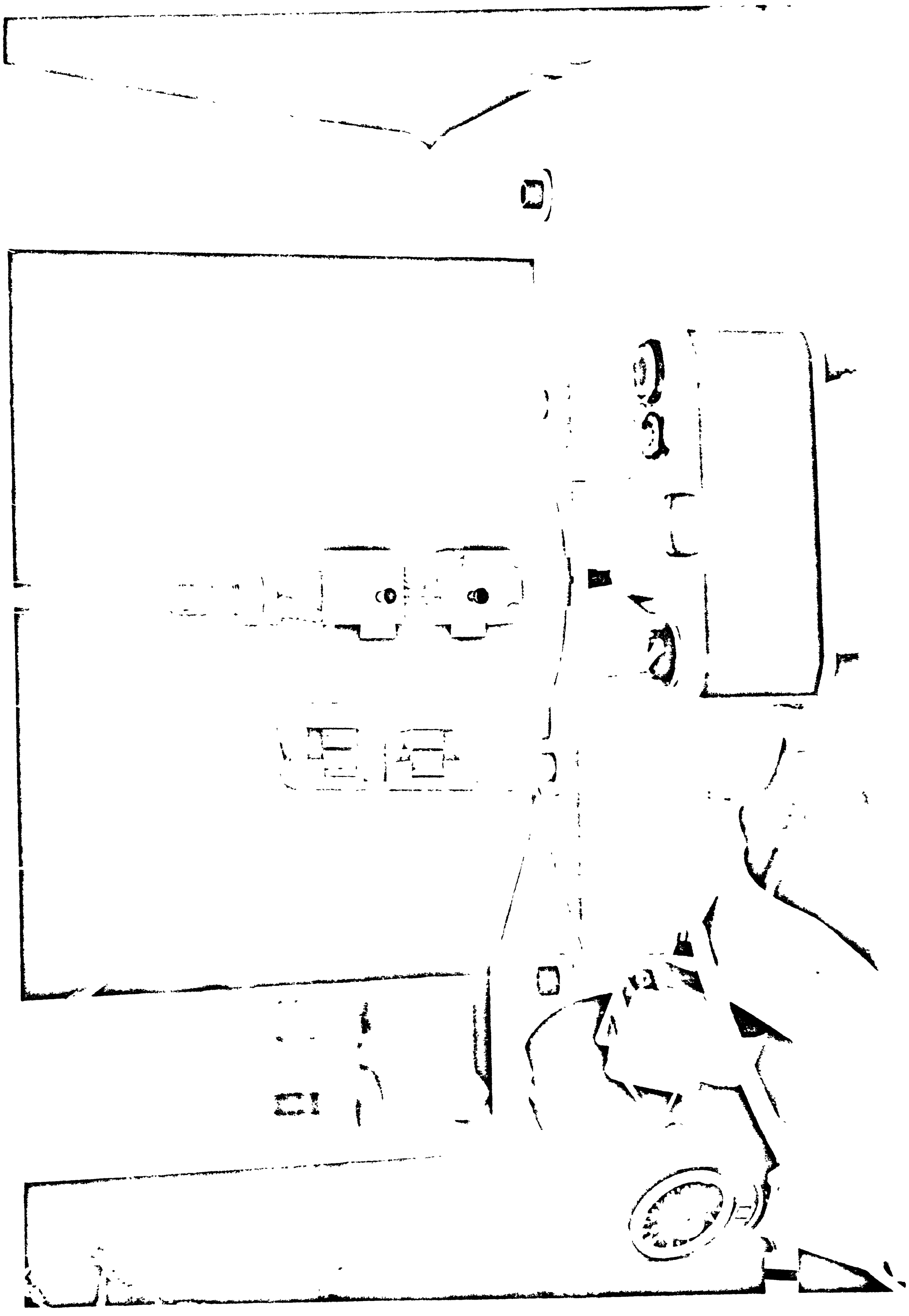

Figure 11. Dynamic Tension Test Set-Up

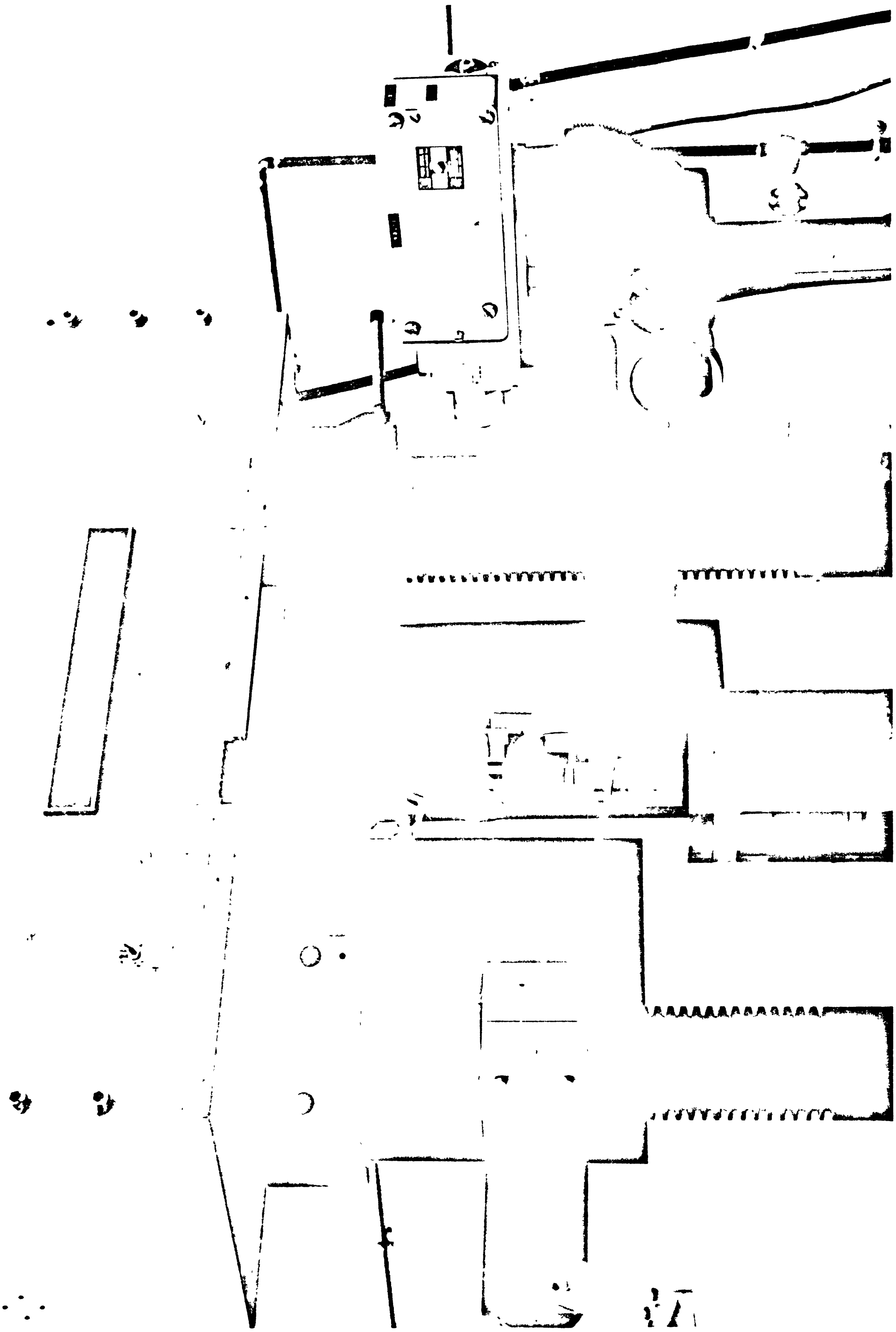

3.1.2 Biaxial Tension Tests

Biaxial tension tests could be performed on tissues which were membraneous in nature and had suitably uniform regions of material (approximately 2.5 inches in diameter). The biaxial tension test apparatus is shown schematically in Figure 12. Also shown is a thickness transducer for use in static biaxial tests. Figure 13 shows an assembly drawing of the finalized test apparatus and Figure 14 is a photograph of the device with a rubber sheet trial specimen in place. The device was mounted on an air chamber with a quick-opening solenoid valve as shown in Figure 15. For dynamic operation, the air chamber was charged with compressed air at about 100 psi with the solenoid valve closed. The valve was then opened and the membrane inflated to failure dynamically in approximately 10 msec.

Preparation of the test specimen involved cutting a roughly circular sample of the tissue with a diameter slightly larger than the 2 inch diameter rubber O-ring seal. Using the locating plate shown in Figure 16, an O-ring was placed on the circular center boss and the tissue laid on the boss and O-ring top surface. The tissue was bonded to the O-ring with Eastman 910 adhesive and then a circular grid was imprinted on it with the stamp shown in Figure 16. The O-ring then acted as a support and centering device for transferring the specimen to the test device where it was clamped in place by the top sealing ring shown in Figure 13.

The pressure acting on the membrane was measured by a Kistler piezoelectric pressure transducer and the deformation was recorded as shown in Figure 17 using a Photosonics 1B movie camera at 1000 pps. The synchronization of the pressure trace and the movie was obtained with an initial event strobe and timing marks on the film and light beam oscillograph trace. The analysis techniques used for this test are detailed in Appendix I.

Figure 12. Schematic Representation of the Biaxial Tension Test Apparatus

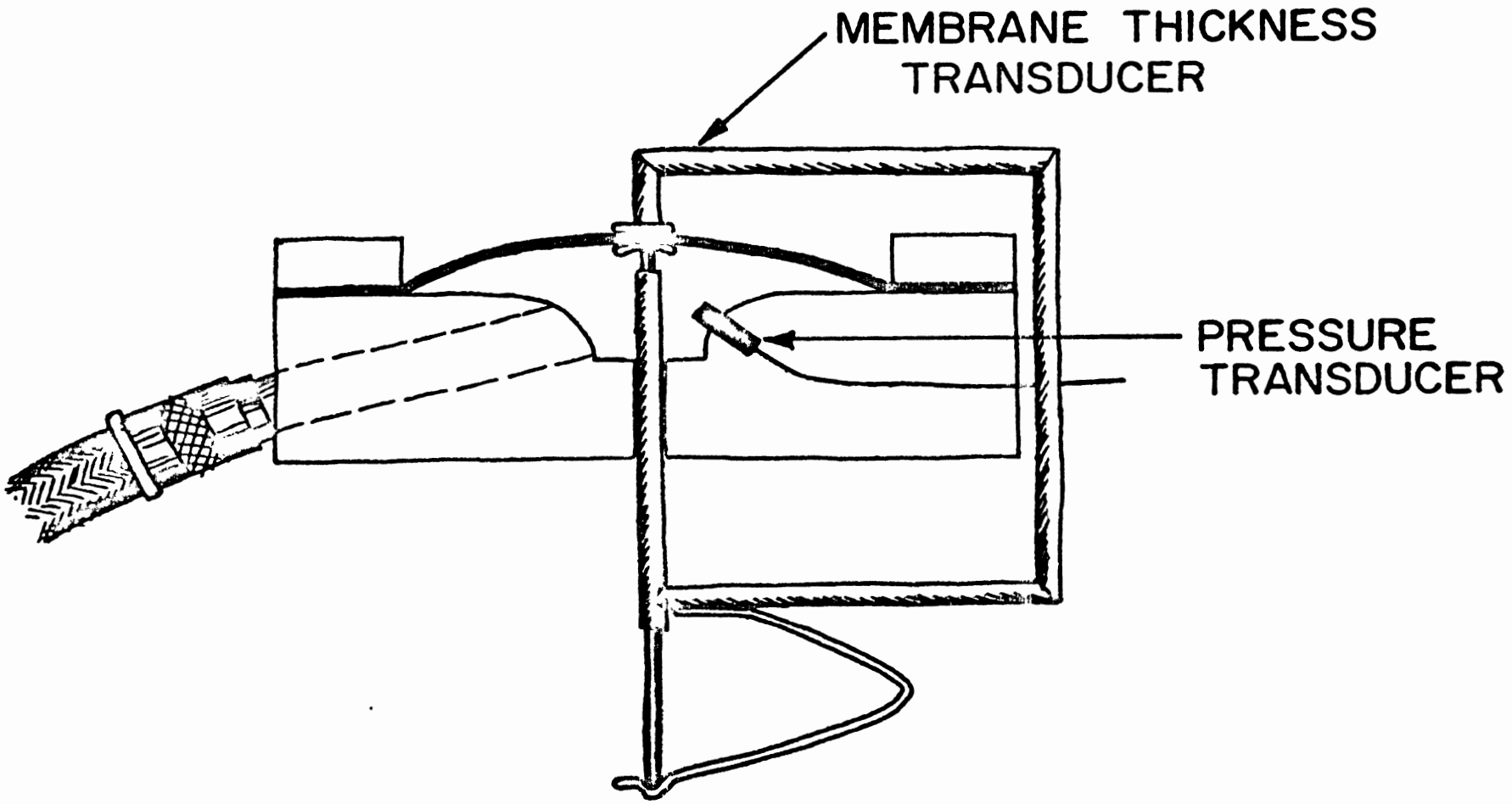
MEMBRANE THICKNESS
TRANSDUCER
PRESSURE
TRANSDUCER

Figure 13. Assembly Drawing of Biaxial Tension Test Apparatus

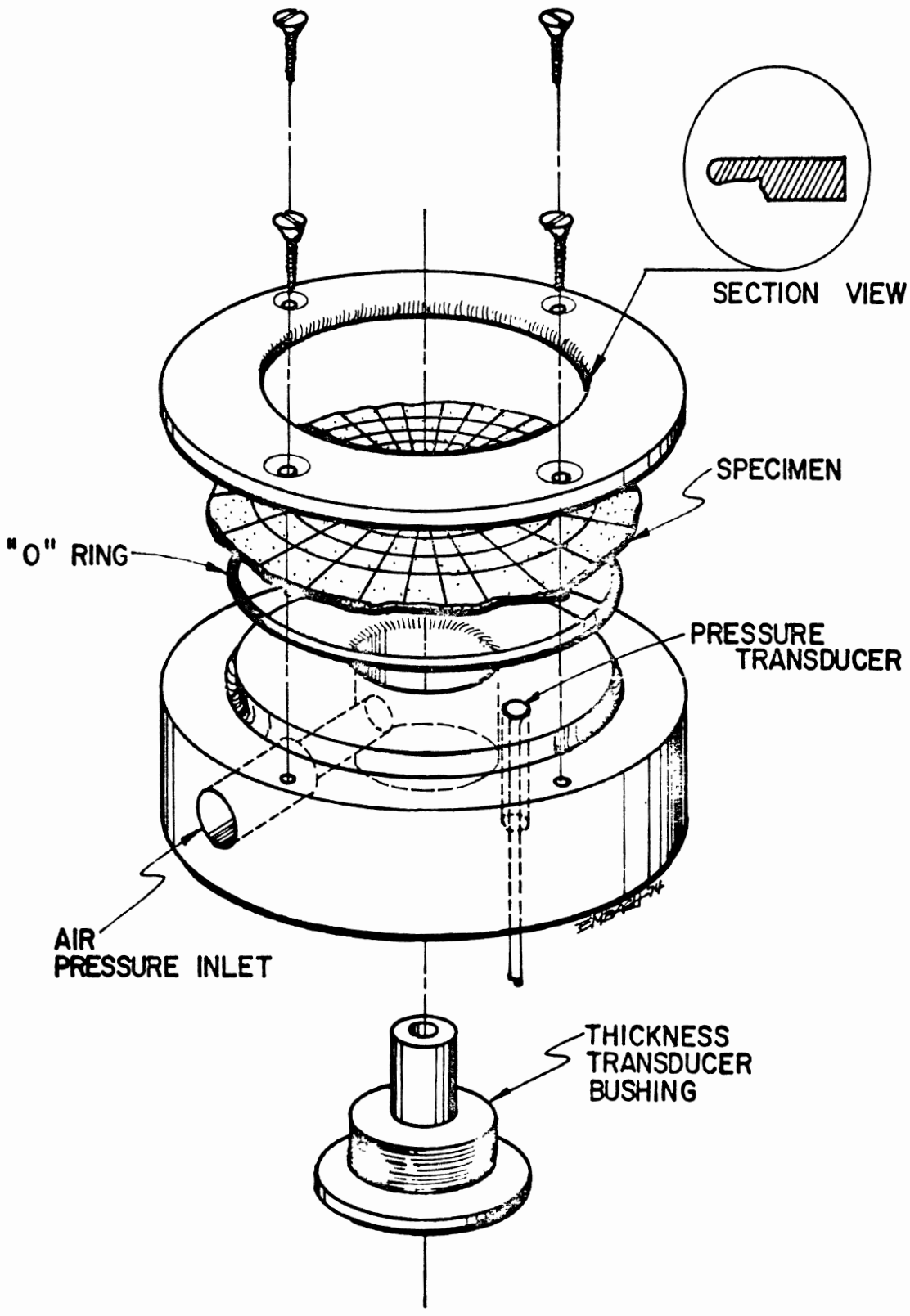
SECTION VIEW
SPECIMEN
"O" RING
PRESSURE TRANSDUCER
AIR PRESSURE INLET
THICKNESS TRANSDUCER BUSHING

Figure 14. Biaxial Test Set-Up
(Rubber Sample Shown)

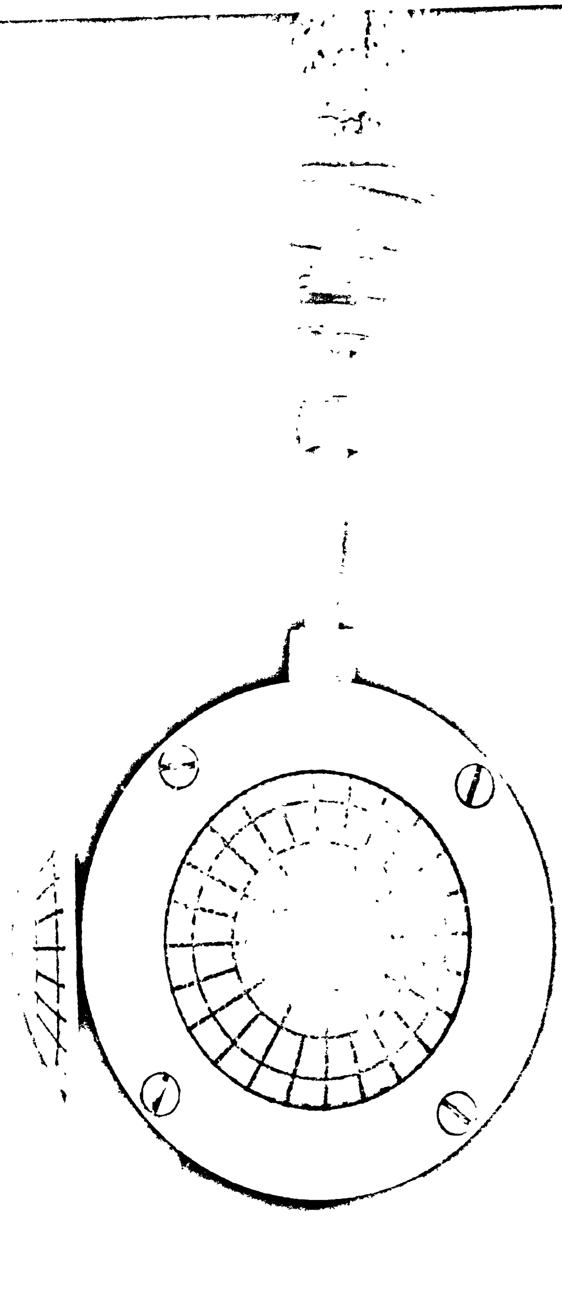

Figure 15. Biaxial Test Set-Up Showing Pressure Chamber

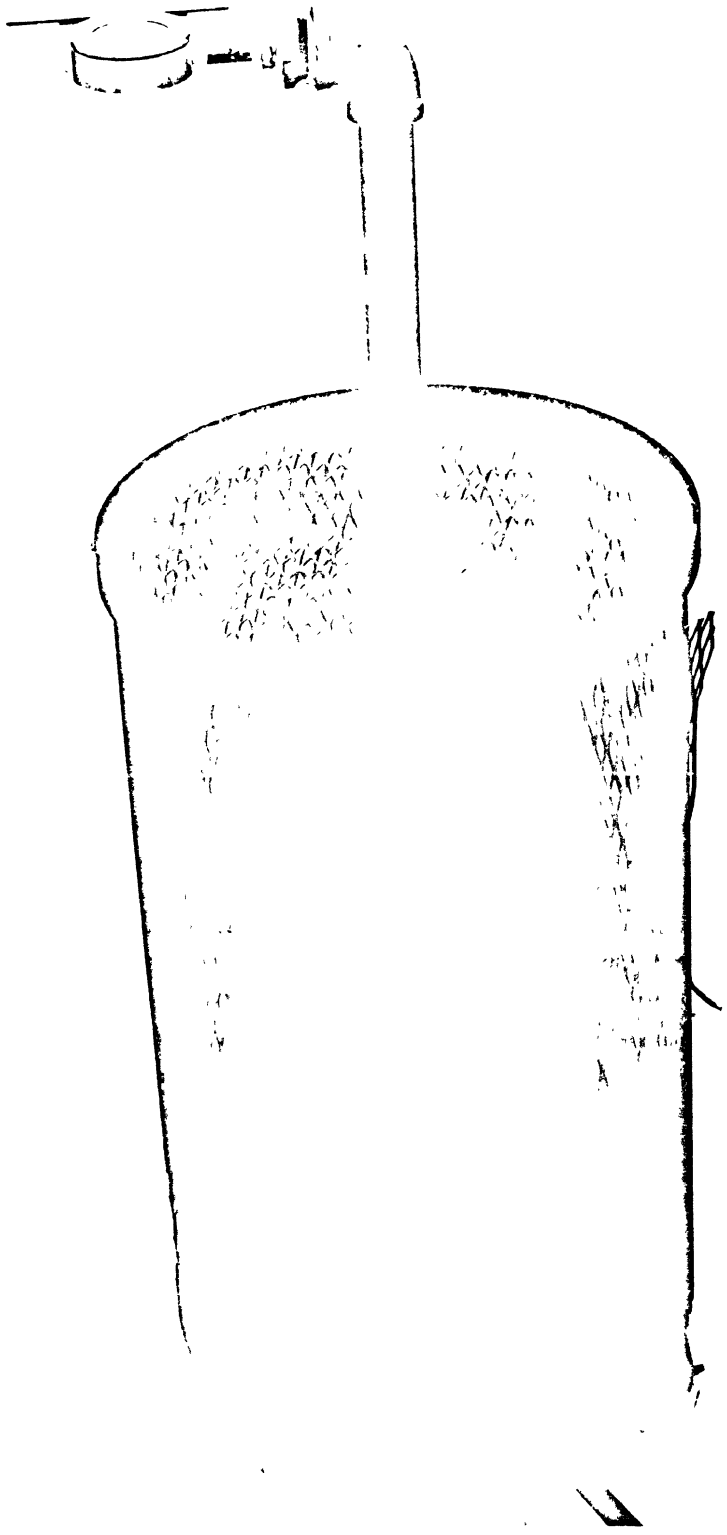

Figure 16. Biaxial Tension Specimen Grid Stamp and Fixture

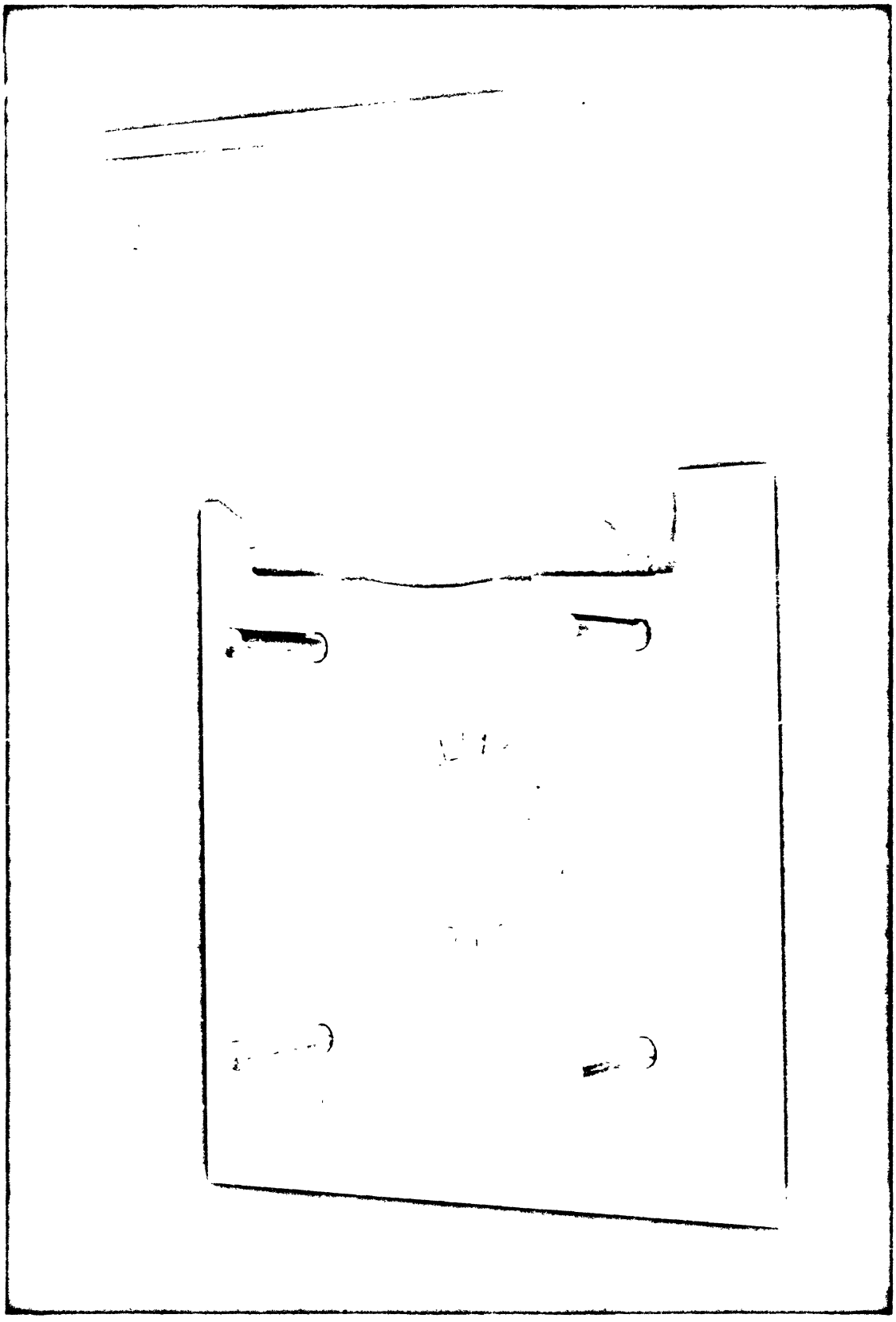

Figure 17. Schematic Representation of the Biaxial Tension Strain Recording Technique

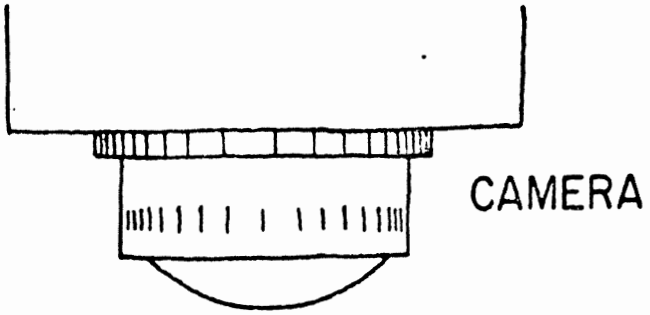
CAMERA

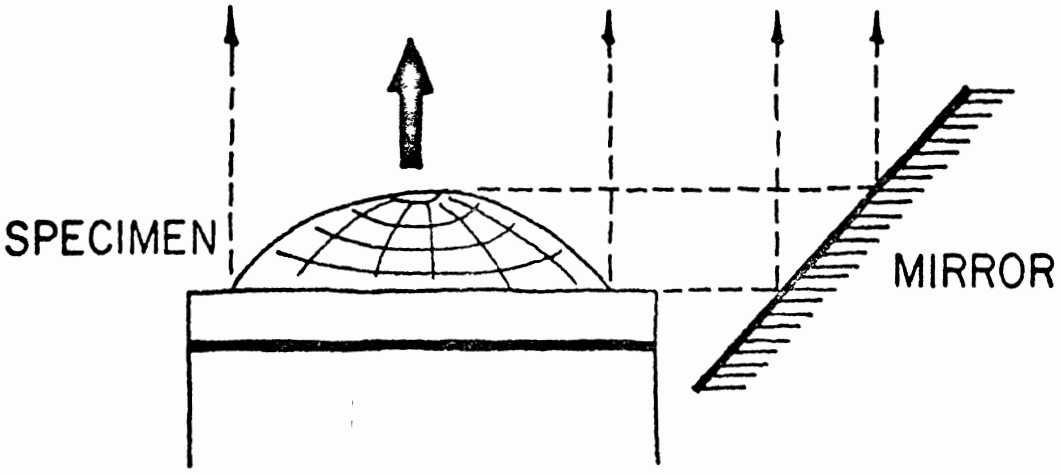
SPECIMEN
MIRROR

3.1.3 Structural Tests

Three tissue types which required testing in what could be termed a structural mode were the intercostal muscles, the intervertebral ligaments and the lungs. Each test had its own unique requirements as described below.

The intercostal muscles are short muscles lying between pairs of ribs. Due to the short length and the insertion of the muscle to adjacent ribs it was decided to test the muscle and its ribs as a unit. Short segments (about 1/2 to 3/4 inches in length) were cut along the ribs and the rib segments were used as the means of loading the muscle by pinning the rib segments into grips. Such an arrangement is shown in Figure 18. In the example shown, two pins were used in each rib segment. In some tests a single central pin was used in each rib segment. The load was measured as in the uniaxial tension tests. The strain in the muscle was measured by grip displacement and was calculated as an extension ratio based on the initial rib to rib spacing.

The intervertebral ligament test required the design of a specimen holding fixture which would allow a specimen consisting of a sectioned vertebral column of two vertebral bodies and the associated rib, to be loaded in three directions in sequence. The fixture with a specimen mounted is shown in Figure 19. In order to measure the three-dimensional motion of the rib relative to the vertebral column, the target shown attached to the rib was used. This target system also served to apply the load to the specimen as shown in Figure 20. The load was applied to the target fixture through a C-ring attached to a flexible wire from the load cell. A 45° mirror was used to obtain the second view of the target system to provide complete three dimensional information. The motion of the target was photographically recorded.

Figure 18. Intercostal Muscle Specimen and Grips

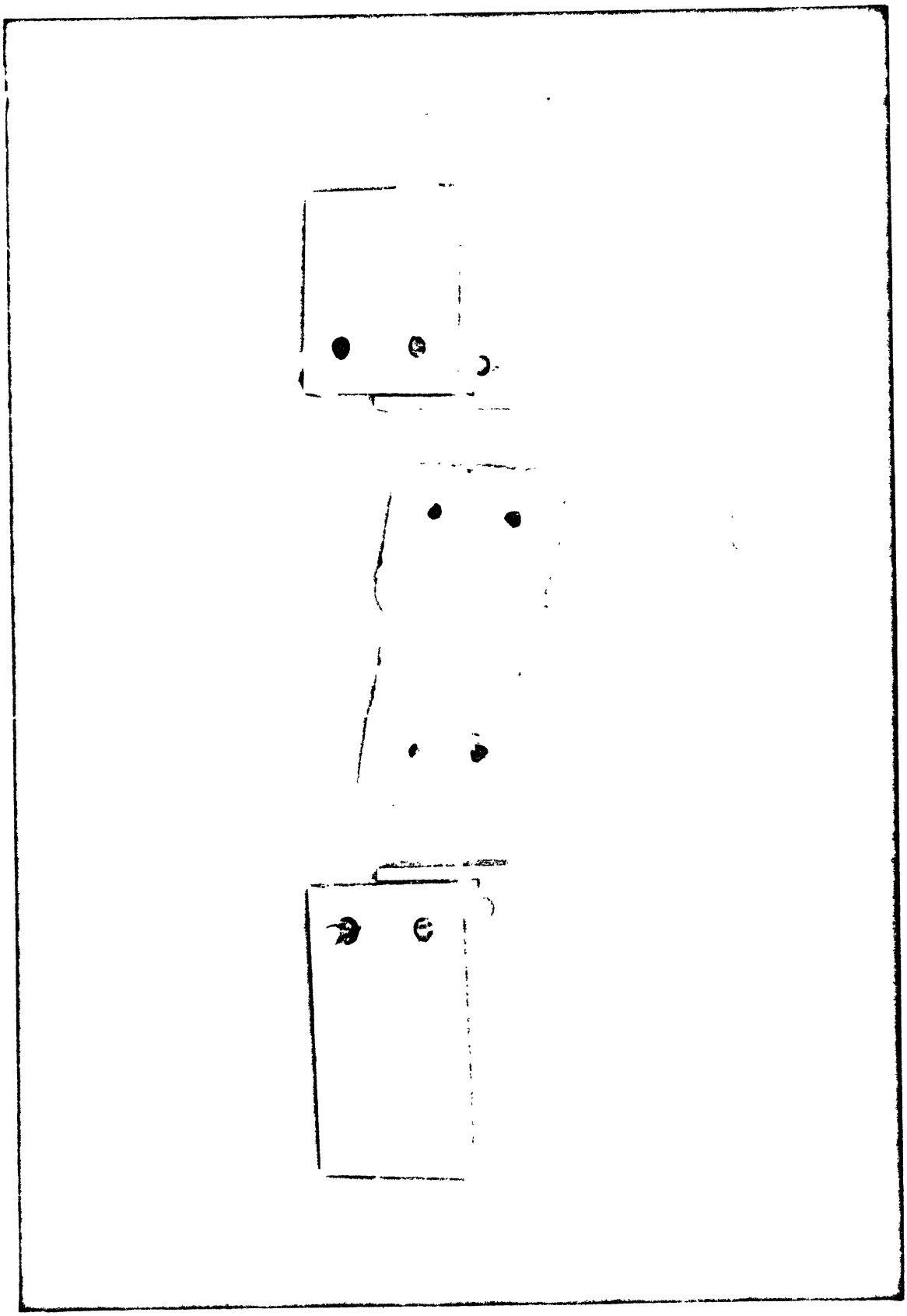

Figure 19. Intervertebral Ligament Test Fixture

1
2
3
4
5

Figure 20. Invertebral Ligament Test Set-Up

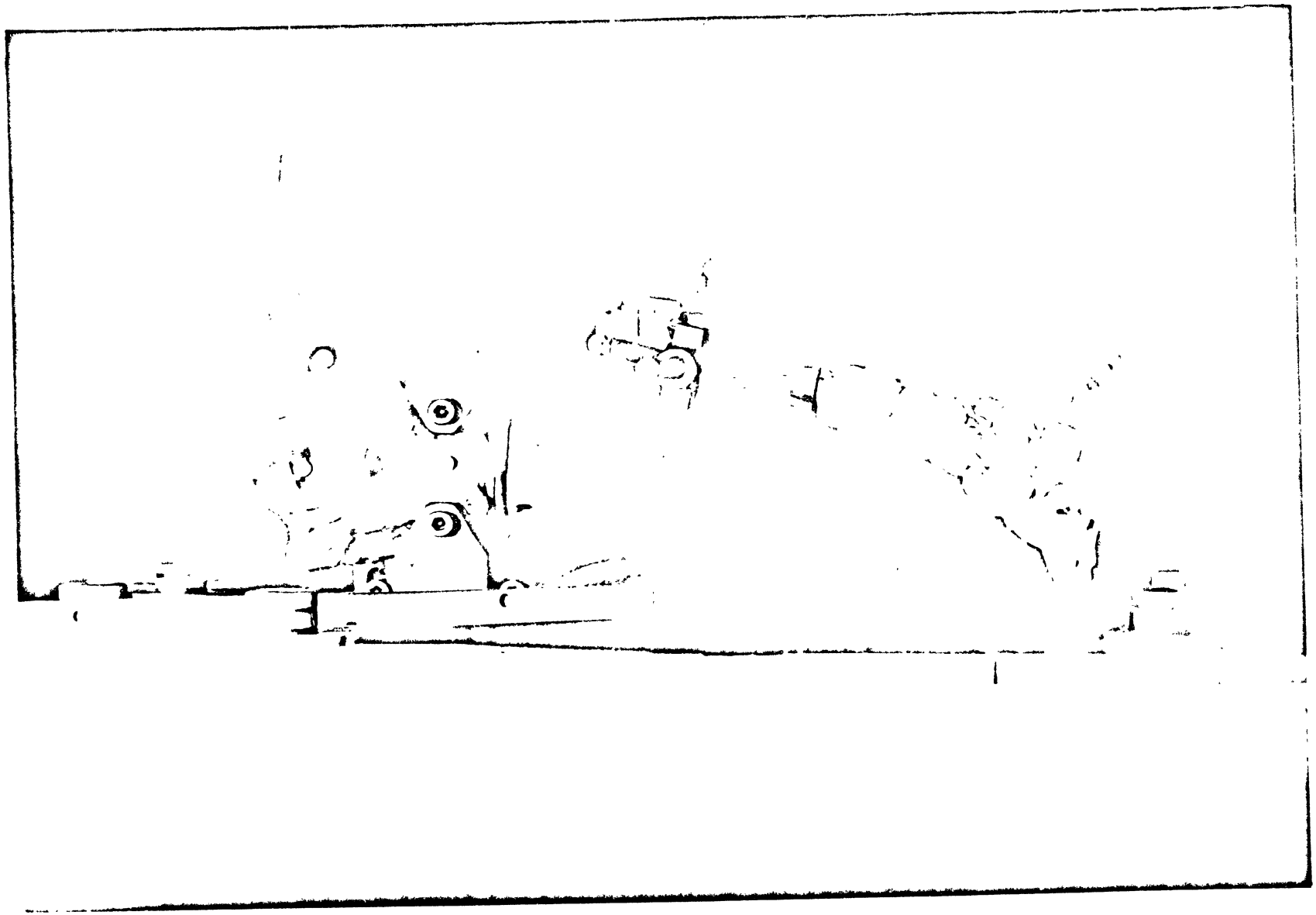

This system was used only in the Instron for static tests.

The determination of the mechanical properties of the tissue of the lung presented many difficult technical problems. In the in vivo state, lung tissue is filled with air and is highly compressible. However, when an excised sample of lung tissue with a shape suitable for materials property testing is tested in vitro, the tissue is no longer air filled and thus is not representative of the in vivo state. This problem has plagued investigators in lung mechanics for many years.

The mathematical model of the thorax being developed at FIRL has characterized the lung as an elastic foundation which interacts accordingly with organs such as the heart during impact. In view of this simplified model of the lung, it would appear that a lung structural test would be of greater use in supplying data for the modeling effort. The lung structural test was performed on Rhesus monkeys. The experiment included in vivo and post mortem tests.

The monkey was anaesthetized with an I.V. injection of Sodium Pentobarbitol (300 mg). A tracheostomy was performed and a Harvard Respirator connected to provide respiration with a tidal volume of 30 ml, at a rate of 30 breaths per minute and an expiratory back pressure of 5 cm of water. The skin over the left half of the thoracic cage was then removed and half an inch portion of the fifth rib and surrounding musculature cut out to expose the middle portion of the pulmonale lobus medium. The monkey was placed on a specifically designed adjustable table and positioned so that the exposed lung surface could be impacted laterally with probe. The probe (3 inches length), in series with a Kistler 931 A load link, was mounted on an Unholtz Dickie linear shaker as shown in Figure 21. A linear accelerometer was also mounted on the shaker head and the two signals were added in

Figure 21. Lung Structural Test Set-Up

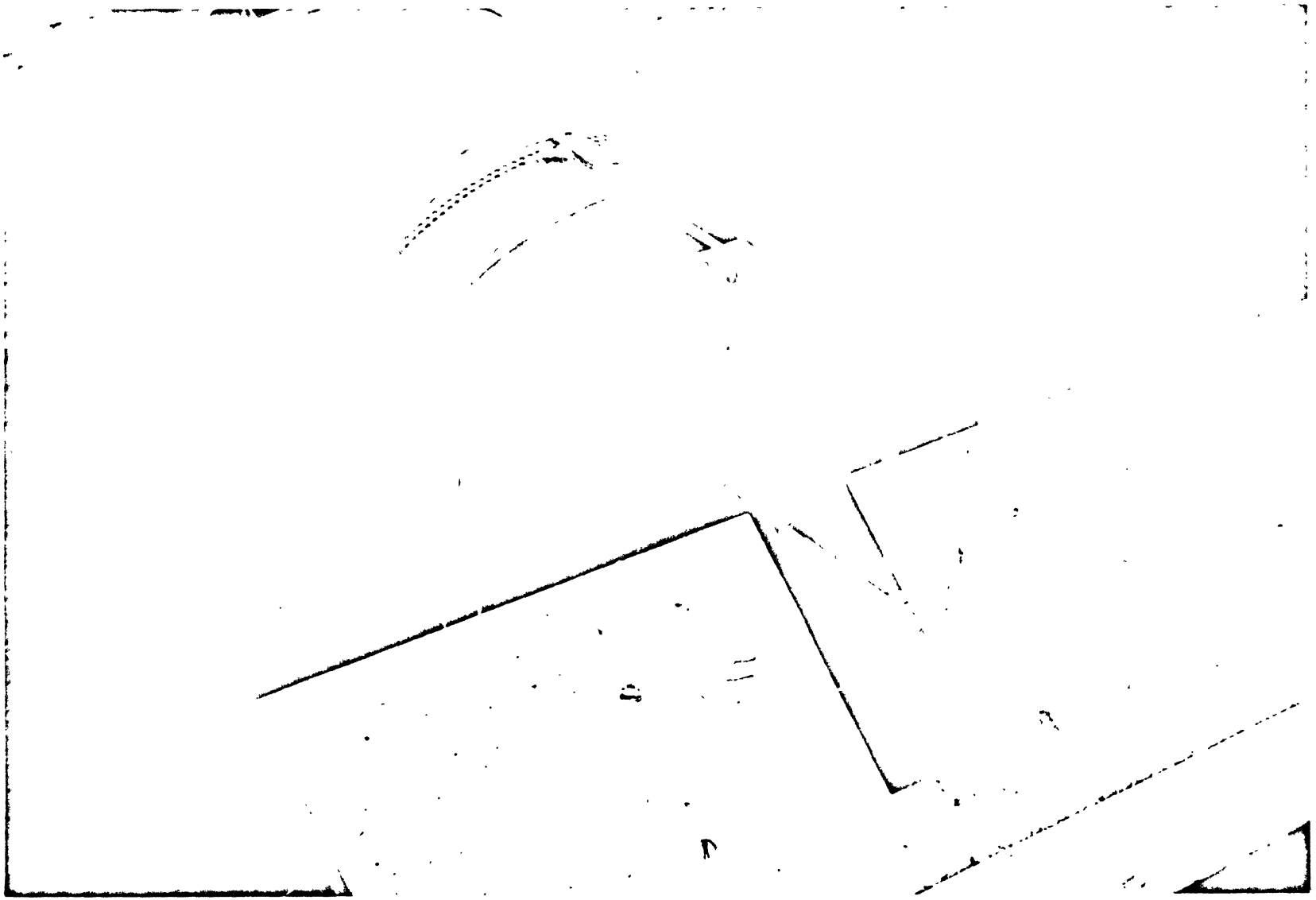

a differential amplifier. With appropriate balancing of the signals, the inertial effect was cancelled out from the load cell output. The probe travel was measured optically by a Physitect GAGE-it unit by measuring the relative movement of the flaps mounted on the shaker head and base. Two types of tests were run with this apparatus; single pulse rapid load-unload tests and driving-point impedance sweeps.

In the single pulse tests, the probe travel was adjusted to 0.4 inches stroke and single cycle at a frequency of 50 Hz. The lung was placed so that it just touched the probe. Impacts were made both at the end of expiration and inspiration. The monkey was then moved and a small middle portion of the third left rib removed to expose the lobus superior and similar tests conducted at that site.

The heart beat was checked with a stethoscope before and after tests, and no abnormal arrhythmias noticed.

The monkey was then sacrificed with an overdose of Sodium Pentobarbitol and the above tests repeated immediately and twice more at intervals of 30 minutes. The monkey was removed from the test lab and stored in a refrigerator at a temperature of 35° F and removed 24 hours later. The lungs were removed from the thoracic cavity, placed in a stainless steel tray and connected to the respirator. The same tests as detailed before were conducted on the left and the right lungs at room temperature. The cycling frequency of the shaker was changed to 5 Hz and similar tests were conducted again.

The driving point impedance tests were carried out in generally the same manner as above. One difference was the use of a half cylinder of rigid polyethylene to enclose the in vitro lung against the steel support tray. This tended to produce a volumetric enclosure of the lung similar to that in the in situ case. In addition, another probe of twice the cross-sectional

area of the original probe was used as well as the original probe of the single pulse tests. Two monkeys were tested for the driving point impedance tests, one was 5.5 kg (LT-3) and the other weighed 5.1 kg (LT-4).

3.1.4 Data Reduction Techniques

As mentioned previously, the load-time (or pressure-time) traces for every test were recorded along with synchronization pulses on a light beam oscillograph strip recorder. The corresponding strain data required a rather lengthy analysis procedure in which each single frame of film (either 35 mm in the static tests and 16 mm in the dynamic tests) was projected and the resulting enlarged image was carefully traced onto paper to produce a permanent record of the strain grid. The series of tracings for each test were measured and the resulting extension ratios calculated as indicated in Appendix A.

4.0 TISSUE SOURCES AND TESTING PRIORITY

The human tissues tested in this program were fresh unembalmed tissues obtained at autopsy at the Veterans Administration Hospital in Ann Arbor. The material specimens were tested as soon as they were obtained, or in cases where this was not possible, they were stored in refrigerated physiological saline solution until used. Specimens were obtained from 13 individuals as indicated in Table 1, Summary of Tissue Source Data. It had been anticipated at the beginning of the program that more donors than the 13 would have been available. This did not occur for two reasons. The first was an unusual reduction in the number of autopsies performed during parts of the testing phase of the program. A more significant reason however, is apparent when the cause of death and gross pathologic diagnoses column of Table 1 is studied. In almost every case complications of one thoracic organ or another are involved. In many autopsies the situation was such that no suitable tissues could be obtained due to severe involvement of the thoracic organs in the pathology of the subject. Thus, only a fraction of the autopsies performed at the VA Hospital produced any suitable samples at all. Many of the conditions noted in Table 1 are characteristic of the older population (the average age at death of the individuals in Table 1 is 69.5 years when the one young person (20 years) is excluded). The primary tissues studied in the program (ordered in decreasing importance to the FIRL modelling) are:

1. Intercostal muscle
2. Cardiac muscle (left ventricle)
3. Aorta
4. Pericardium
5. Lungs
6. Diaphragm

7. Vertebral ligaments

8. Esophagus

9. Trachea and Bronchi

In addition to human tissue samples, Rhesus monkey tissue samples of high priority tissues were also tested in the program. The monkey tissues were obtained from animals used on other HSRI studies. A limited number of live Rhesus monkeys were used in this program to study the lung structural characteristics.

TABLE 1

SUMMARY OF TISSUE SOURCE DATA

#	AUTOPSY NUMBER	SEX	AGE YEARS	HEIGHT ft-in	WEIGHT lbs	CAUSE OF DEATH AND GROSS PATHOLOGIC DIAGNOSES
1	3	M	77	5'11"	150	Squamous cell carcinoma of lung. Fibrous pericardial adhesions. Generalized arteriosclerosis. Hypercalcemia.
2	4	M	82	5'10"	140	Respiratory insufficiency. Bronchopneumonia. Right ventricular myocardia hypertrophy. Severe calcific atheriosclerosis of aorta.
3	6	M	60	-	170	Bronchogenic carcinoma of right lobe. Occlusive coronary arterial atherosclerosis. Metastases in diaphragm. Diabetes mellitus.
4	8	M	77	5' 8"	170	Massive gastrointestinal hemorrhage. Duodenal ulcer. Occlusive calcific, coronary artery atherosclerosis. Arteriolonephrosclerosis. Generalized atherosclerosis.
5	9	M				Chronic pancreatic insufficiency. Lobular pneumonia. Carcinoma of the lung. Pulmonary edema. Chronic alcoholism.
6	10	M	77	5'10"	120	Carcinoma of the lung. Hemopericardium. Brown atrophy of heart and skeletal muscle.
7	56	M	61	6' 4"	171	Right hemothorax. Osteogenic sarcoma metastatic to lung. Calcific abdominal aorta atherosclerosis.
8	57	M	64	6' 7"	148	Bilateral, confluent lobular pneumonia. Carcinoma of the lung. Arterialnephrosclerosis. Myocardial hypertrophy.
9	58	M	63	-	101	Atherosclerotic cardiovascular disease. Severe pulmonary edema. Aortic and focal coronary atherosclerosis.
10	70	M	54	5'10"	210	Sepsis. Multiple abscesses of left lung. Cerebral Infarction. Asthma. Chronic bronchitis.
11	74	M	20	5'11"	142	Hodgkin's Disease in mediastinal abdominal, and para-aortic lymph nodes and liver.

TABLE 1 (continued)

SUMMARY OF TISSUE SOURCE DATA

#	AUTOPSY NUMBER	SEX	AGE YEARS	HEIGHT ft-in	WEIGHT lbs	CAUSE OF DEATH AND GROSS PATHOLOGIC DIAGNOSES
12	76	M	82	5' 0"	94	Prostatic hypertrophy. Septicemia. Severe coronary atherosclerosis. Moderate dilation of thoracic aorta. Dehydration.
13	81	M	68	5' 9"	99	Stage 4 Cancer of Prostate. Idiopathic hypercalcemia for six years. Widespread prostatic carcinoma.

5.0 TEST PROGRAM RESULTS

5.1 GENERAL

Tests were performed on samples of all of the following human tissues:

1. Intercostal muscle
2. Cardiac Muscle (left ventricle)
3. Aorta (Ascending, Arch and Descending)
4. Pericardium
5. Lungs (Rhesus monkey only)
6. Diaphragm
7. Intervertebral Ligaments
8. Esophagus
9. Trachea and Bronchi

In addition, tests were performed on many of the same tissues from Rhesus monkeys. These tests are reported as an aggregate at the end of this section with the exception of the lung tests which are reported separately.

The numbers of tests obtained on each tissue type varies and reflects a combination of factors; the priority or importance of the tissue to the FIRL modelling effort, the availability of a particular tissue at autopsy and the degree of difficulty which the tissue presents in making a suitable specimen.

The test results are presented in four formats:

1. Engineering stress-strain curves for each test (presented in this section.)
2. Tables of the reduced data for each test (presented in Appendix C & D)
3. Average dynamic stress-strain curves for each tissue type (presented in Section 6.0).
4. Tables of the average dynamic stress-strain behavior (presented in Section 6.0).

5.1.1 Intercostal Muscle Test Results

The tests on intercostal muscle are presented in Figure 22. Due to variations in specimen thickness which did not seem to relate to load carrying ability, it was decided to not use the thickness to calculate tensile stress, but instead to use only the load per unit width of the specimen. This helped reduce scatter and can be justified in that the muscle tissue itself only carries part of the load between the ribs in the passive state and that connective tissue between the ribs, which carries most of the load, is not represented by a total thickness measurement. The tables in Appendix C list the individual test specimen thicknesses. The structural nature of these tests precluded a more complete strain analysis of the tissue behavior.

The tissue samples used in these tests came from two donors, one who was young (20 years old) but emaciated, and one who was older but heavy. In general the tissue from the heavy person (series 74) was more extensible than for the lighter weight person (series 70) but the strengths were comparable. Comparison of the static results with the dynamic results indicate about a 50% increase in tensile strength in the dynamic case but with only a slight reduction in extension.

5.1.2 Cardiac Muscle (Left Ventricle)

Samples of left ventricular tissue were tested both parallel to the muscle fiber and transverse to the fiber direction. The results (as shown in Figures 23 and 24) indicate a pronounced increase in tensile strength at dynamic strain rates with the strength parallel to the fibers being about three times that across the fibers. A similar relation was found in static tests reported by Yamada (13).

Figure 22. Human Intercostal Muscle Tension Test Results

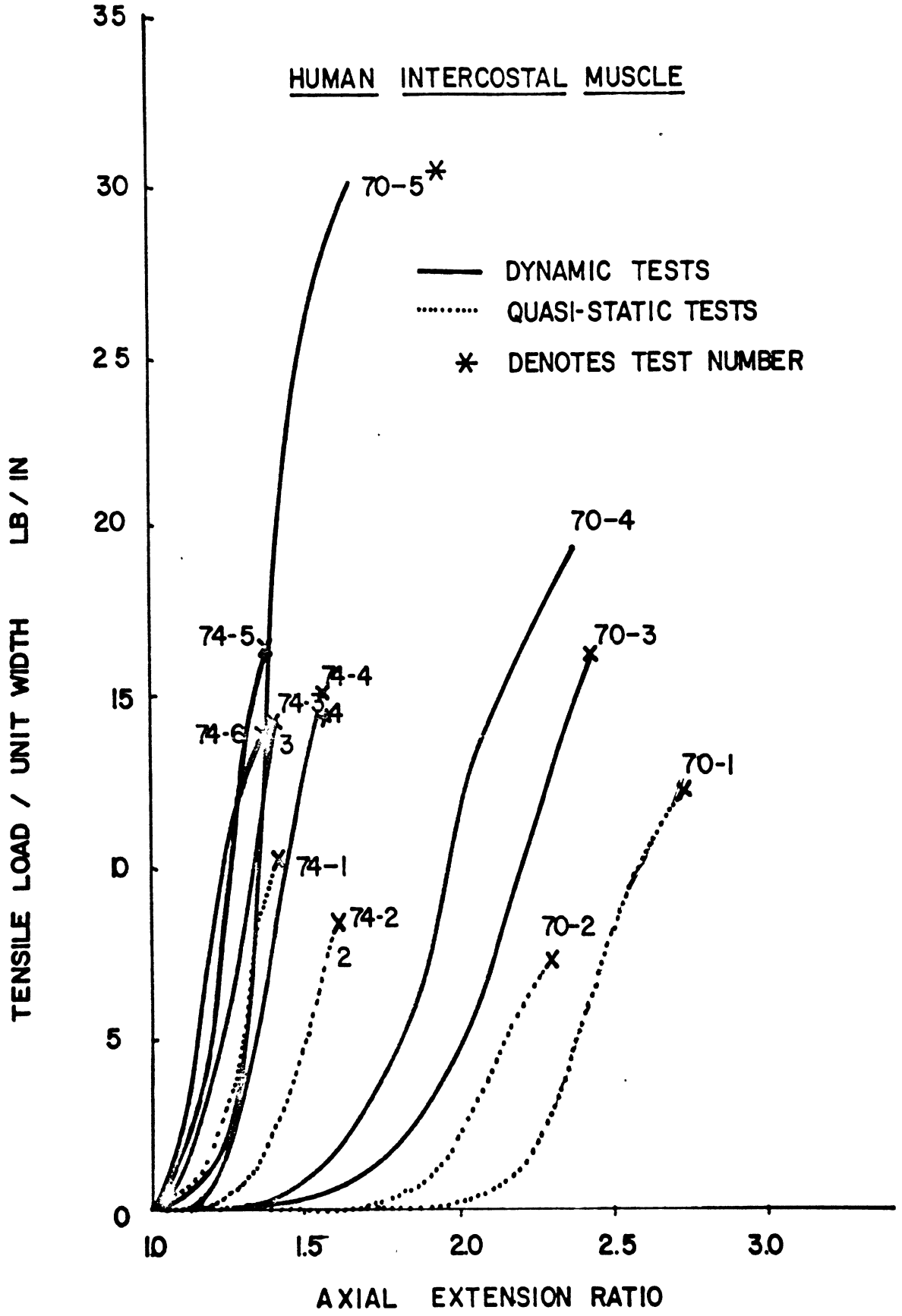
HUMAN INTERCOSTAL MUSCLE
DYNAMIC TESTS
QUASI-STATIC TESTS
* DENOTES TEST NUMBER
70-5*
70-4
70-3
70-2
70-1
74-5
74-4
74-3
74-6
3
4
74-1
74-2
2
TENSILE LOAD / UNIT WIDTH LB / IN
AXIAL EXTENSION RATIO
0
5
10
15
20
25
30
35
1.0
1.5
2.0
2.5
3.0

Figure 23. Human Cardiac Muscle (Left Ventricle) Tension Test Results, Direction of Loading Parallel to Muscle Fibers

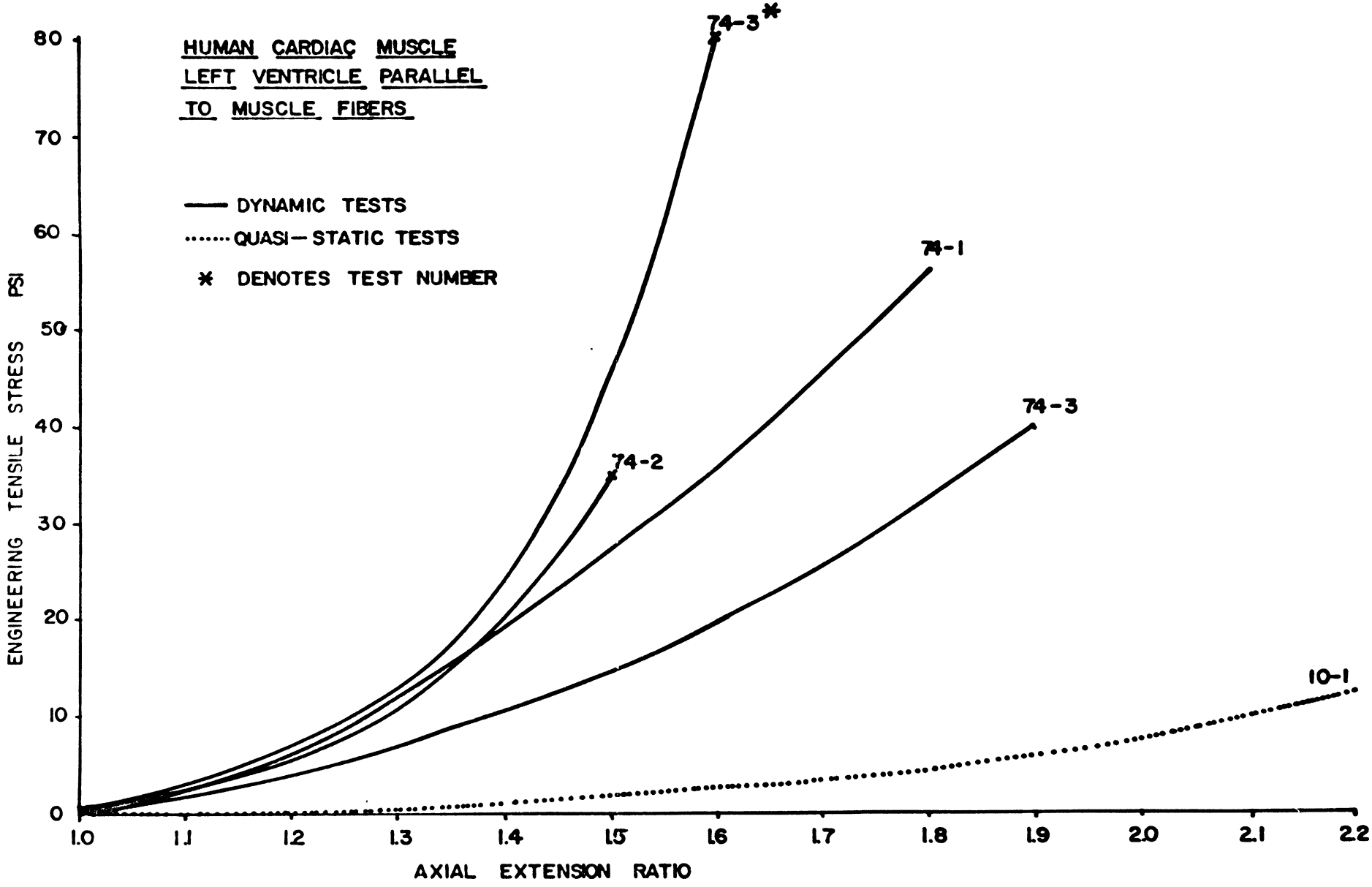
HUMAN CARDIAC MUSCLE
LEFT VENTRICLE PARALLEL
TO MUSCLE FIBERS
DYNAMIC TESTS
QUASI—STATIC TESTS
* DENOTES TEST NUMBER
74-3*
74-1
74-3
74-2
10-1
ENGINEERING TENSILE STRESS PSI
AXIAL EXTENSION RATIO
0
10
20
30
40
50
60
70
80
1.0
1.1
1.2
1.3
1.4
1.5
1.6
1.7
1.8
1.9
2.0
2.1
2.2

Figure 24. Human Cardiac Muscle (Left Ventricle) Tension Test Results, Direction of Loading Across Muscle Fibers

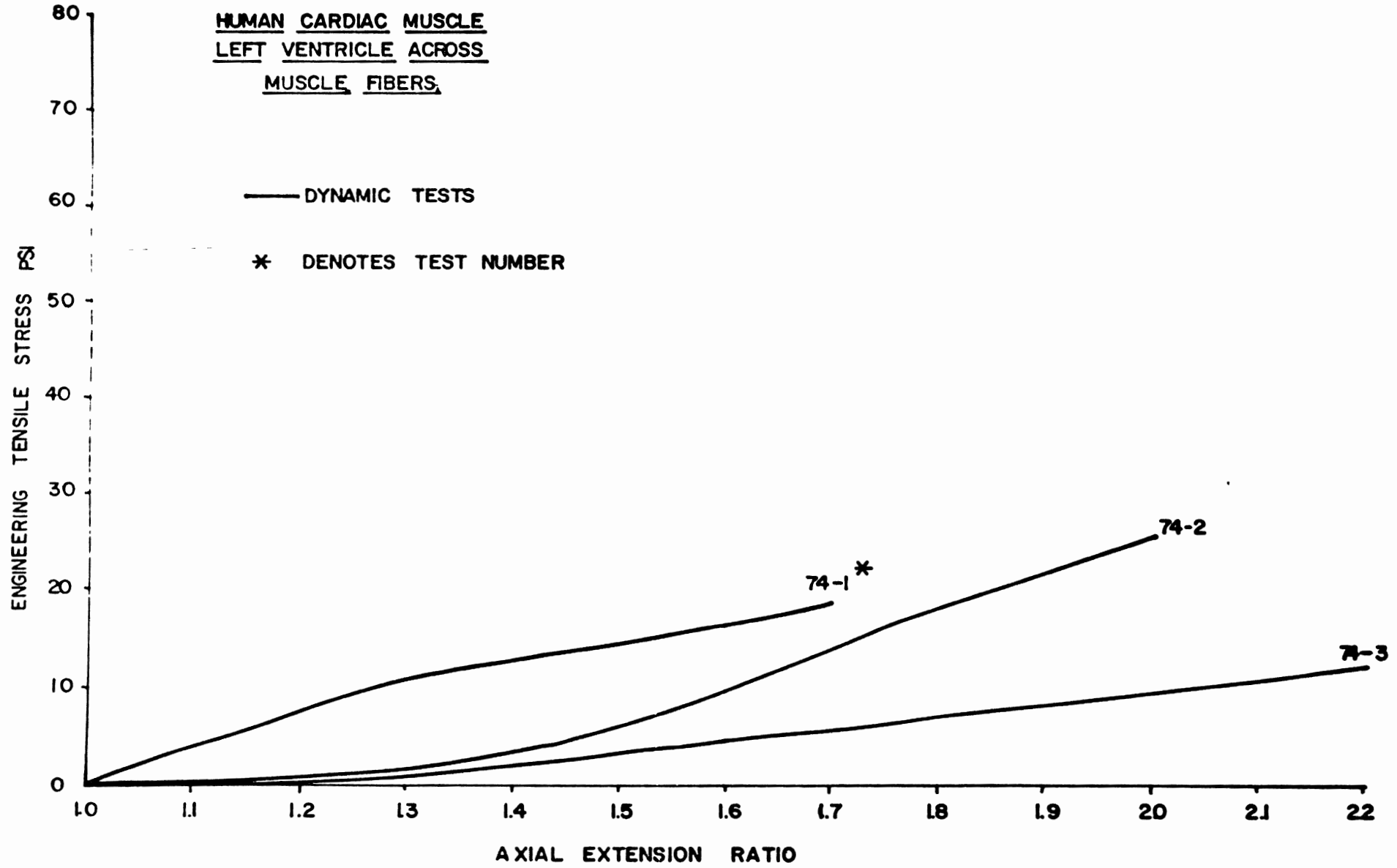
HUMAN CARDIAC MUSCLE
LEFT VENTRICLE ACROSS
MUSCLE FIBERS
DYNAMIC TESTS
* DENOTES TEST NUMBER
ENGINEERING TENSILE STRESS PSI
80
70
60
50
40
30
20
10
0
1.0
1.1
1.2
1.3
1.4
1.5
1.6
1.7
1.8
1.9
2.0
2.1
2.2
AXIAL EXTENSION RATIO
74-1 *
74-2
74-3

5.1.3 Aorta

Tests were performed on samples of the ascending aorta, aortic arch and descending thoracic aorta. Test directions were longitudinal to the vessel and transverse to the vessel. The test results are shown for each specimen location and orientation in Figures 25, 26, 27, 28, 29 and 30. As in other tissues marked,strain effects are present with respect to static data. Also evident are large variations in the low stress extensibility of the material, a manifestation of pathological condition.

5.1.4 Pericardium

Only a few tests of the pericardium were performed, mainly due to the difficulty in obtaining suitable samples of this tissue. The results are shown in Figure 31.

5.1.5 Lung Structural Tests

Lung tests were performed only on Rhesus monkey lungs. The tests were performed both in vivo, post mortem in situ and in vitro. In all cases the lung was inflated by a respirator. The tests which consisted of single pulse loading of the lung showed very pronounced rate effects as demonstrated in Figure 32 where the 50 Hz equivalent pulse produced almost five times the forces of the 5 Hz equivalent pulse with the 50 Hz force peak corresponding to maximum probe velocity rather than maximum deflection.

The driving point impedance tests results on two monkeys shown in Figures 33, 34, 35, 36, 37, and 38 also show the viscous nature of the lung. At low frequencies (below approximately 20-30 Hz) the response is spring-like while above these frequencies large damping effects predominate. Note that the general response of the lung in vivo and in vitro is similar although specific details vary with probe diameter and animal.

Figure 25. Human Ascending Aorta Test Results, Direction of Loading Longitudinal to Vessel

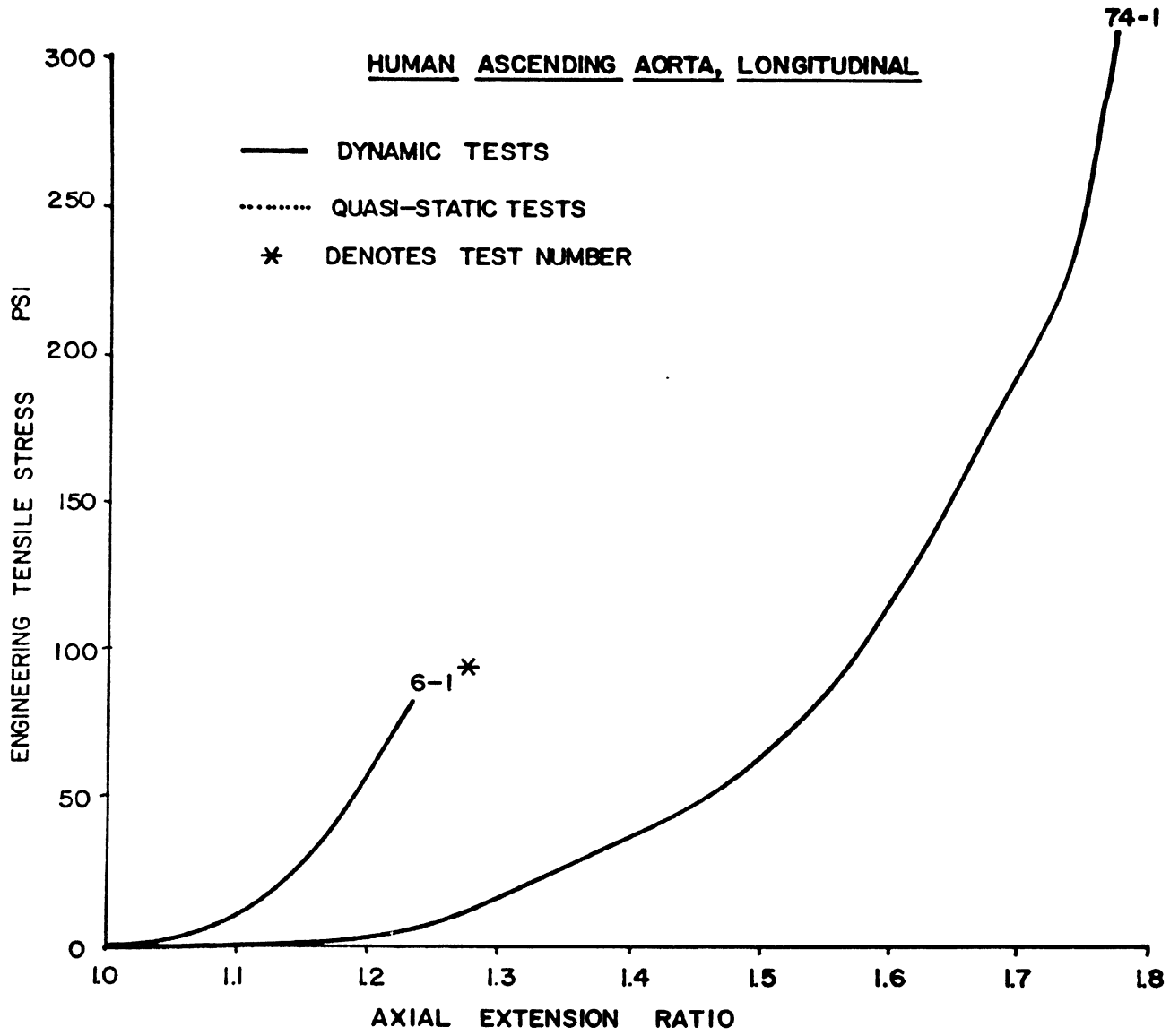
HUMAN ASCENDING AORTA, LONGITUDINAL
DYNAMIC TESTS
QUASI-STATIC TESTS
* DENOTES TEST NUMBER
74-1
6-1*
ENGINEERING TENSILE STRESS PSI
300
250
200
150
100
50
0
1.0
1.1
1.2
1.3
1.4
1.5
1.6
1.7
1.8
AXIAL EXTENSION RATIO

Figure 26. Human Ascending Aorta Test Results, Direction of Loading Transverse to Vessel

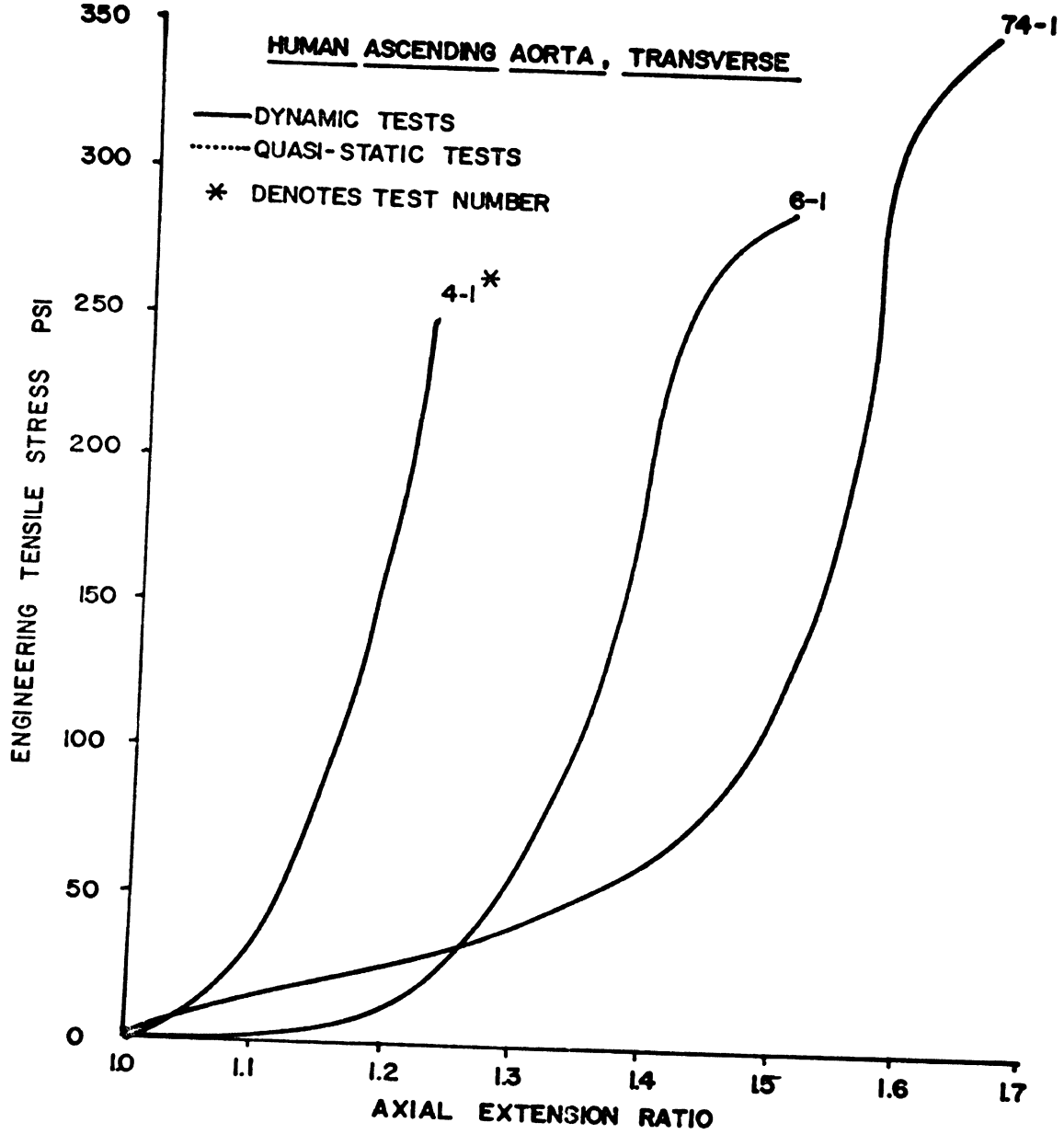
HUMAN ASCENDING AORTA, TRANSVERSE
DYNAMIC TESTS
QUASI-STATIC TESTS
* DENOTES TEST NUMBER
74-1
6-1
4-1*
ENGINEERING TENSILE STRESS PSI
350
300
250
200
150
100
50
0
1.0
1.1
1.2
1.3
1.4
1.5
1.6
1.7
AXIAL EXTENSION RATIO

Figure 27. Human Aortic Arch Test Results, Direction of Loading Longitudinal to Vessel

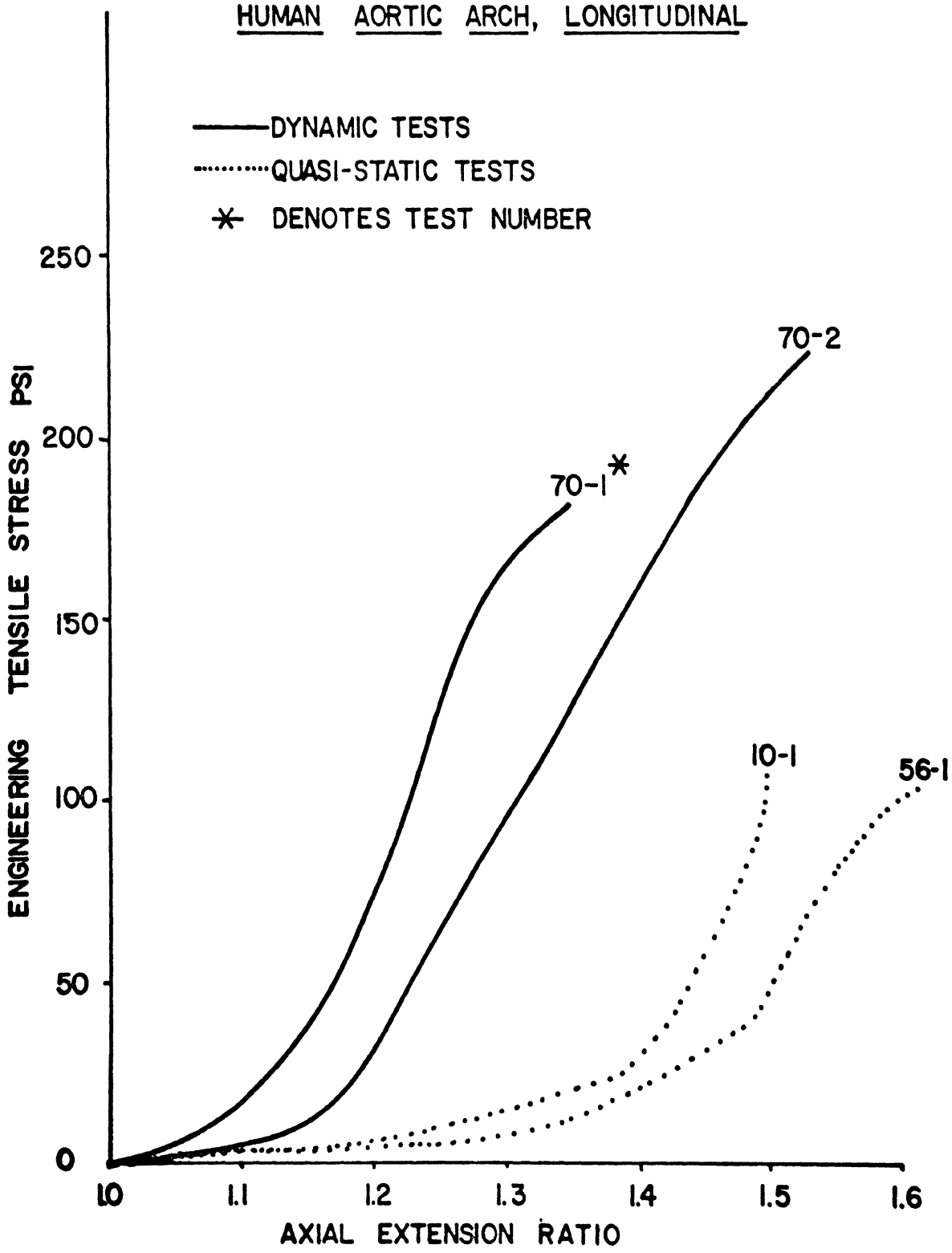
HUMAN AORTIC ARCH, LONGITUDINAL
DYNAMIC TESTS
QUASI-STATIC TESTS
DENOTES TEST NUMBER
ENGINEERING TENSILE STRESS PSI
250
200
150
100
50
0
70-2
70-1*
10-1
56-1
1.0
1.1
1.2
1.3
1.4
1.5
1.6
AXIAL EXTENSION RATIO

Figure 28. Human Aortic Arch Test Results, Direction of Loading Transverse to Vessel

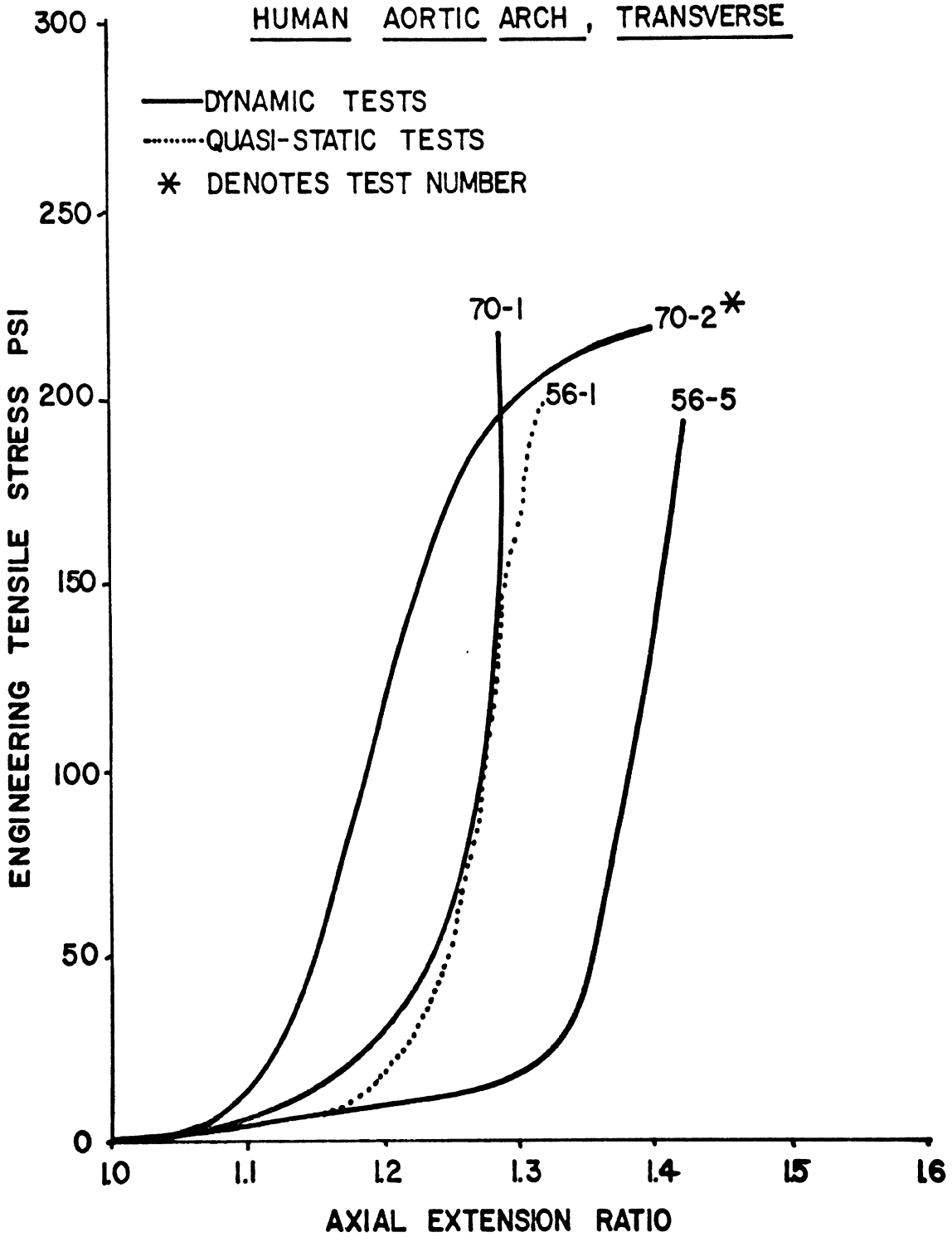
HUMAN AORTIC ARCH, TRANSVERSE
DYNAMIC TESTS
QUASI-STATIC TESTS
* DENOTES TEST NUMBER
ENGINEERING TENSILE STRESS PSI
300
250
200
150
100
50
0
70-1
70-2*
56-1
56-5
1.0
1.1
1.2
1.3
1.4
1.5
1.6
AXIAL EXTENSION RATIO

Figure 29. Human Descending Aorta, Test Results, Direction of Loading Longitudinal to Vessel

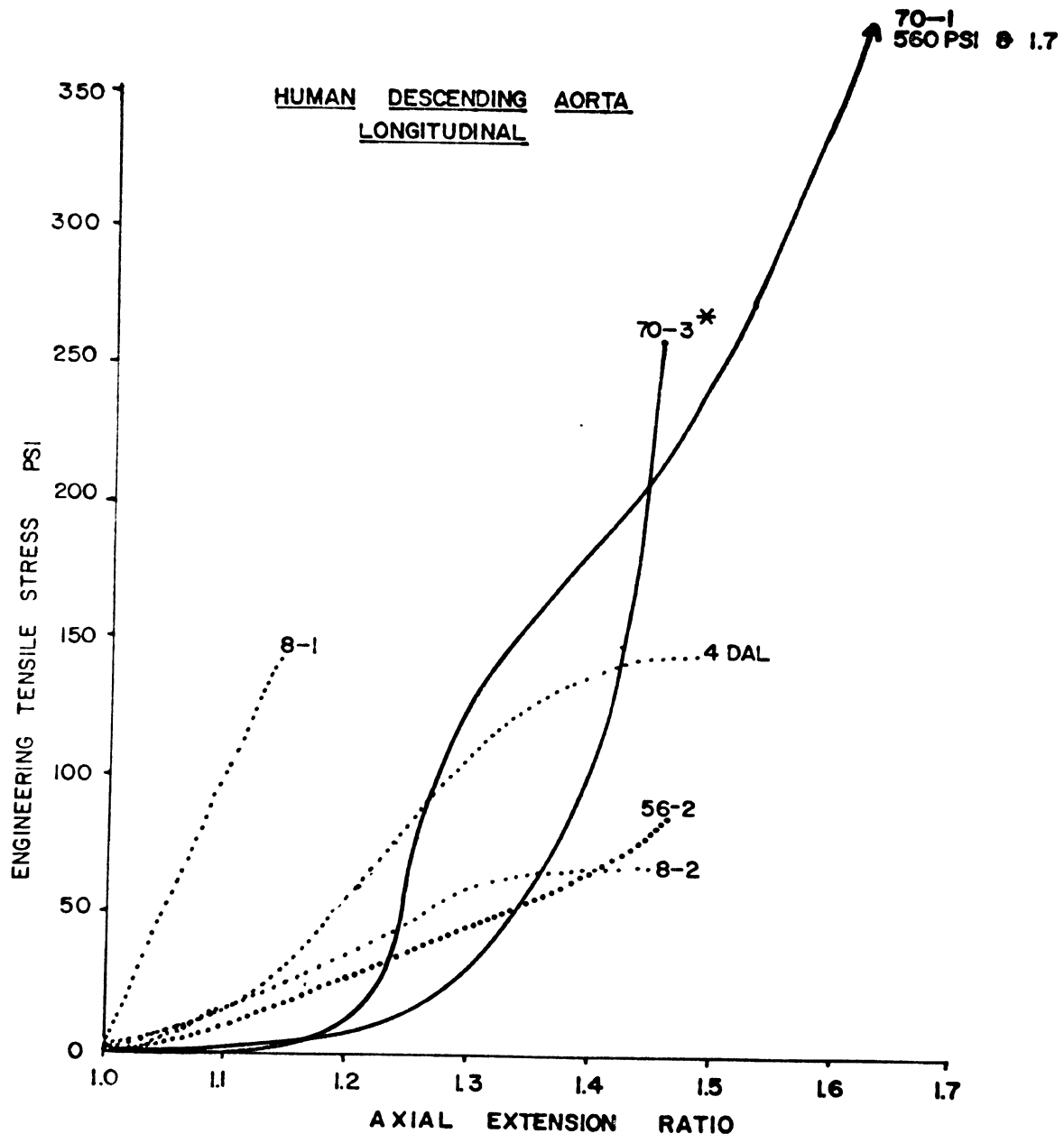
HUMAN DESCENDING AORTA
LONGITUDINAL
70-1
560 PSI @ 1.7
70-3*
8-1
4 DAL
56-2
8-2
ENGINEERING TENSILE STRESS PSI
350
300
250
200
150
100
50
0
1.0
1.1
1.2
1.3
1.4
1.5
1.6
1.7
AXIAL EXTENSION RATIO

Figure 30. Human Descending Aorta Test Results, Direction of Loading Transverse to Vessel

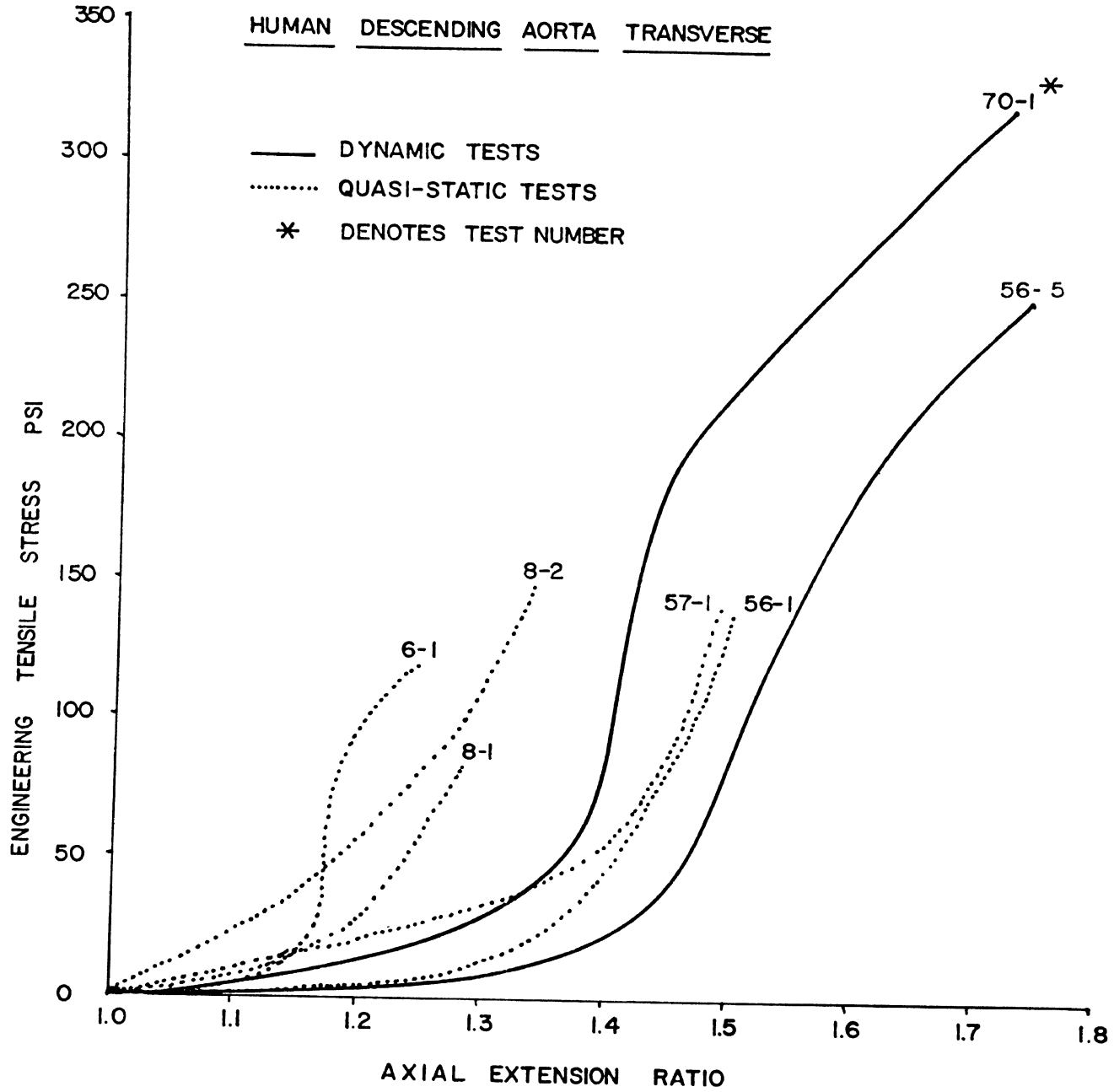
HUMAN DESCENDING AORTA TRANSVERSE
DYNAMIC TESTS
QUASI-STATIC TESTS
* DENOTES TEST NUMBER
70-1 *
56-5
8-2
57-1
56-1
6-1
8-1
ENGINEERING TENSILE STRESS PSI
350
300
250
200
150
100
50
0
1.0
1.1
1.2
1.3
1.4
1.5
1.6
1.7
1.8
AXIAL EXTENSION RATIO

Figure 31. Human Pericardium Test Results

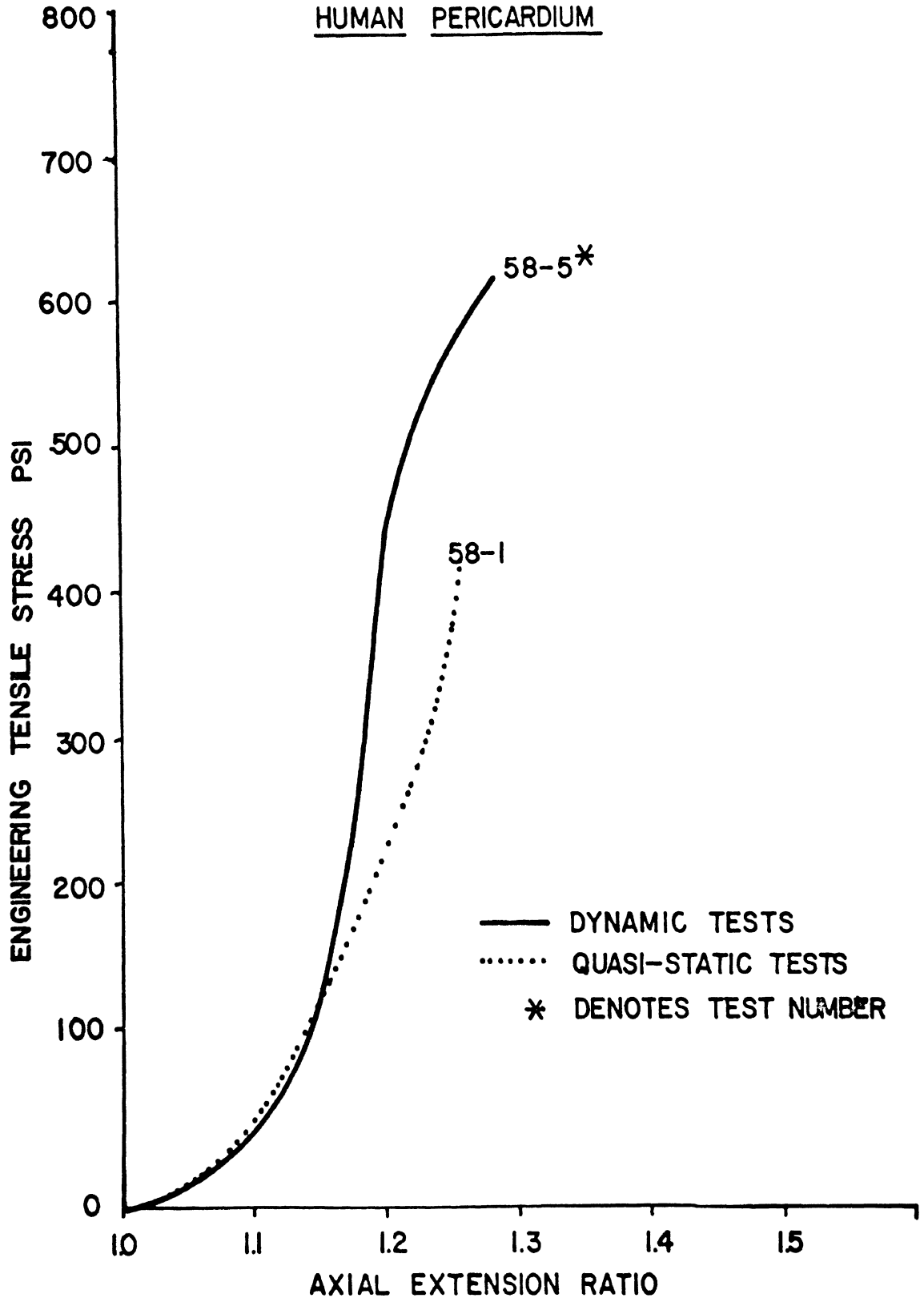
HUMAN PERICARDIUM
800
700
600
500
400
300
200
100
0
ENGINEERING TENSILE STRESS PSI
58-5*
58-1
DYNAMIC TESTS
QUASI-STATIC TESTS
* DENOTES TEST NUMBER
1.0
1.1
1.2
1.3
1.4
1.5
AXIAL EXTENSION RATIO

Figure 32. Pulse Load Deflection Curves for Rhesus Monkey Lung Test LT-2

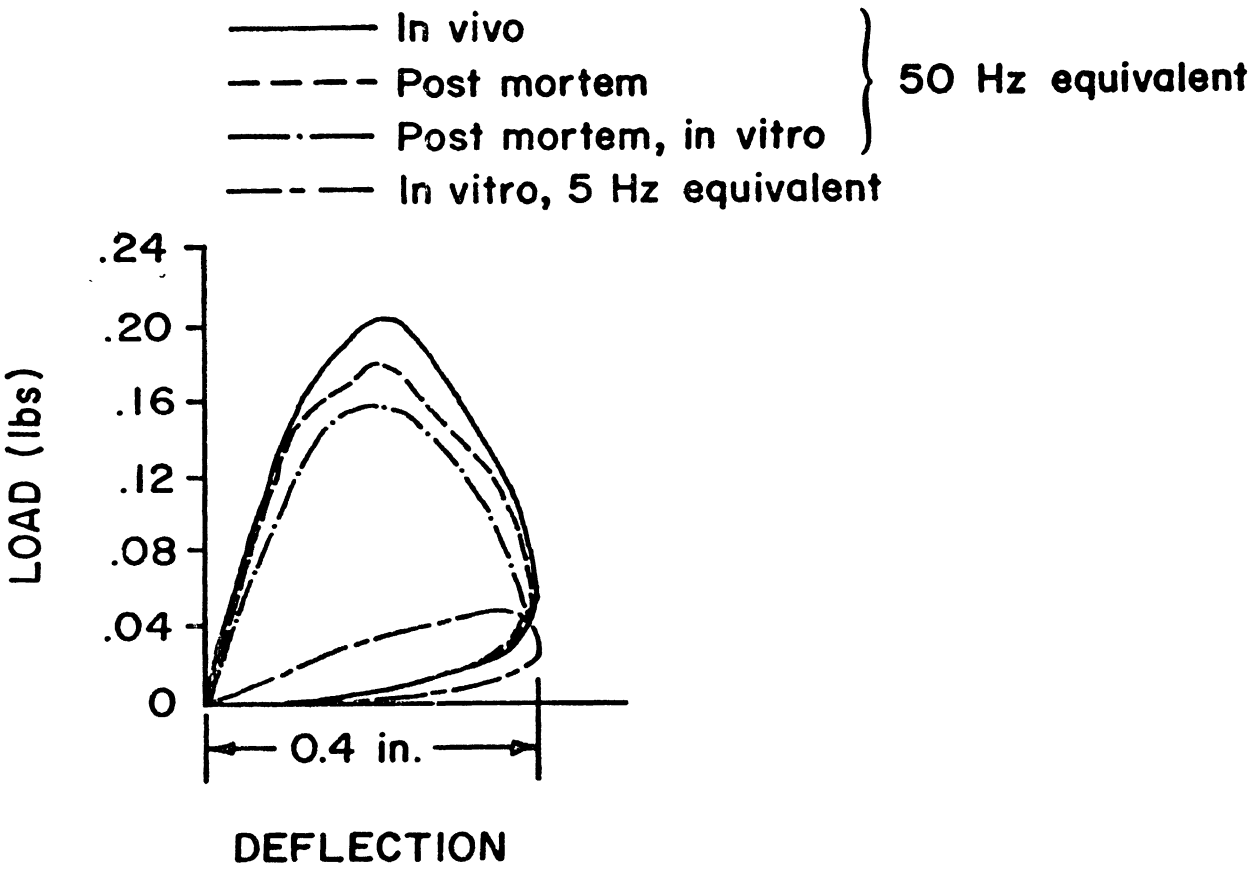
In vivo
Post mortem
Post mortem, in vitro
50 Hz equivalent
In vitro, 5 Hz equivalent
.24
.20
.16
.12
.08
.04
0
LOAD (lbs)
0.4 in.
DEFLECTION

Figure 33. Mechanical Impedance Curves for Inflated Rhesus Lungs in Situ (Post Mortem) Test LT-3 Large Probe

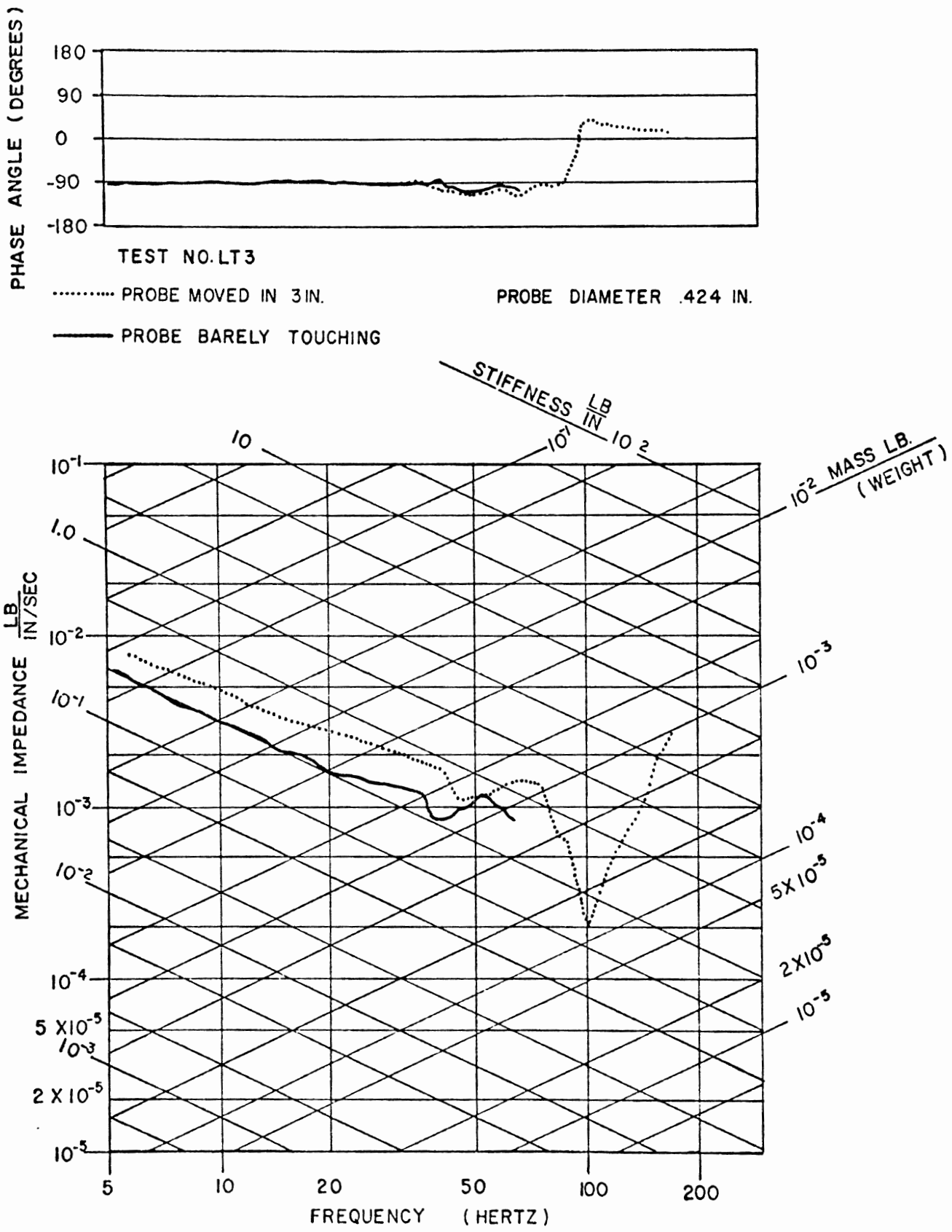

MECHANICAL IMPEDANCE CURVES FOR INFLATED RHESUS LUNGS IN SITU (POST MORTEM)

Figure 34. Mechanical Impedance Curves for Inflated Rhesus Lungs In Vitro Test LT-3 Large Probe

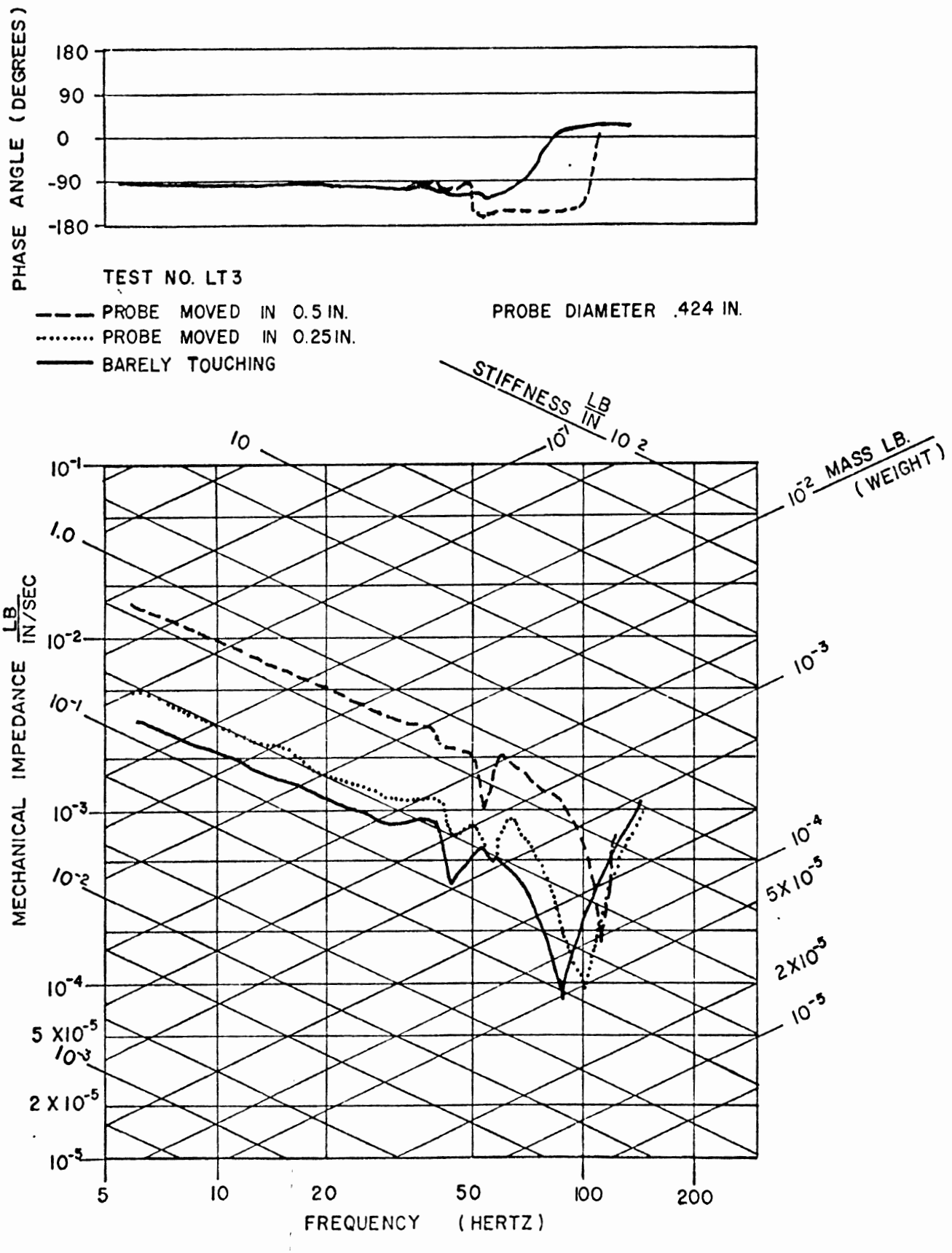

MECHANICAL IMPEDANCE CURVES FOR INFLATED RHESUS LUNGS IN VITRO

Figure 35. Mechanical Impedance Curves for Inflated Rhesus Lungs in Vitro Test LT-3 Small Probe

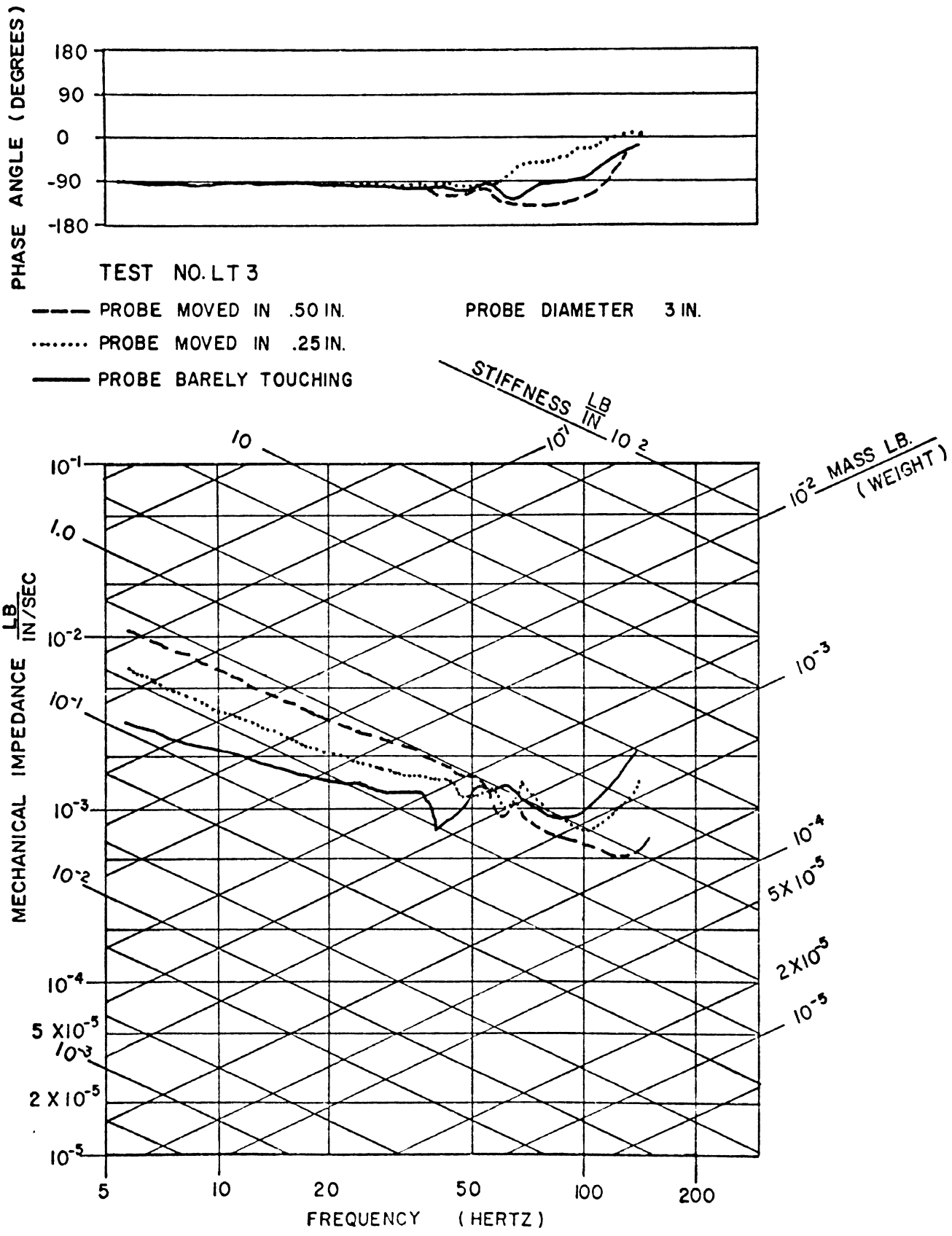

MECHANICAL IMPEDANCE CURVES FOR INFLATED RHESUS LUNGS IN VITRO

Figure 36. Mechanical Impedance Curves for Rhesus Lungs in Vivo Test LT-4 Large Probe

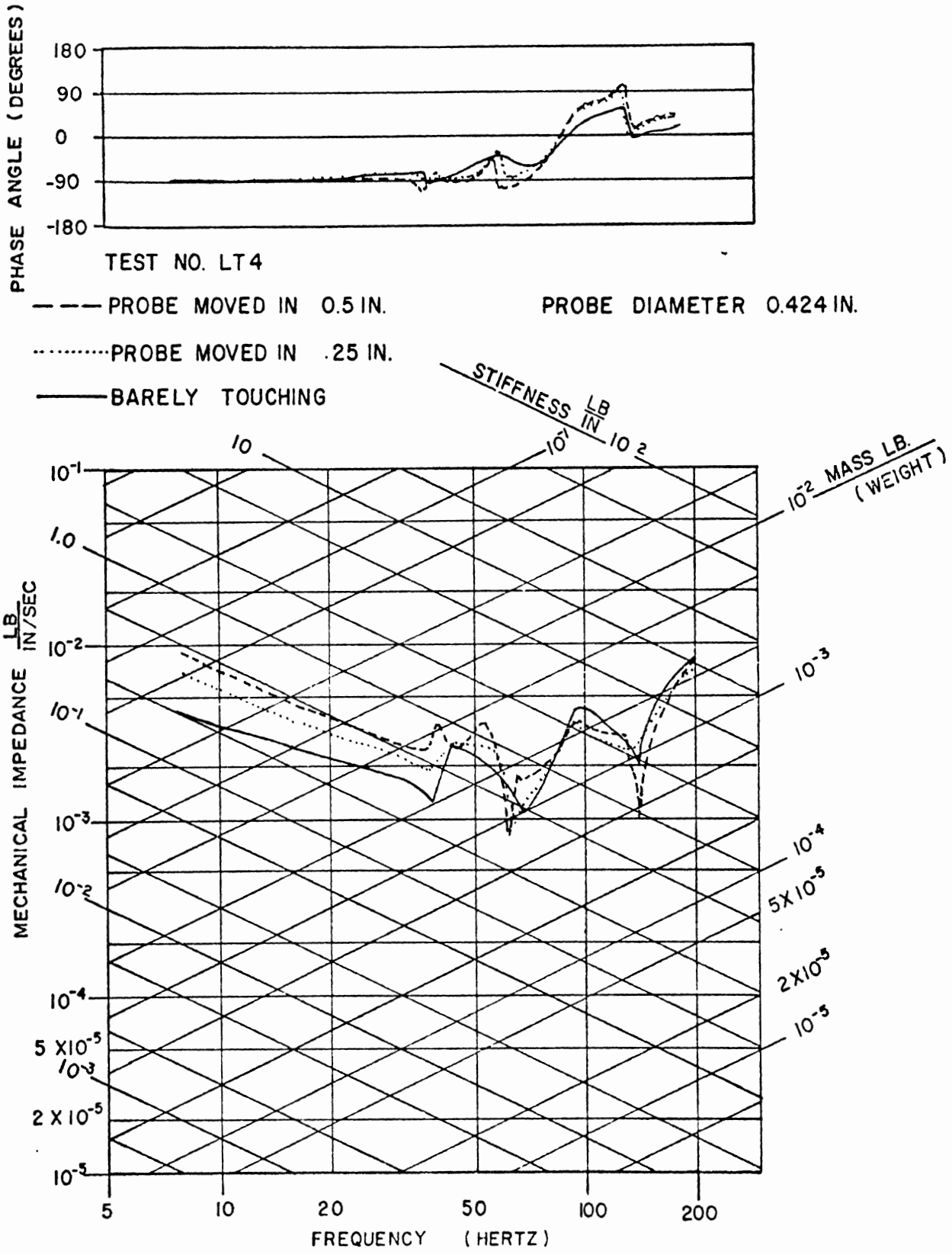

MECHANICAL IMPEDANCE CURVES. FOR RHESUS LUNGS

IN VIVO

Figure 37. Mechanical Impedance Curves for Rhesus Lungs in Vitro Test LT-4 Large Probe

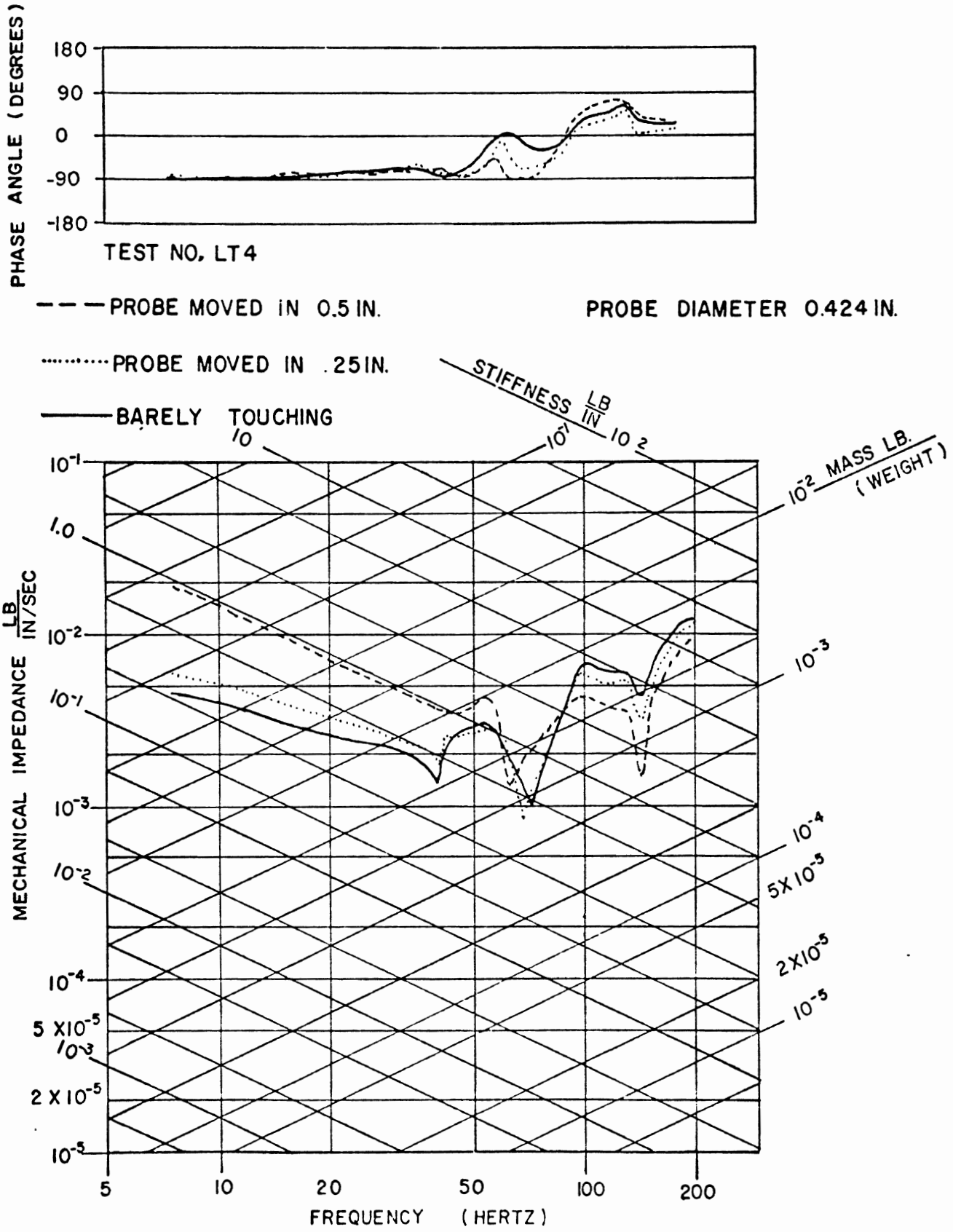

MECHANICAL IMPEDANCE CURVES FOR RHESUS LUNGS IN VITRO

Figure 38. Mechanical Impedence Curves for Inflated Rhesus Lungs In Vitro Test LT-4 Small Probe

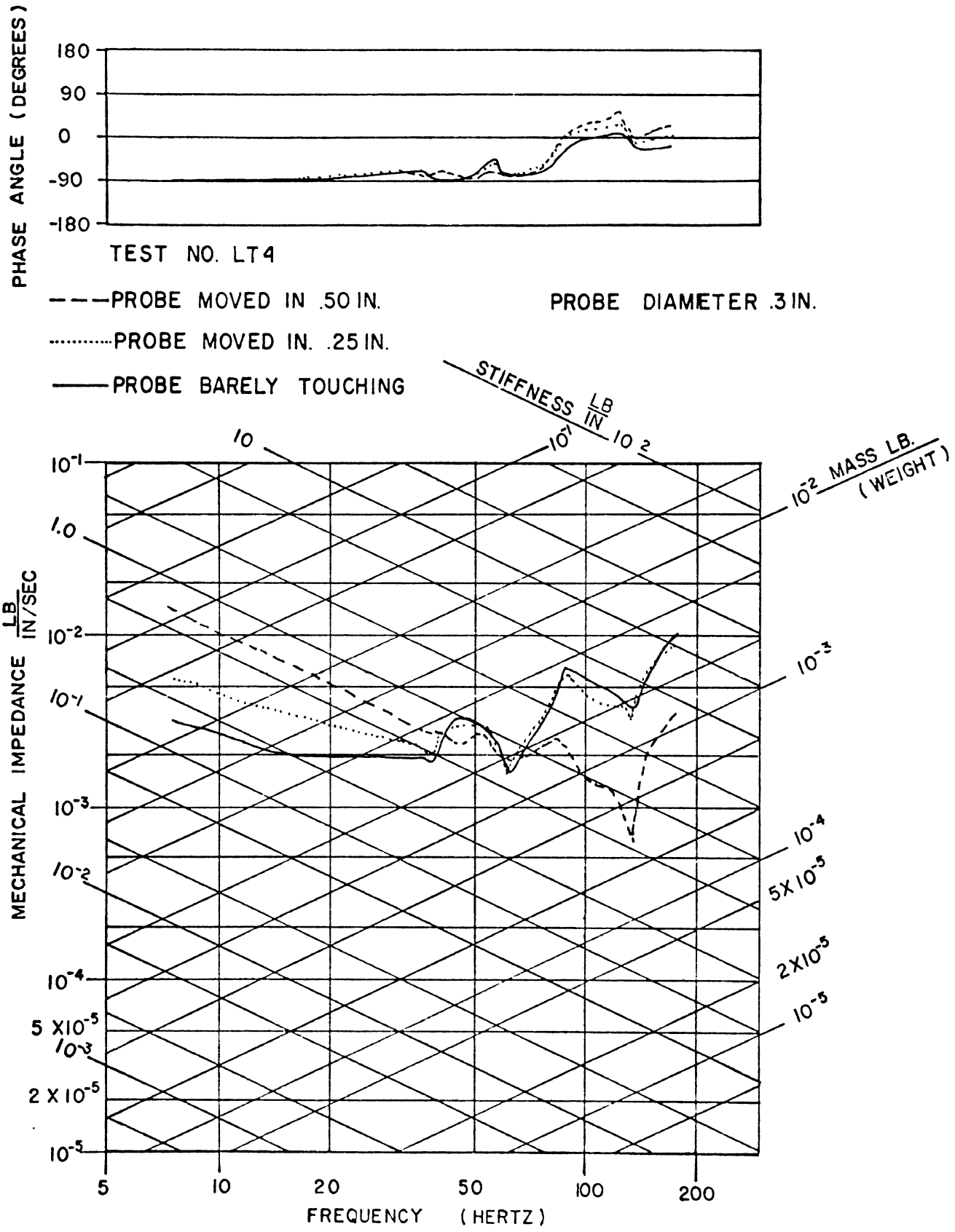

MECHANICAL IMPEDANCE CURVES FOR INFLATED RHESUS LUNGS IN VITRO

5.1.6 Diaphragm

The diaphragm proved quite suitable for testing both in suitability for specimens and availability at autopsy. The diaphragm test specimen orientation was denoted with respect to the fiber orientation of the muscle layer which is sandwiched between two layers of connective tissue membrane. The orientations were across the fibers and parallel to the fibers. The test results for the tests in these orientations are shown in Figures 39 and 40. The behavior of the diaphragm when tested parallel to the muscle fibers was not as rate sensitive as other tissue types, however, the strength across the fibers did increase with strain rate.

Sufficiently large samples of diaphragm were available to allow biaxial tension testing of the tissue. Two tests were performed with dynamic loading (about 10 msec. to failure). The general nature of the deformation patterns in the membrane as it inflated indicated that large anisotropy effects were not evident. Analysis of the failure stresses are strains yielded a biaxial extension ratio of $\lambda = 1.55$ and a corresponding biaxial engineering stress of 700 psi.

5.1.7 Intervertebral Ligament Test

Due to extreme difficulty in obtaining suitable samples (the removal of the sample from the body involves cutting near the joint of interest), only one sample was obtained for testing in the program. The tests were performed by loading the rib segment first downward in the superior-inferior direction, then laterally in the left-right direction and finally in the anterior-posterior direction. It was only in the S-I test direction (the direction in which the costovertebral joint usually moves) where the displacements and rotations were great enough to make accurate measurements of the rib motion. This data was resolved in terms of moments about the A-P and L-R axes of the joint with

Figure 39. Human Diaphragm Test Results, Direction of Loading Across Muscle Fibers

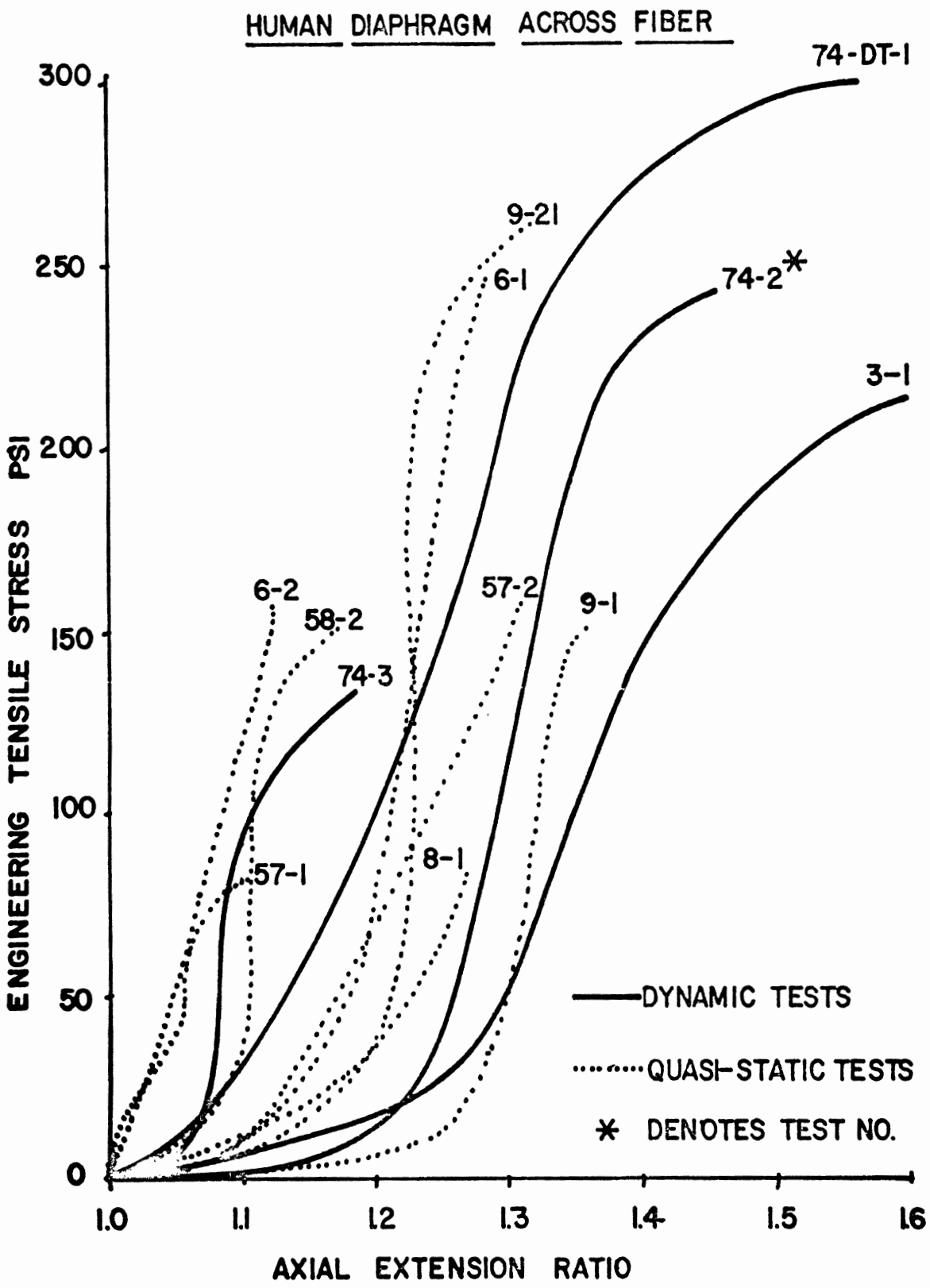
HUMAN DIAPHRAGM ACROSS FIBER
74-DT-1
9-21
6-1
74-2*
3-1
6-2
58-2
57-2
9-1
74-3
57-1
8-1
300
250
200
150
100
50
0
ENGINEERING TENSILE STRESS PSI
DYNAMIC TESTS
QUASI-STATIC TESTS
* DENOTES TEST NO.
1.0
1.1
1.2
1.3
1.4
1.5
1.6
AXIAL EXTENSION RATIO

Figure 40. Human Diaphragm Test Results, Direction of Loading Parallel to Muscle Fibers

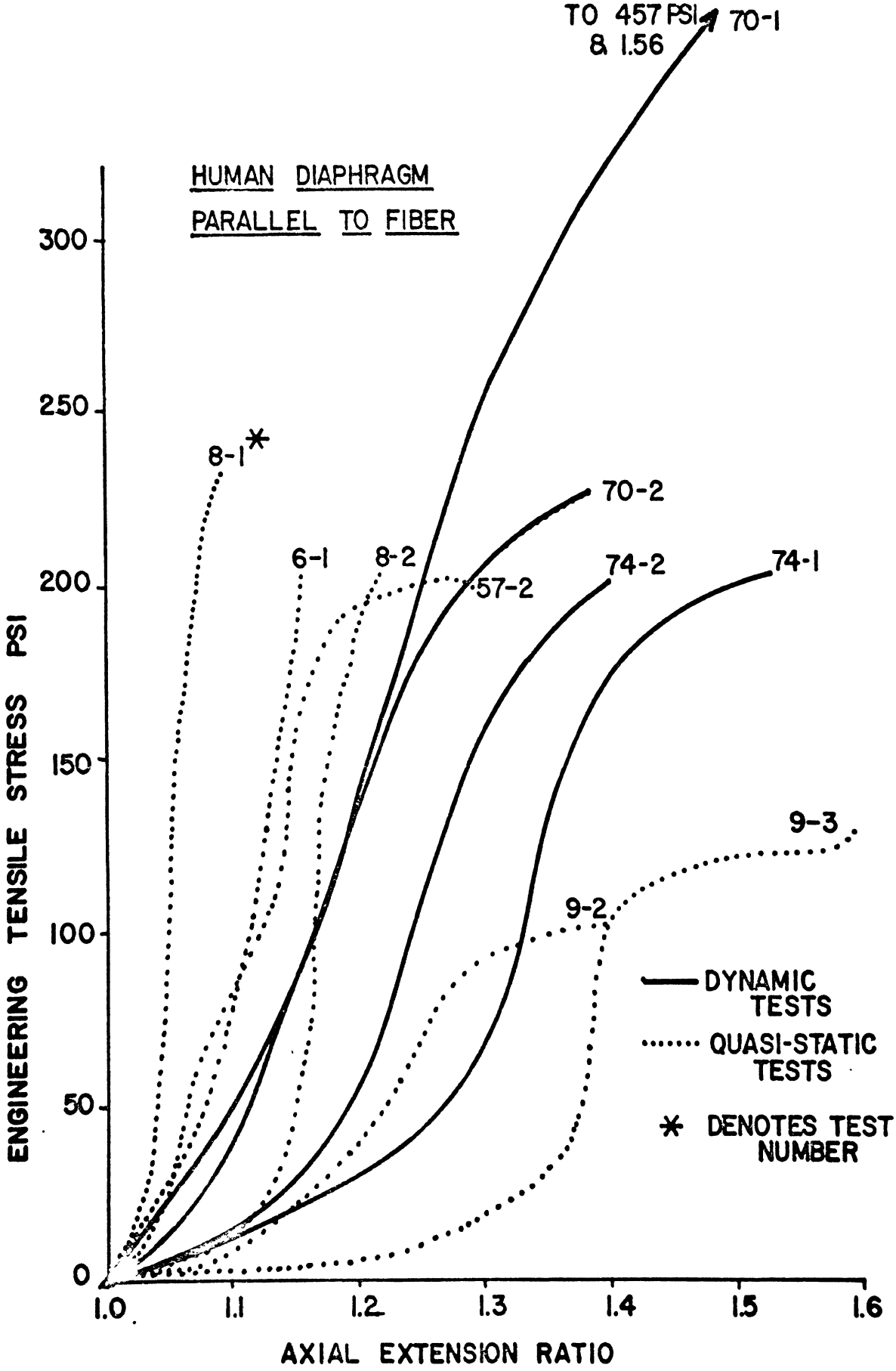
TO 457 PSI & 1.56
70-1
HUMAN DIAPHRAGM
PARALLEL TO FIBER
300
250
200
150
100
50
0
8-1*
70-2
6-1
8-2
57-2
74-2
74-1
9-3
9-2
DYNAMIC TESTS
QUASI-STATIC TESTS
* DENOTES TEST NUMBER
ENGINEERING TENSILE STRESS PSI
1.0
1.1
1.2
1.3
1.4
1.5
1.6
AXIAL EXTENSION RATIO

the major motion being a rotation about the A-P axis. These responses are shown in Figure 41. The response of the joint in the other directions of loading were similar to the response of the joint about the L-R axis in Figure 41.

5.1.8 Esophagus, Trachea and Bronchi

Only a limited number of tests on these tissues were performed. The results are shown in Figures 42 and 43. The esophagus demonstrated the usual rate sensitivity of about 100% increase in strength dynamically. Only static tests on the trachea and bronchi were performed. Due to the cartilagenus rings present in the sample, the test should really be considered a structural test rather than a basic test of the membrane between rings.

5.1.9 Rhesus Monkey Tissue Test Results

Uniaxial tension tests were performed on Rhesus monkey aorta, diaphragm and esophagus. The resulting data are shown in Figures 44, 45, 46, 47, 48 and 49. The tissues exhibited rate sensitivity comparable to the human tissues. The monkey tissues were generally stronger than the human tissues (with the exception of the esophagus) although if a comparison is made of tissue strengths based on comparable ages (i.e. the monkeys were young adults) using static data on humans from Yamada (13) the differences are not great. The main difference appears to be the generally greater extensibility of the monkey tissues.

Figure 41. Human Intervertebral Ligament Test Results, Costo-vertebral Joint Response to Superior-Inferior (Downward) Loading

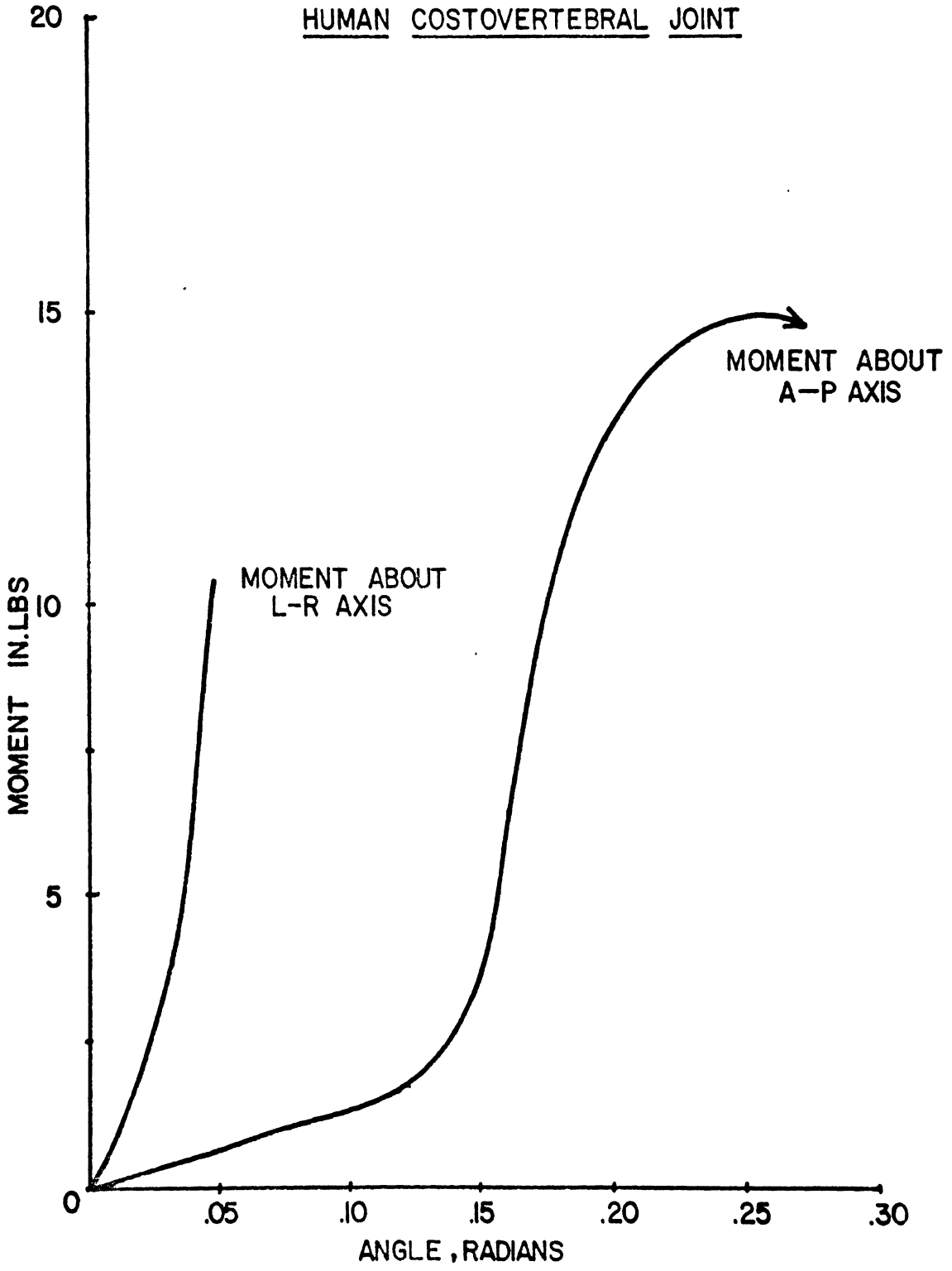
HUMAN COSTOVERTEBRAL JOINT
20
15
10
5
0
MOMENT IN.LBS
MOMENT ABOUT
L-R AXIS
MOMENT ABOUT
A-P AXIS
.05
.10
.15
.20
.25
.30
ANGLE, RADIANS

Figure 42. Human Esophagus Test Results, Direction of Loading Longitudinal to Organ

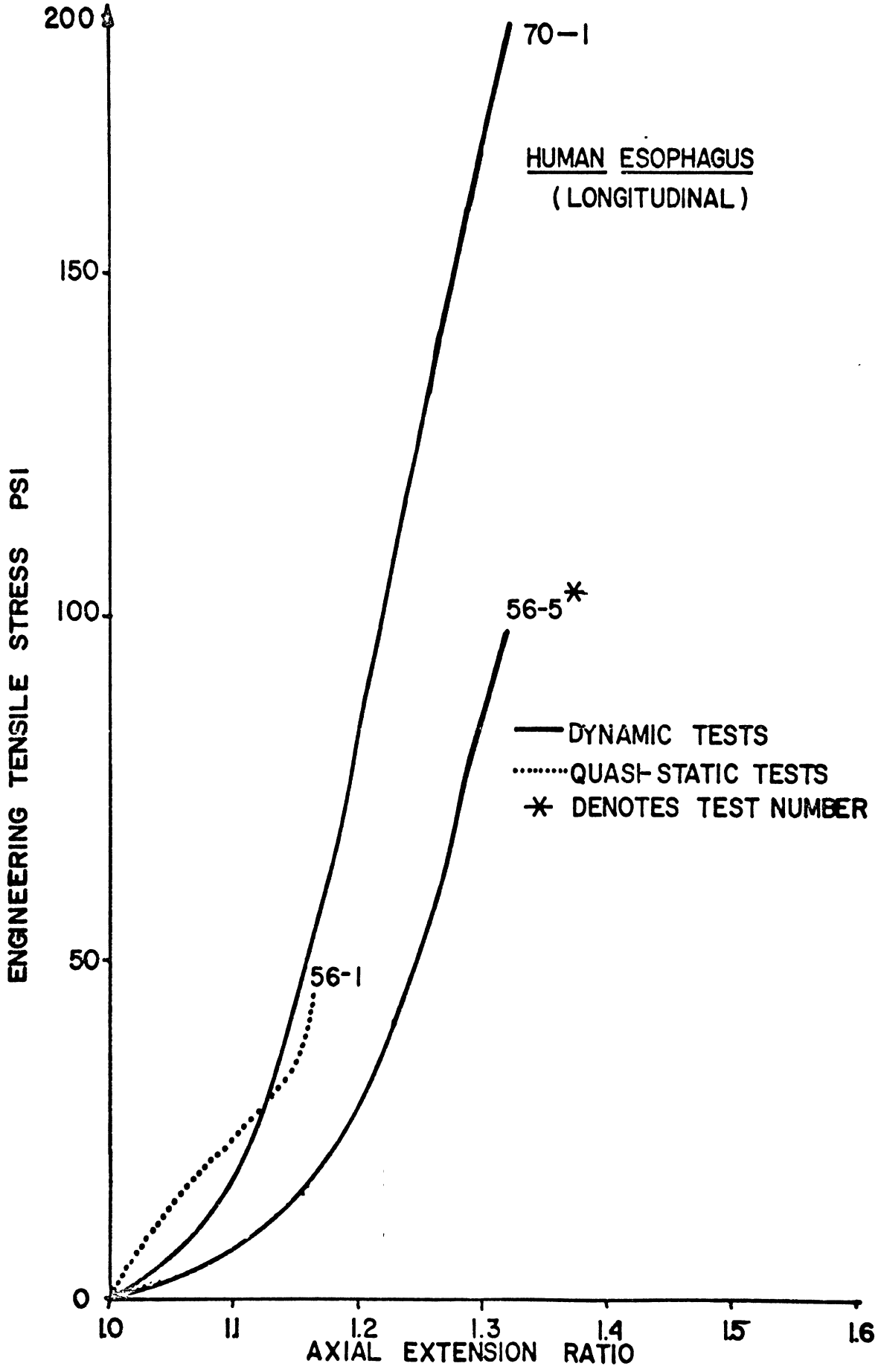
200
150
100
50
0
ENGINEERING TENSILE STRESS PSI
70-1
HUMAN ESOPHAGUS
(LONGITUDINAL)
56-5*
56-1
DYNAMIC TESTS
QUASI-STATIC TESTS
* DENOTES TEST NUMBER
1.0
1.1
1.2
1.3
1.4
1.5
1.6
AXIAL EXTENSION RATIO

Figure 43. Human Trachea and Brochus Test Results, Direction of Loading Longitudinal to Organ

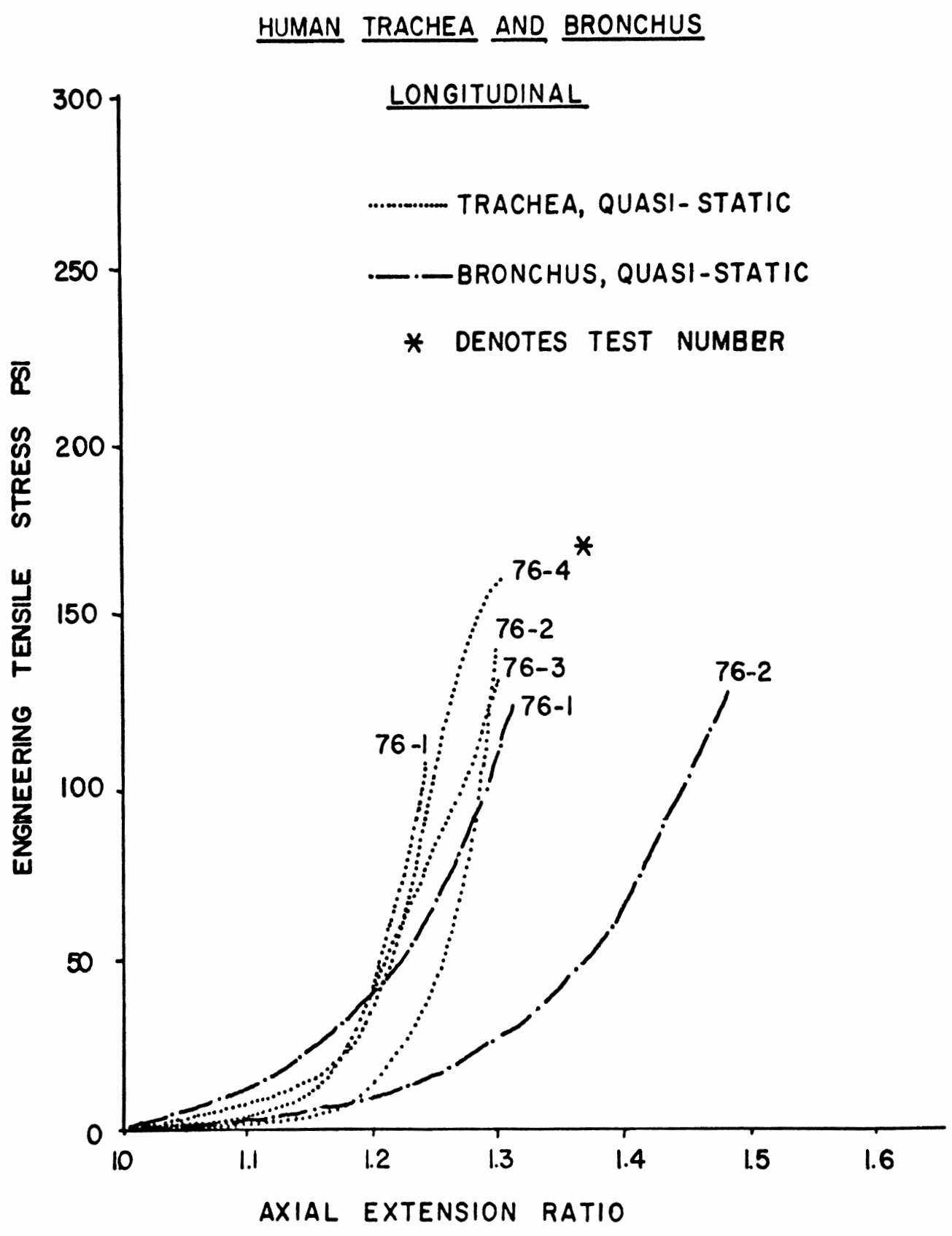
HUMAN TRACHEA AND BRONCHUS
LONGITUDINAL
TRACHEA, QUASI-STATIC
BRONCHUS, QUASI-STATIC
* DENOTES TEST NUMBER
ENGINEERING TENSILE STRESS PSI
300
250
200
150
100
50
0
76-4 *
76-2
76-3
76-1
76-1
76-2
1.0
1.1
1.2
1.3
1.4
1.5
1.6
AXIAL EXTENSION RATIO

Figure 44. Rhesus Monkey Ascending Aorta Test Results, Direction of Loading Transverse to Vessel

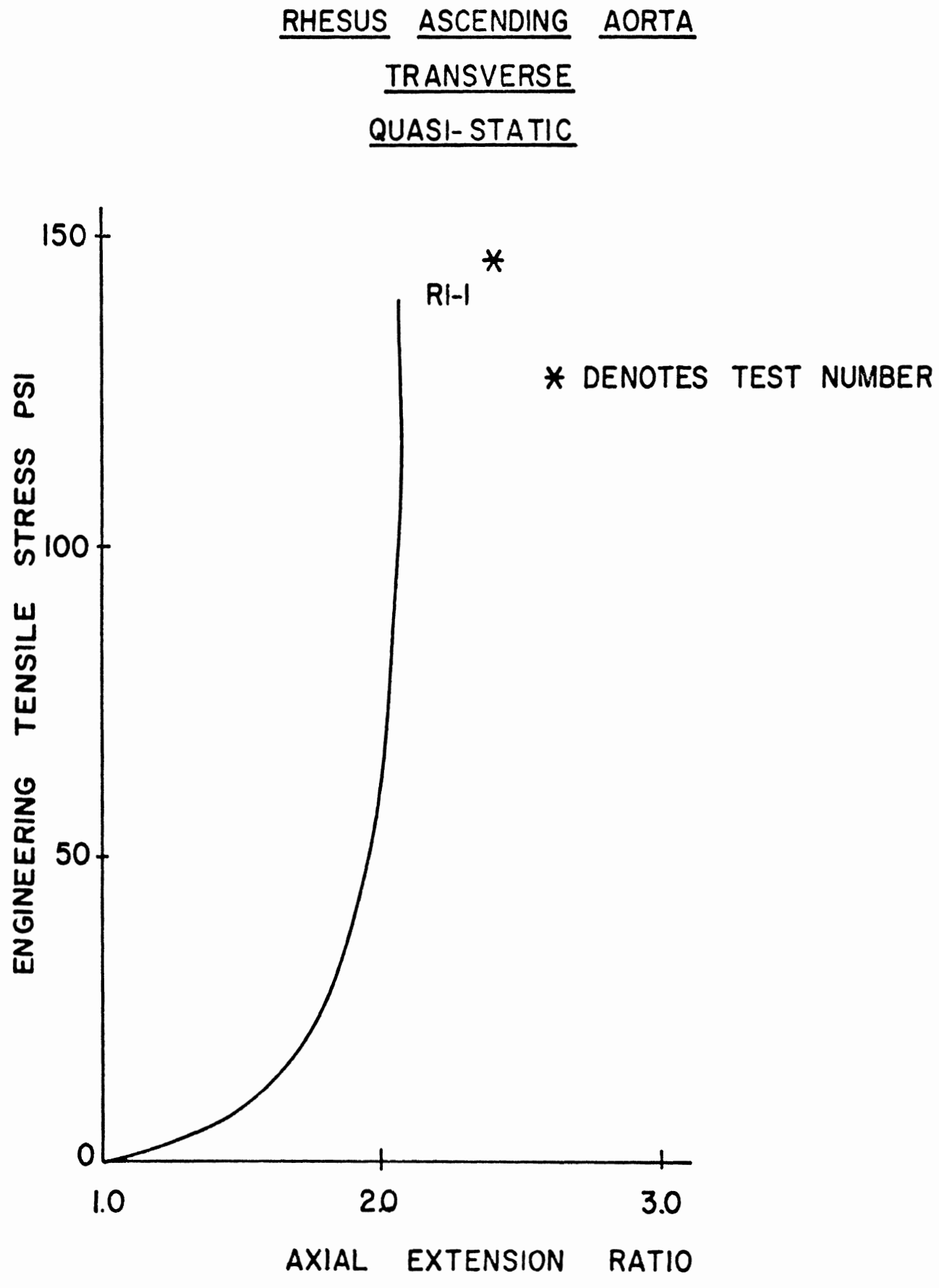
RHESUS ASCENDING AORTA
TRANSVERSE
QUASI-STATIC
150
100
50
0
RI-1
* DENOTES TEST NUMBER
ENGINEERING TENSILE STRESS PSI
1.0
2.0
3.0
AXIAL EXTENSION RATIO

Figure 45. Rhesus Monkey Descending Aorta Test Results, Direction of Loading Longitudinal to Vessel

RHESUS DESCENDING AORTA

LONGITUDINAL

QUASI-STATIC

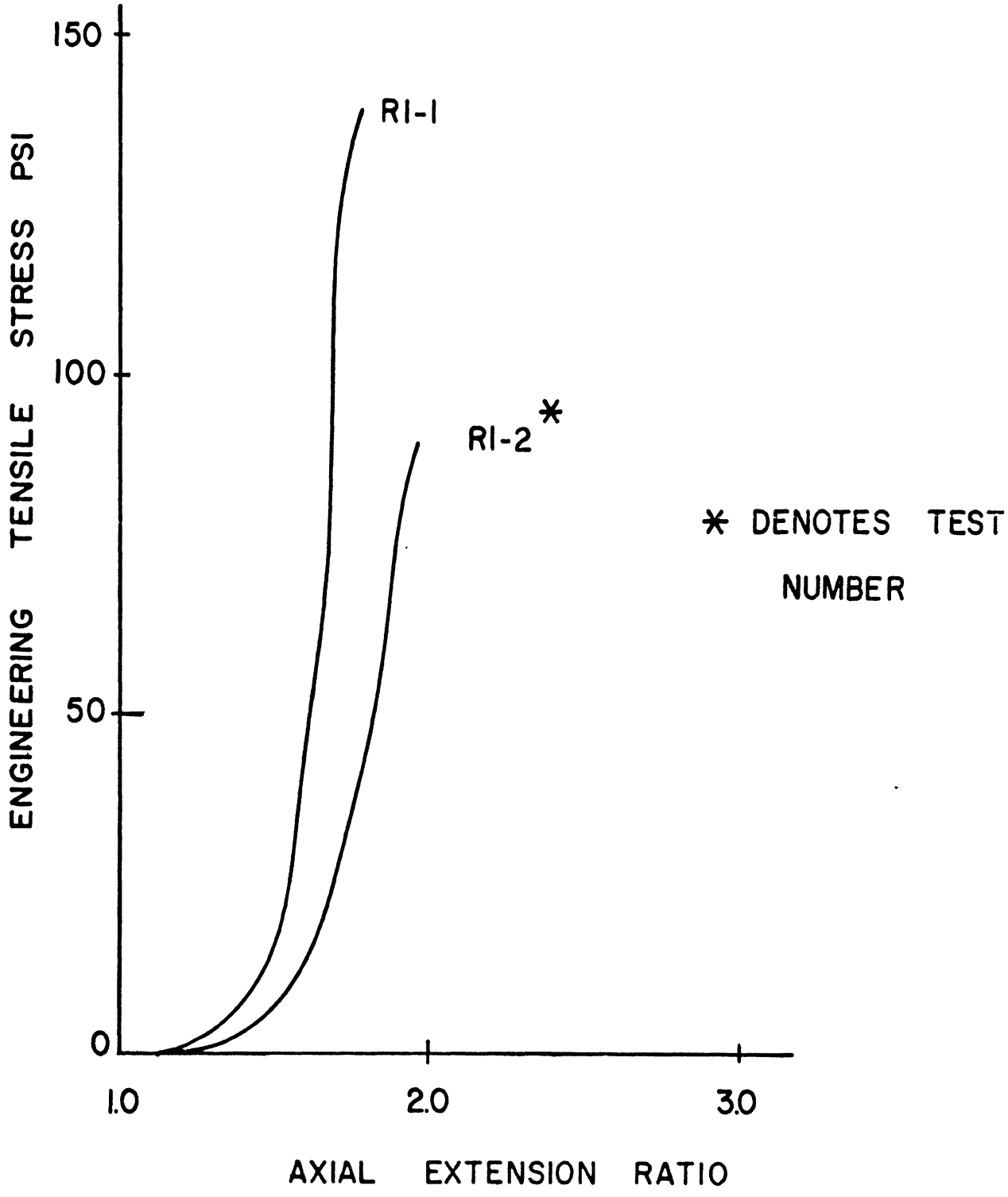

Figure 46. Rhesus Monkey Descending Aorta Test Results, Direction of Loading Transverse to the Vessel

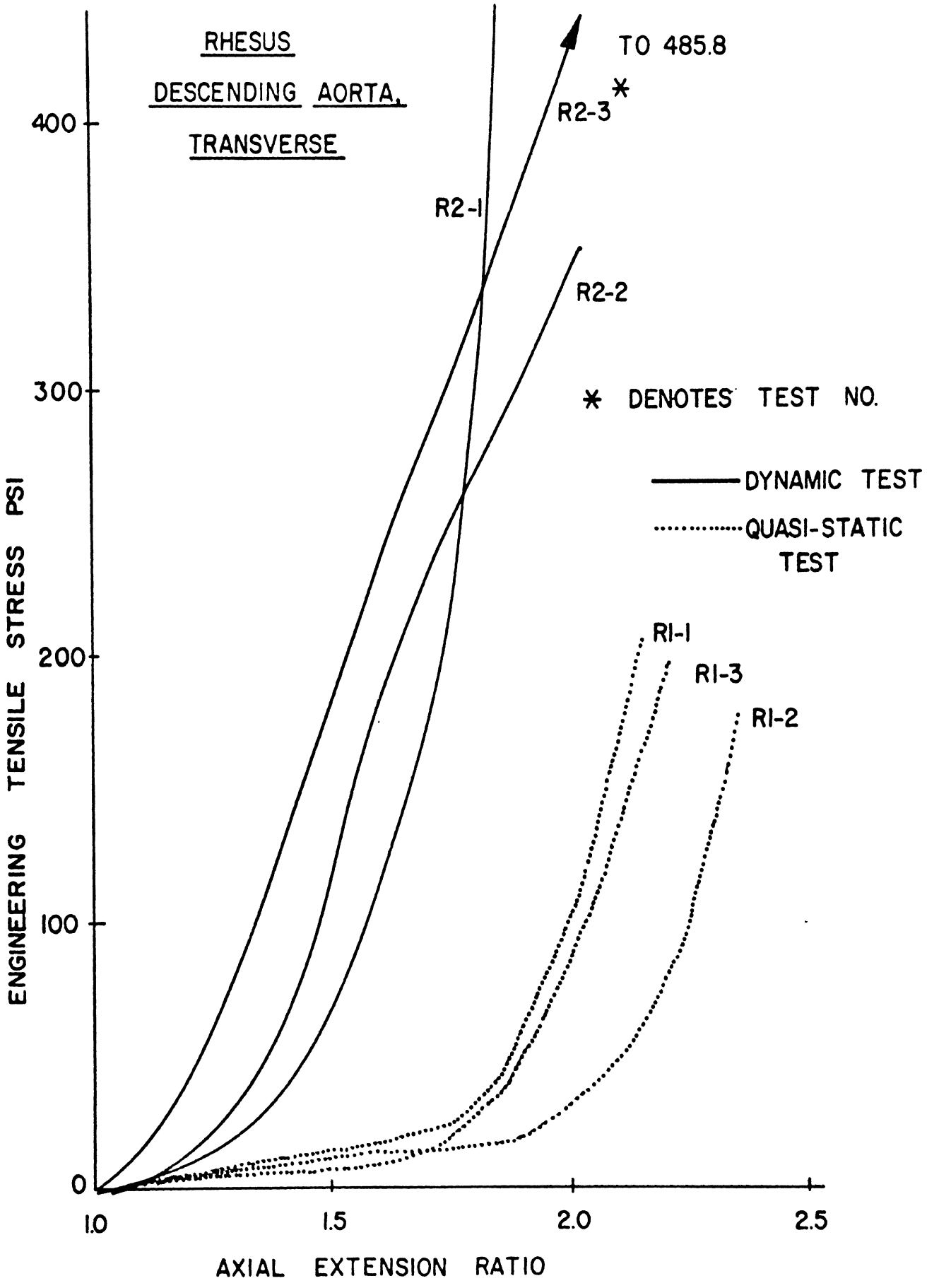
RHESUS
DESCENDING AORTA,
TRANSVERSE
TO 485.8
R2-3
R2-1
R2-2
* DENOTES TEST NO.
DYNAMIC TEST
QUASI-STATIC TEST
RI-1
RI-3
RI-2
400
300
200
100
0
1.0
1.5
2.0
2.5
ENGINEERING TENSILE STRESS PSI
AXIAL EXTENSION RATIO

Figure 47. Rhesus Monkey Diaphragm Test Results

RHESUS DIAPHRAGM, QUASI-STATIC

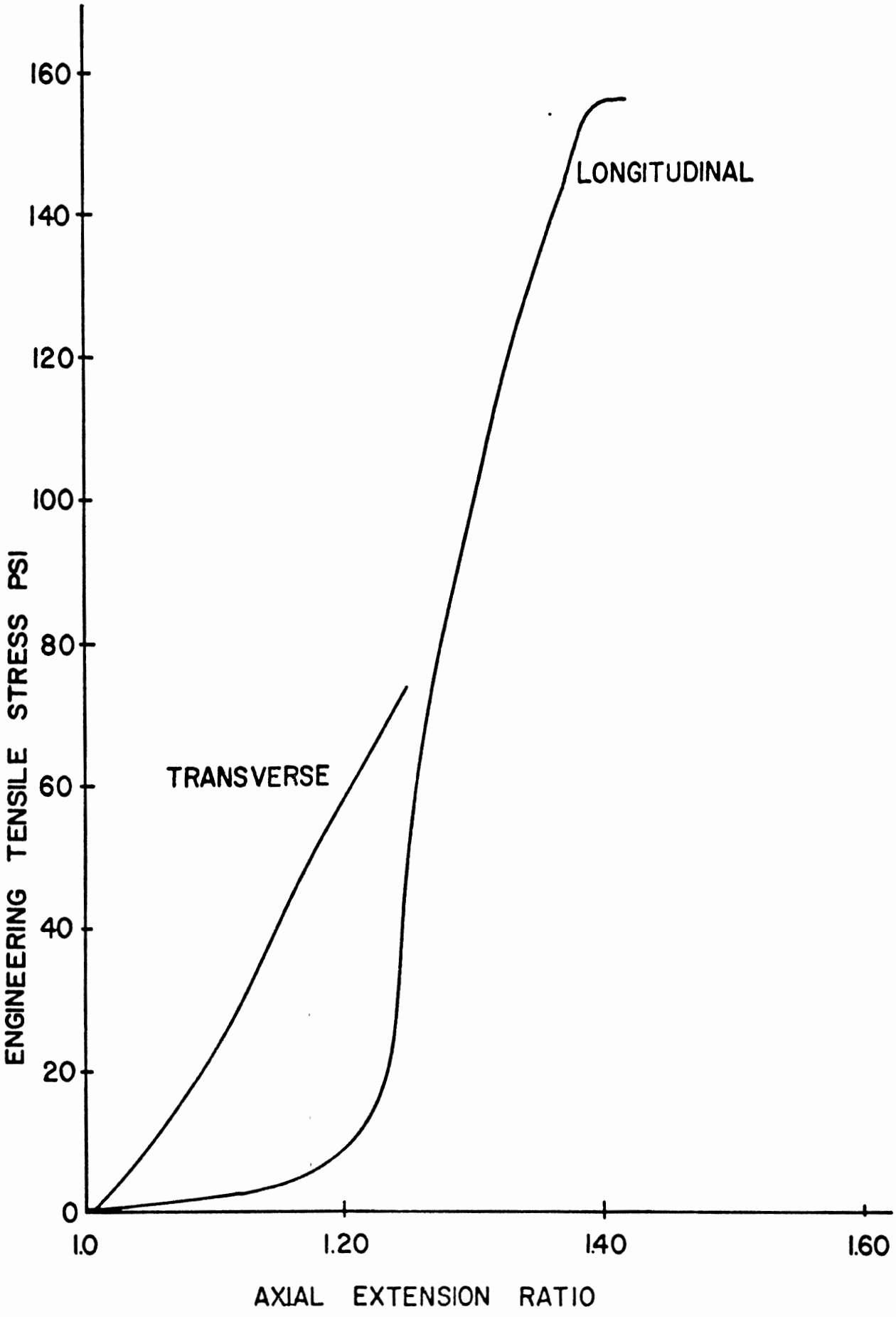

Figure 48. Rhesus Monkey Esophagus Test Results, Direction of Loading Longitudinal to Organ

RHESUS ESOPHAGUS

LONGITUDINAL, QUASI-STATIC

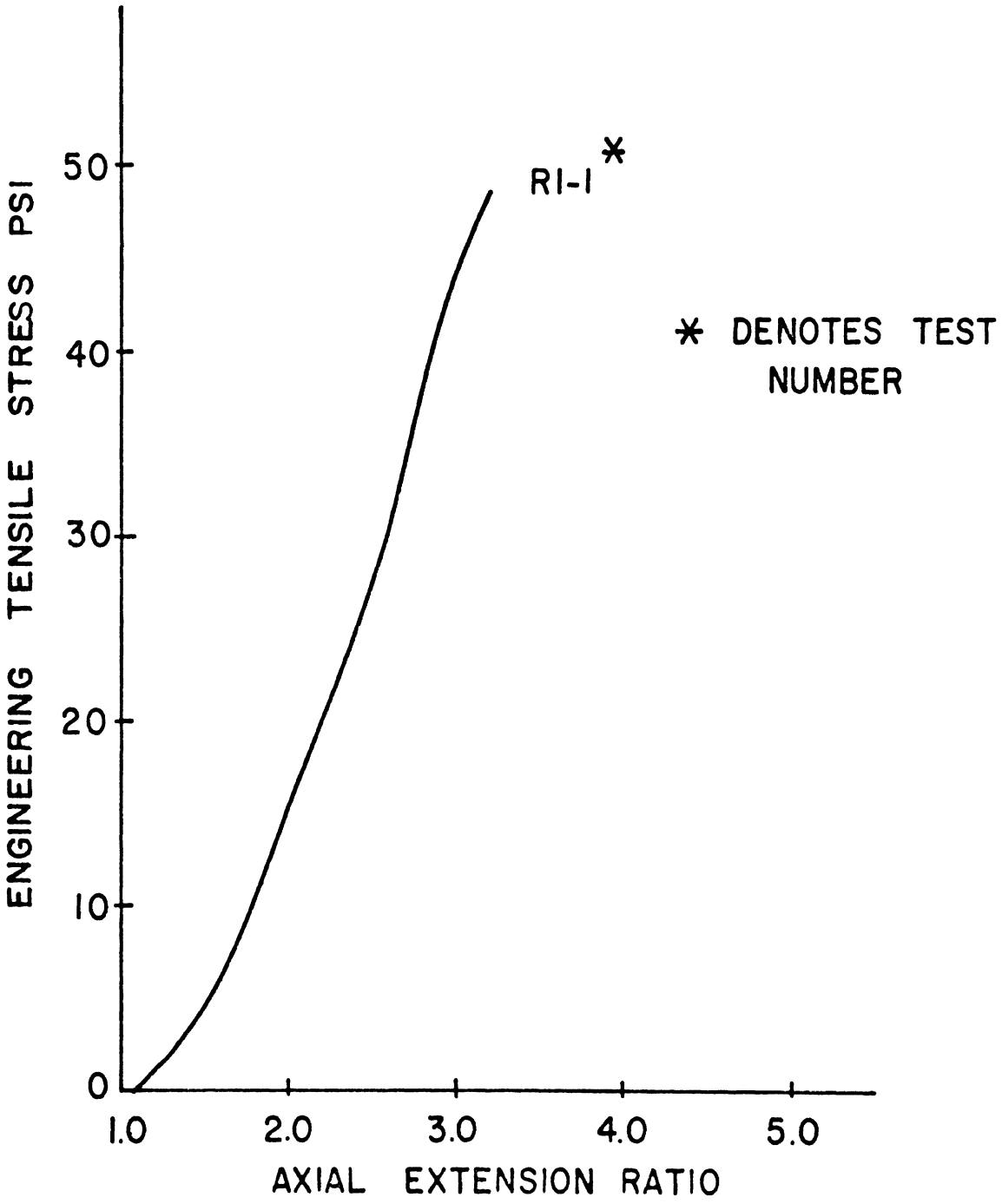

Figure 49. Rhesus Monkey Esophagus Test Results, Direction of Loading Transverse to the Organ

RHESUS ESOPHAGUS, TRANSVERSE

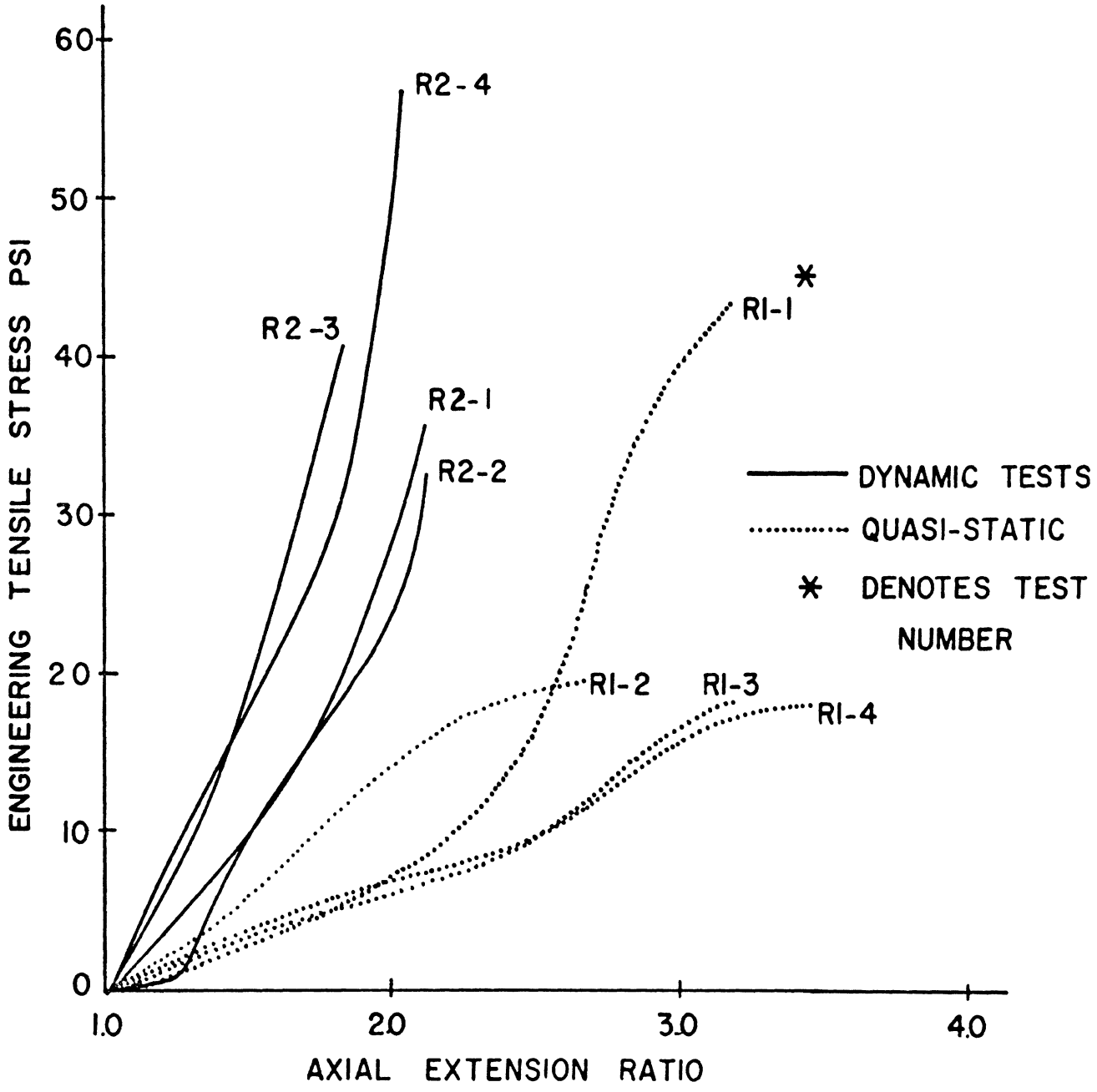

6.0 SUMMARY AND CONCLUSIONS

6.1 General Program Summary

This program has produced a bibliography of over 500 entries on the subjects of soft tissue mechanical properties and test techniques. The majority of these articles have been abstracted and are presented in Volume III of this report.

The knowledge obtained in performing the literature search has been incorporated into the experimental program carried out in this project. Test techniques on soft tissue testing have been specially adapted to the needs of the experimental program and unique test equipment developed to allow high speed dynamic testing of tissue samples in uniaxial tension and biaxial tension. The data produced this project on the dynamic mechanical properties of thoracic tissues of the human and the Rhesus monkey are unique and represent the first time that these tissues have been characterized at strain rates comparable to those produced in thoracic trauma associated with automotive accidents.

While the data presented here by no means represents a complete description of the tissues tested, either in the statistical sense or in the continuum mechanics sense, the data does represent a definitive first step in characterizing the dynamic behavior of these tissues and their failure mechanisms.

6.1.1 Test Results Summary

Examination of the test results in Section 5.0 reveals that the stress-strain response of the tissues varies over a wide range. In order to summarize the response for each tissue to provide average response curves the following reduction technique was used. First, it was noted that the major cause of the variability in response in most tissues was the different extensibility

exhibited by each tissue in the low stress region. Following the lead of other investigators in soft tissue research (1,2) this high extension, low stress region of the curves was treated as a region separate from the stiffer high stress response region, since, in many cases, the pathological conditions found in these tissues manifests itself primarily in the low stress region (e.g. in atherosclerosis (hardening of the arteries) the main effect is the loss of this low stress extensibility while high stress response appears to be relatively unaffected.). In the analysis of the uniaxial tension test data an arbitrary stress level of 20 psi was used to define the upper limit of the low stress region (this corresponds to a typical wall stress in the aorta under physiological conditions). All dynamic stress-extension ratio curves for a particular tissue and loading direction were compared above this stress level by graphically shifting the curves to the $\lambda = 1.00$ point. This shift produced response curves which were generally quite similar. (This is most likely due to the fact that the high stress response of the tissues is controlled by the oriented collagenous connective tissue present in the tissue. This orientation process occurs during the low stress extension.) In order to produce a representative curve for the tissue response the resulting shifted high stress curves where averaged by dividing each curve into four proportional regions represented by the quarter point, the midpoint, the three quarter point and the failure end point. The resulting stress and extension ratio values for those four points were respectively averaged for all the curves of a given type and the average curve plotted. Similarly, the extension ratios for each curve at the 20 psi level were averaged and an average low stress region added graphically to the average high stress response.

Figure 50. Summary Curve of Average Dynamic Response of Human Intercostal Muscle

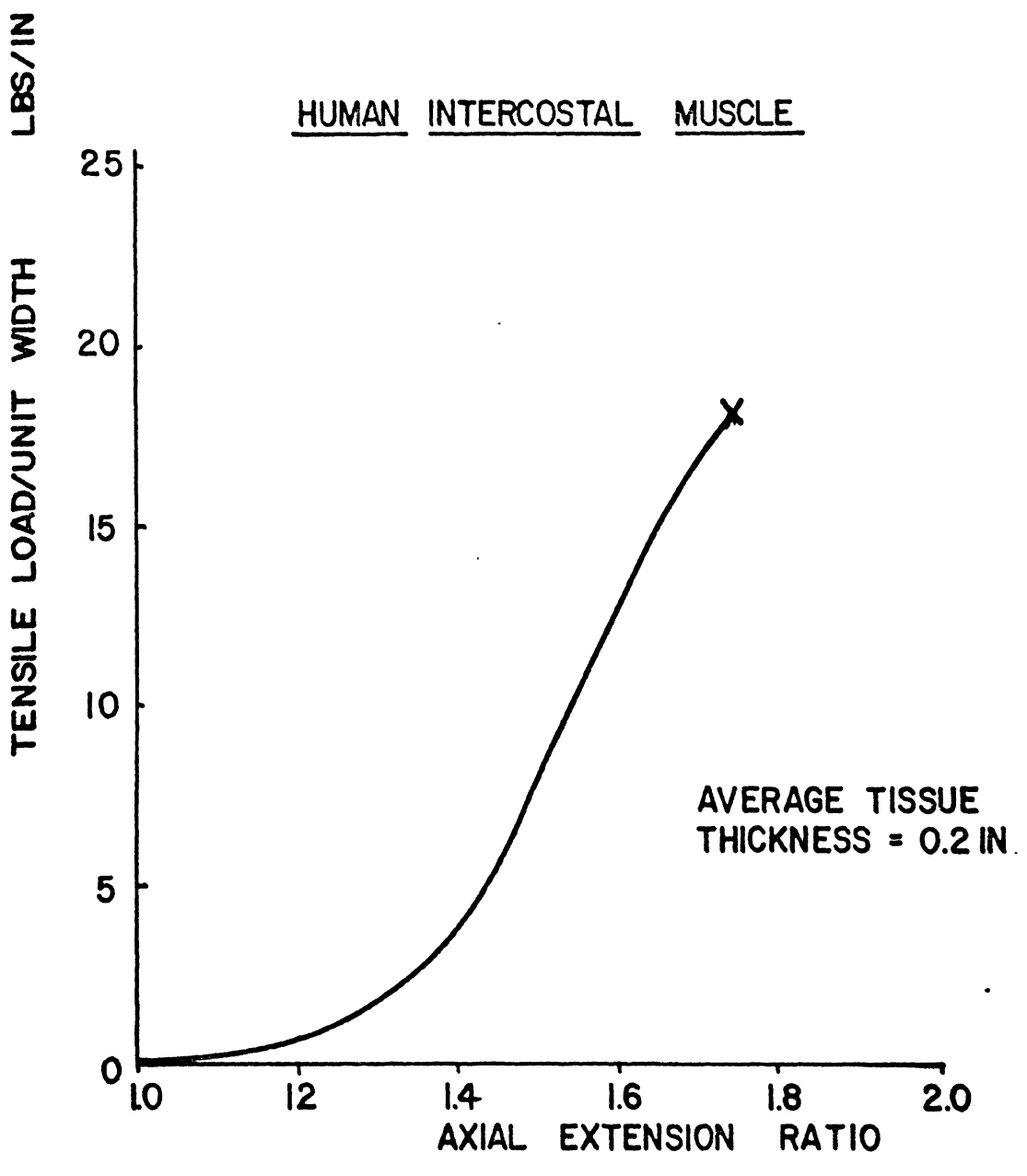
HUMAN INTERCOSTAL MUSCLE
TENSILE LOAD/UNIT WIDTH LBS/IN
25
20
15
10
5
0
1.0
1.2
1.4
1.6
1.8
2.0
AXIAL EXTENSION RATIO
AVERAGE TISSUE
THICKNESS = 0.2 IN.

Figure 51. Summary Curves of Average Dynamic Responses of Human Cardiac Muscle

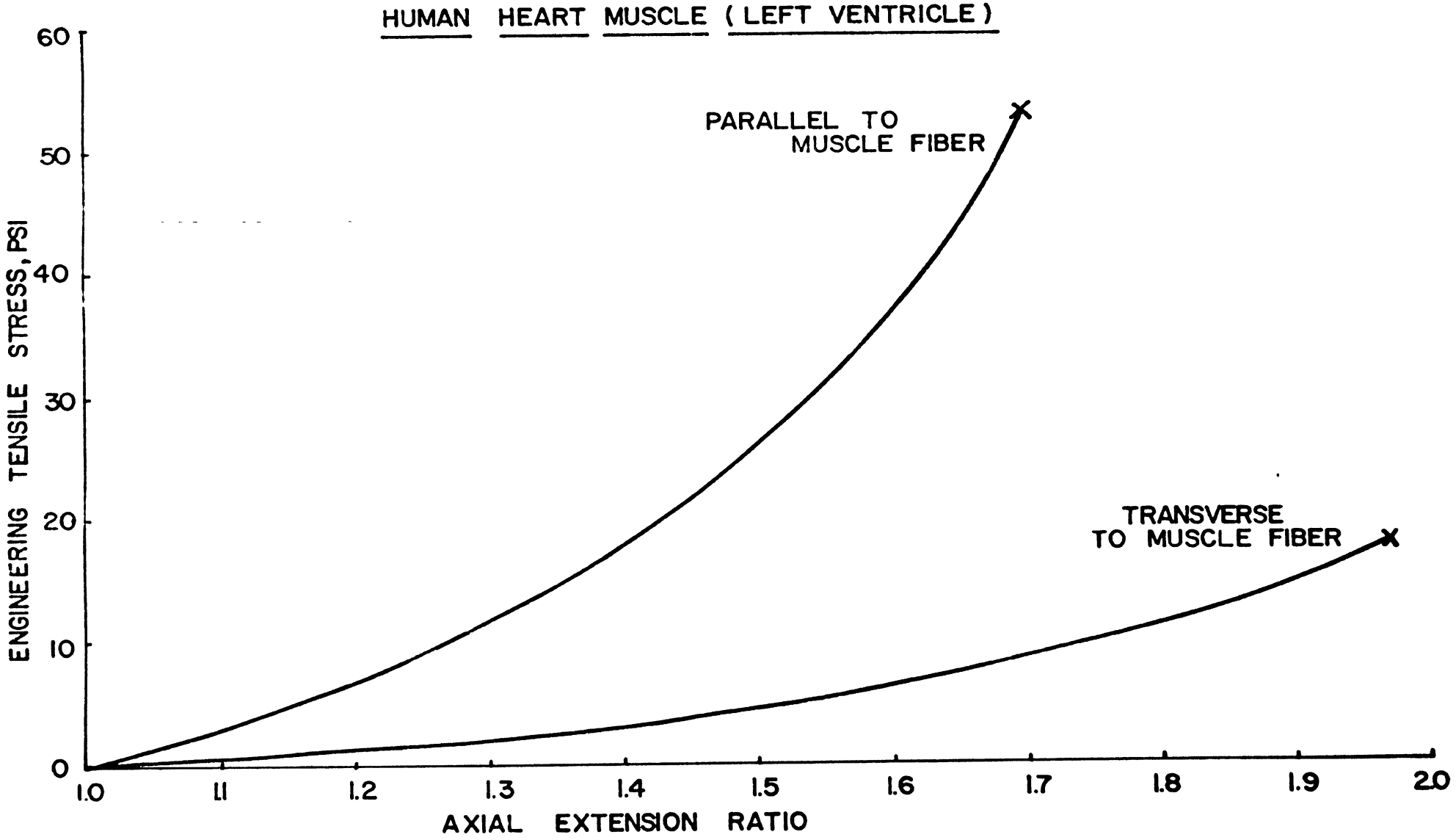
HUMAN HEART MUSCLE (LEFT VENTRICLE)
PARALLEL TO MUSCLE FIBER
TRANSVERSE TO MUSCLE FIBER
ENGINEERING TENSILE STRESS, PSI
60
50
40
30
20
10
0
1.0
1.1
1.2
1.3
1.4
1.5
1.6
1.7
1.8
1.9
2.0
AXIAL EXTENSION RATIO

Figure 52. Summary Curve of Average Dynamic Response of Human Aorta in the Longitudinal Direction

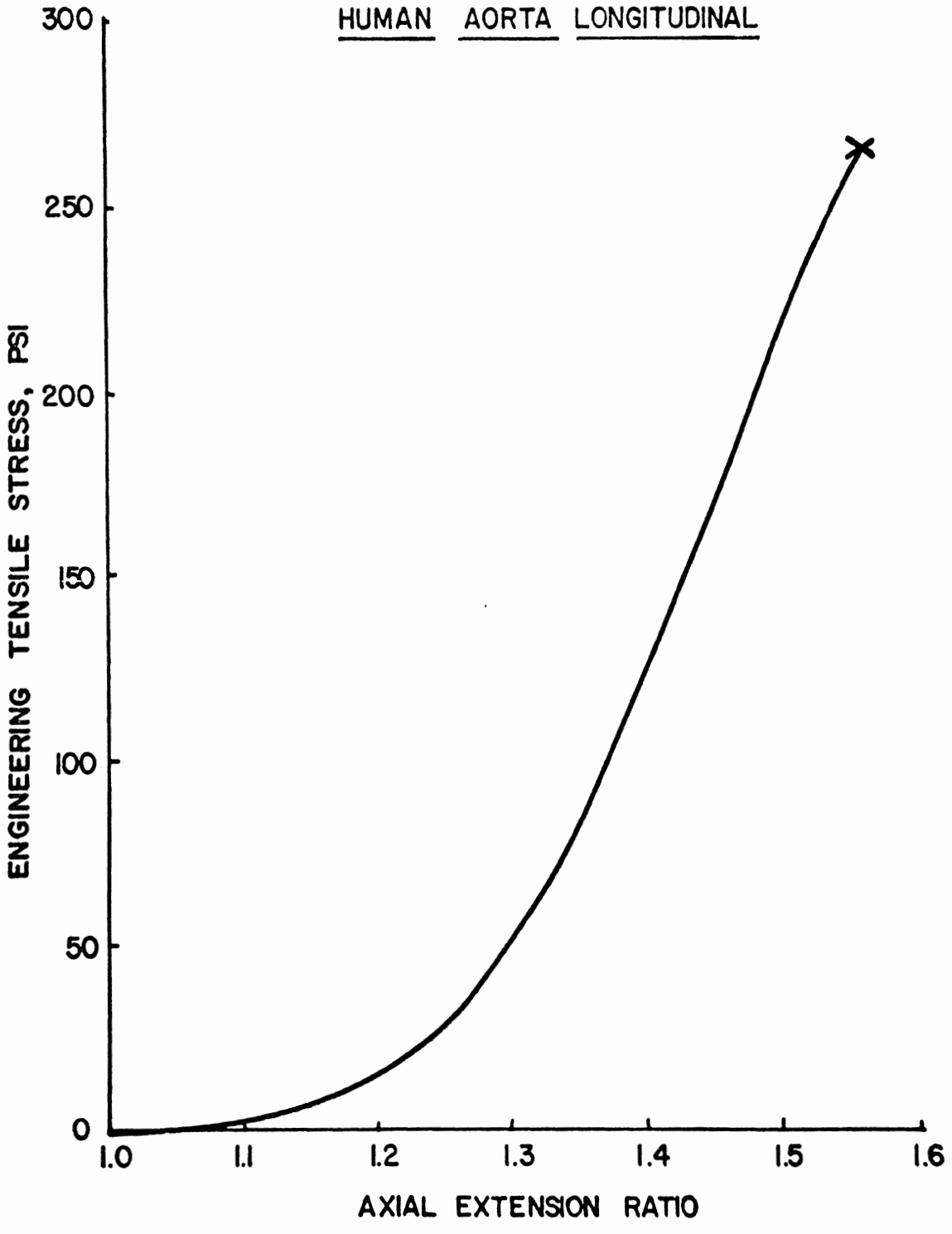
HUMAN AORTA LONGITUDINAL
300
250
200
150
100
50
0
ENGINEERING TENSILE STRESS, PSI
1.0
1.1
1.2
1.3
1.4
1.5
1.6
AXIAL EXTENSION RATIO

Figure 53. Summary Curve of Average Dynamic Response of Human Aorta in the Transverse Direction

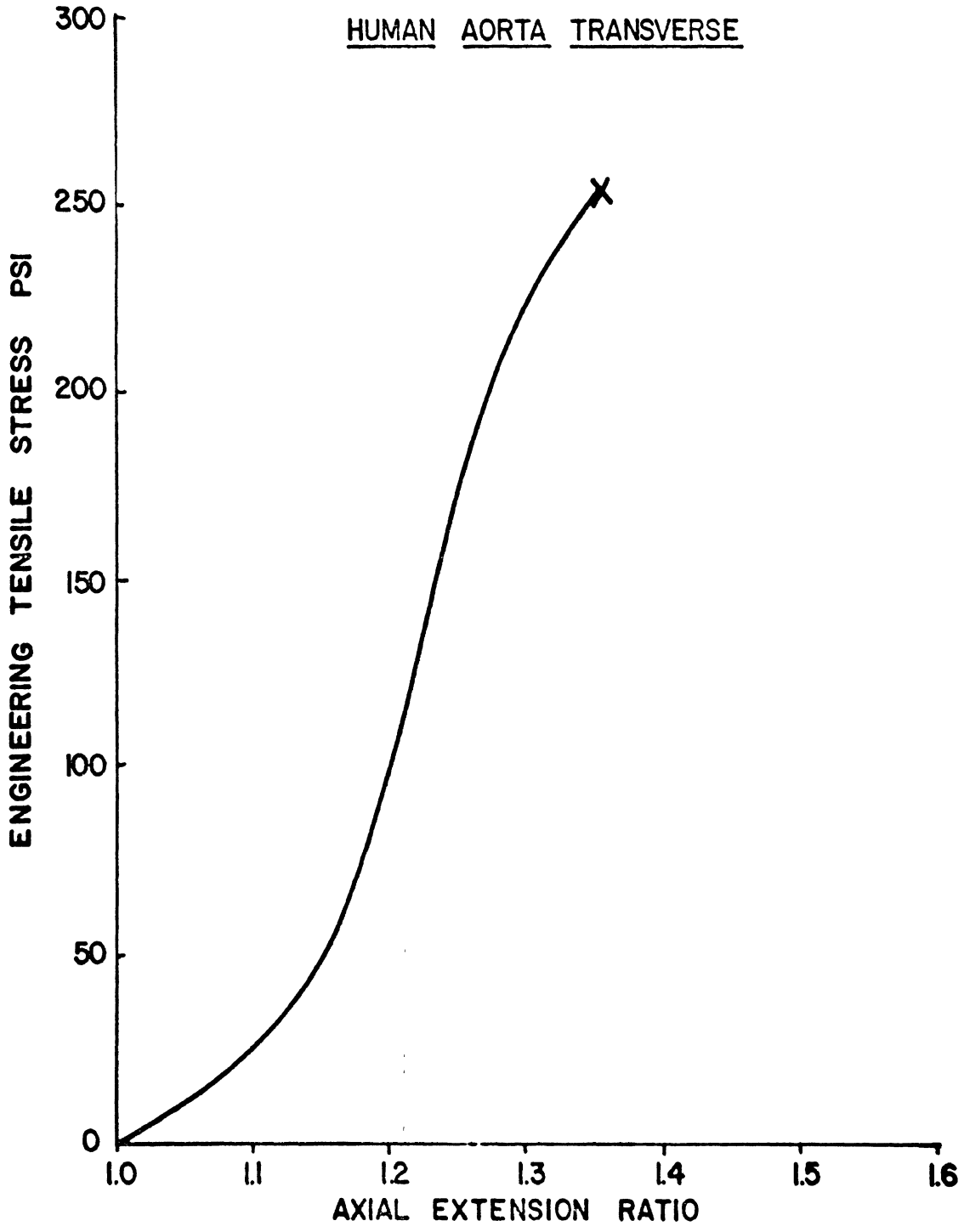
HUMAN AORTA TRANSVERSE
ENGINEERING TENSILE STRESS PSI
300
250
200
150
100
50
0
1.0
1.1
1.2
1.3
1.4
1.5
1.6
AXIAL EXTENSION RATIO

Figure 54. Summary Curve of Dynamic Response of Human Pericardium

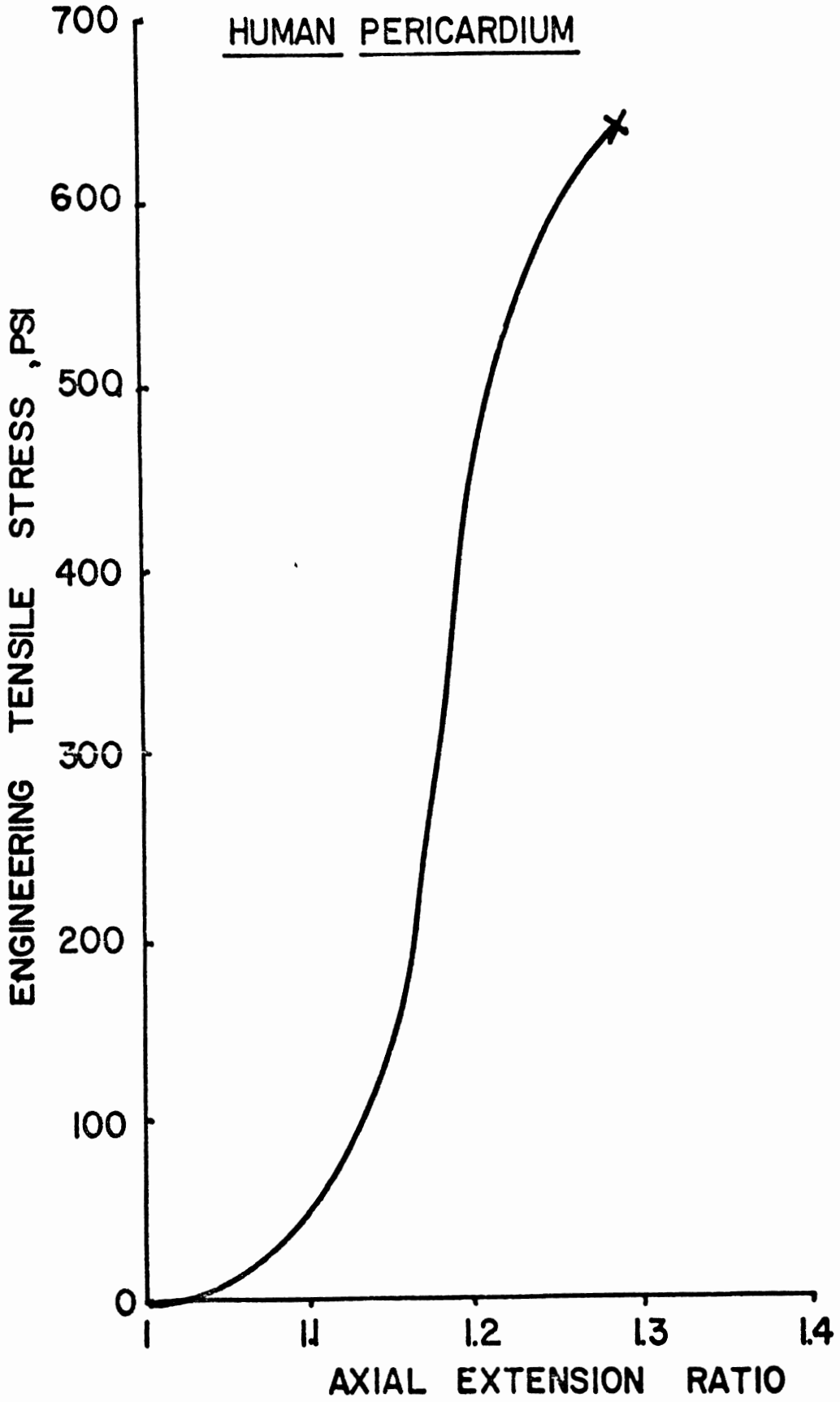
HUMAN PERICARDIUM
700
600
500
400
300
200
100
0
ENGINEERING TENSILE STRESS, PSI
1
1.1
1.2
1.3
1.4
AXIAL EXTENSION RATIO

Figure 55. Summary Curve of Average Dynamic Response of Human Diaphragm Across Muscle Fibers

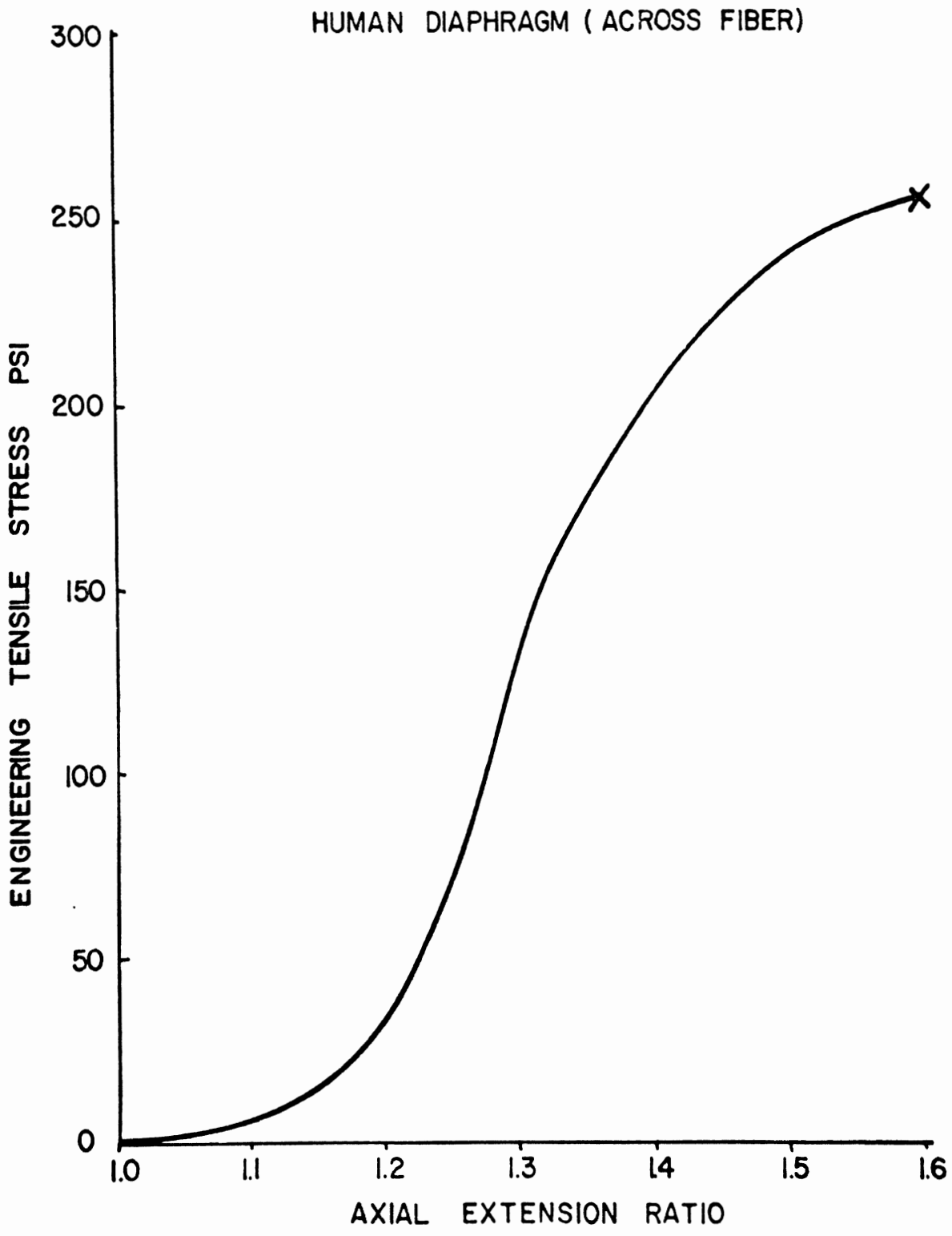
HUMAN DIAPHRAGM (ACROSS FIBER)
ENGINEERING TENSILE STRESS PSI
300
250
200
150
100
50
0
1.0
1.1
1.2
1.3
1.4
1.5
1.6
AXIAL EXTENSION RATIO

Figure 56. Summary Curve of Average Dynamic Response of Human Diaphragm Parallel to Muscle Fibers

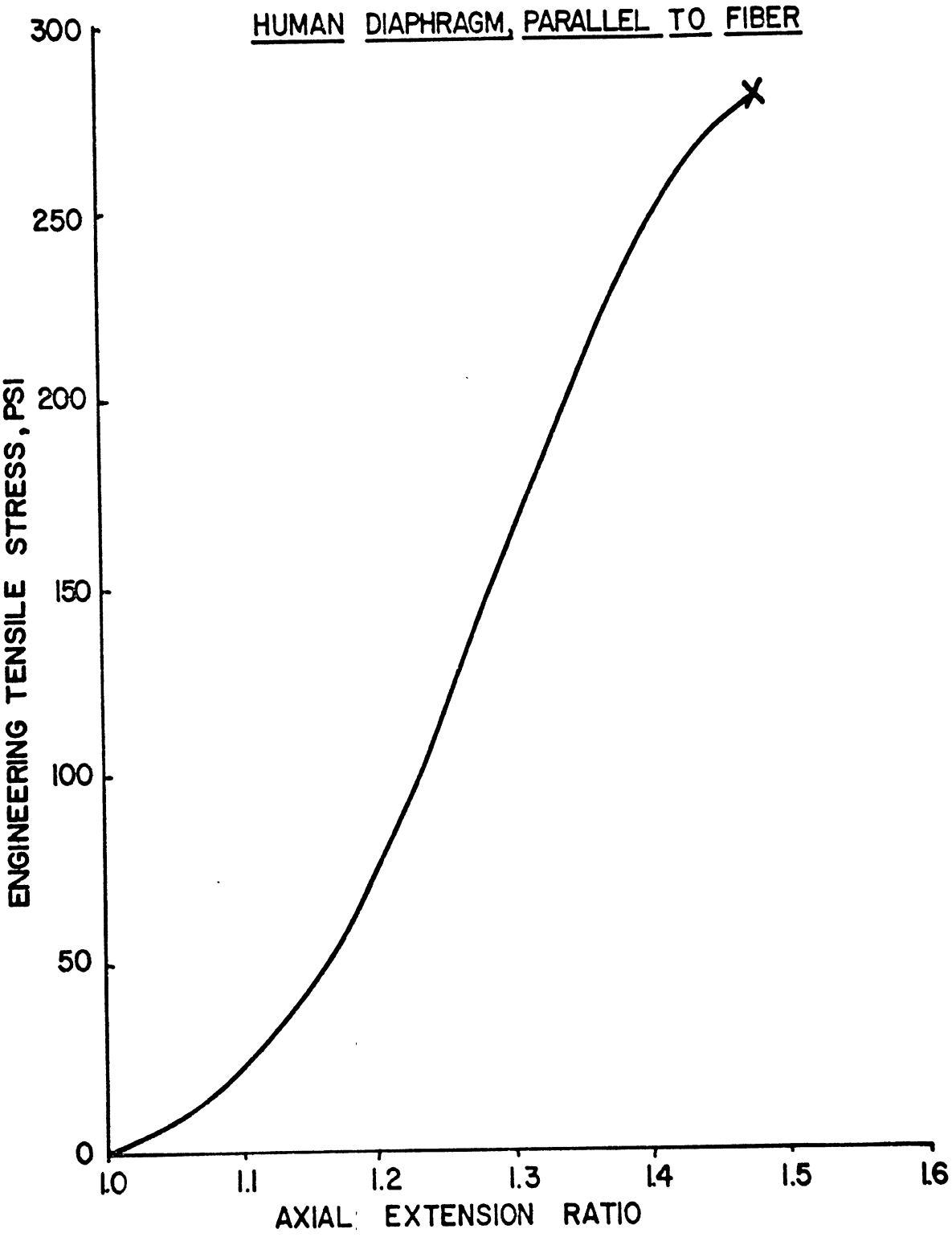
HUMAN DIAPHRAGM, PARALLEL TO FIBER
300
250
200
150
100
50
0
ENGINEERING TENSILE STRESS, PSI
1.0
1.1
1.2
1.3
1.4
1.5
1.6
AXIAL EXTENSION RATIO

Figure 57. Summary Curve of Average Dynamic Response of Human Esophagus in the Longitudinal Direction

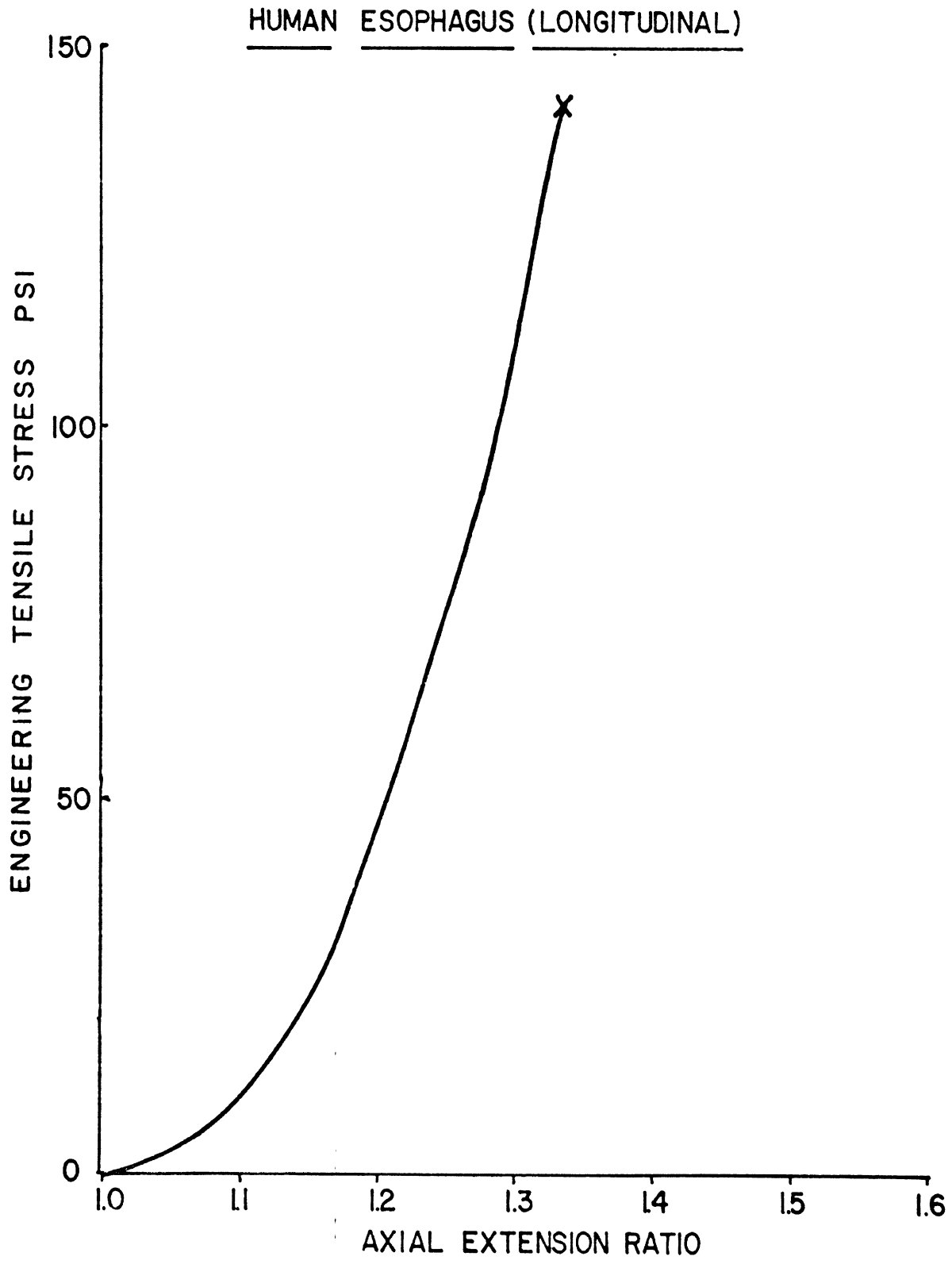
HUMAN ESOPHAGUS (LONGITUDINAL)
150
100
50
0
ENGINEERING TENSILE STRESS PSI
1.0
1.1
1.2
1.3
1.4
1.5
1.6
AXIAL EXTENSION RATIO

Figure 58. Summary curve of Average Dynamic Response of Rhesus Monkey Descending Aorta in the Transverse Direction

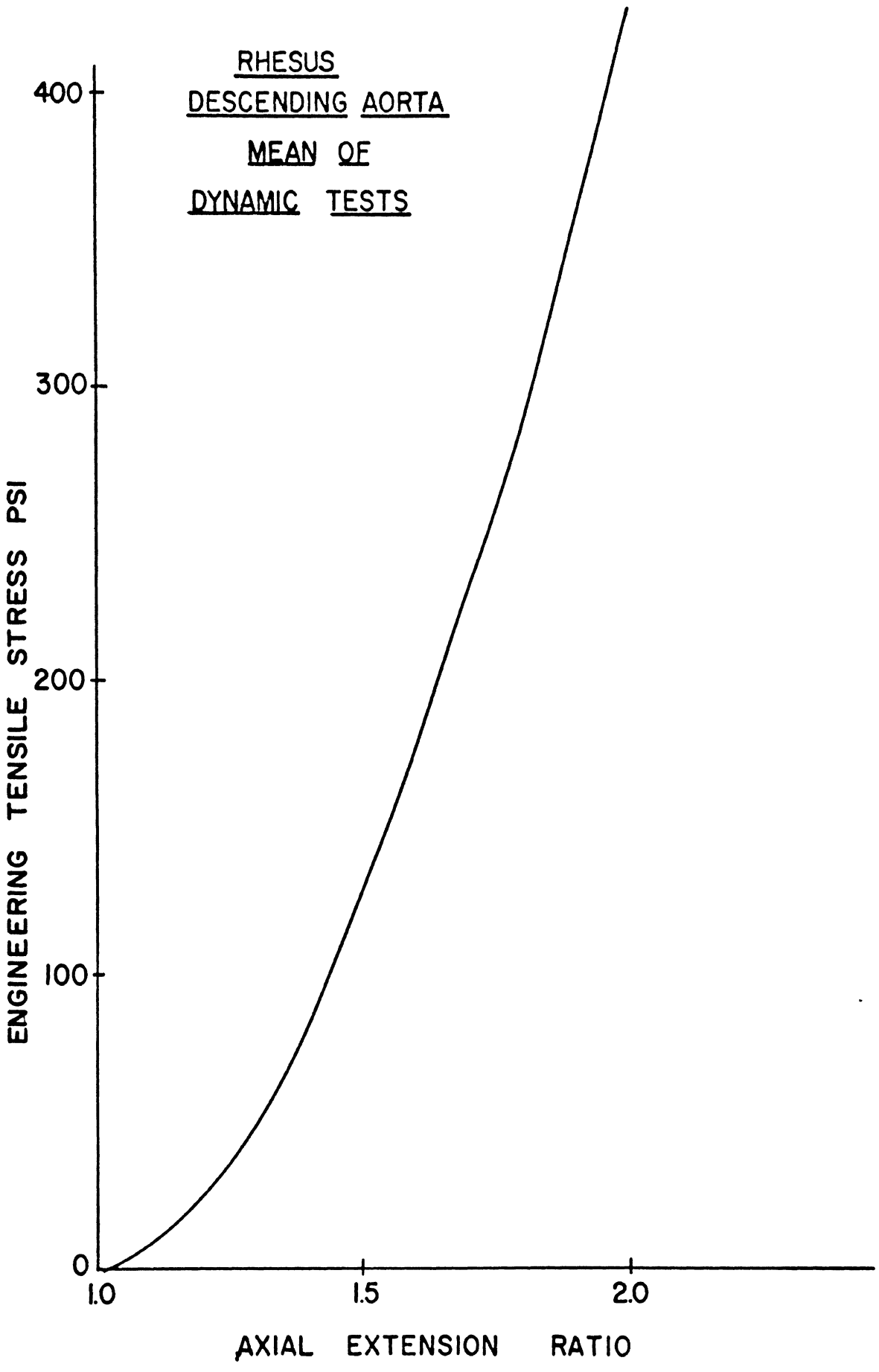
RHESUS
DESCENDING AORTA
MEAN OF
DYNAMIC TESTS
400
300
200
100
0
ENGINEERING TENSILE STRESS PSI
1.0
1.5
2.0
AXIAL EXTENSION RATIO

Figure 59. Summary Curve of Average Dynamic Response of Rhesus Monkey Esophagus in the Transverse Direction

RHESUS ESOPHAGUS, MEAN OF DYNAMIC TESTS

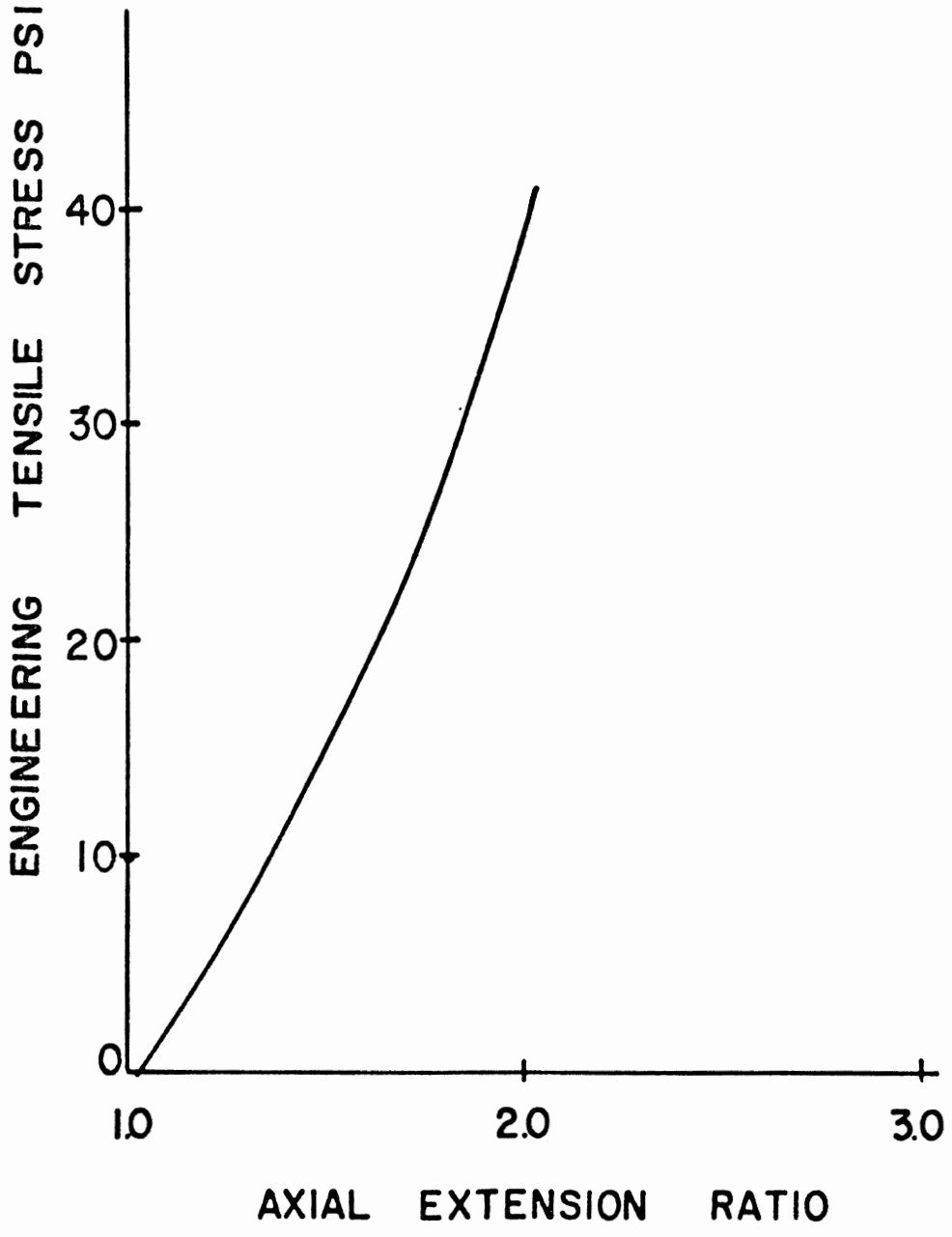

The resulting average dynamic response curves for human intercostal muscle, cardiac muscle, aorta, pericardium, diaphragm and esophagus are shown in Figures 50, 51, 52, 53, 54, 55, 56, and 57. Similar curves for Rhesus monkey aorta and esophagus are shown in figures 58 and 59. Tabular descriptions of these curves are found in Table 2 for human tissues and Table 3 for Rhesus tissues. Also listed in the tables is the calculated true stress based on the assumption of constancy of volume (incompressibility) of the material during deformation. The assumption of incompressibility was checked on many of the tissue tests when good values of thickness extension ratios could be obtained and, in general, the product of the three principal extension ratios was within 10% of unity (i.e. $\lambda_1\lambda_2\lambda_3 = 1$ implies incompressibility). In view of the limited statistical nature of the data obtained on any one tissue and the limited number of different strain rates used in the testing program it is felt that any attempts to fit a constitutive relation to describe the behavior of any of the tissues would be ill-advised. Only with a more detailed long term study of each tissue could a statistically valid constitutive relation be generated. For the purposes of providing data for the FIRL modelling program it is felt that the tabular summary data in Tables 2 and 3 are most appropriate at this time.

Comparison of the dynamic response of the tissues tested with the static tests performed in the program and with the static data of Yamada (13) indicates that although the dynamic stesses produced in the tissues are as much as twice as great as those produced statically the failure strains tend to be similar. This leads to the conclusion that the most appropriate failure mechanism theory for the tissues studied in the program would be a maximum tensile strain theory of failure. This is born out in the biaxial

tension tests of the human diaphragm where the failure strains were similar to the uniaxial tension failure strains. It should be noted, however, that the pathological state of many of the tissues tested reflects the older age group (average age 69.5 years). The static failure strains obtained in the program are comparable to those obtained in the older age groups reported by Yamada (13) and thus, for younger people larger failure strains would be expected.

6.2. Conclusions and Recommendations

The results of this program to obtain information on the mechanical properties of thoracic tissues at high strain rates indicate that the dynamic response of such tissues is considerably different from the static response in terms of stress, but that the strain response is more dependent upon pathological condition of the tissues than upon strain rate. While the scope of the program was not large enough to permit a complete statistical and continuum mechanics representation of each of the nine tissue types studied, the information developed in the program will be of direct use in finite element modelling of the thorax and in helping to understand more clearly the injury mechanisms associated with thoracic trauma. In this connection it would appear that a maximum tensile strain theory of failure would be most appropriate to describe the failure mechanisms observed in many of the tissues studied in the program.

The work carried out in the program must be considered as an initial step towards the complete characterization of the response and failure of thoracic organ tissues. Work should be continued in the future to include a more complete quantification of anisotropy effects and multiaxial load response, to include a more complete statistical quantification of variations in tissue properties due to sex, age and/or physical condition; and to include

the quantification of the effects of physiological deformation states on tissue response and injury modes. Consideration should also be given to extending this type of study to other injury prone areas of the body.

TABLE 2 TABULAR SUMMARY OF AVERAGE DYNAMIC RESPONSE OF HUMAN TISSUES

INTERCOSTAL MUSCLE, PERPENDICULAR TO THE RIBS, AVERAGE DYNAMIC RESPONSE MEAN THICKNESS = 0.2 in.

LOAD/UNIT WIDTH lb/in	AXIAL EXTENSION RATIO
0.0	1.00
0.1	1.05
0.2	1.10
0.5	1.15
0.8	1.20
1.2	1.25
1.8	1.30
2.6	1.35
3.7	1.40
5.5	1.45
7.8	1.50
10.2	1.55
12.6	1.60
14.6	1.65
16.6	1.70
18.0 *F	1.75 *F

*F Indicates Failure

COSTOVERTEBRAL JOINT STATIC LOAD APPLIED IN THE SUPERIOR-INFERIOR DIRECTION (DOWNWARD)

Resultant Moment about A-P Axis in-lbs	Angle Change (Radians)	Resultant Moment about L-R Axis in-lb
0.00	0.0000	0.0
0.20	0.0125	1.0
0.30	0.0250	2.75
0.50	0.0375	5.75
0.75	0.0500	10.00
0.90	0.0625	
1.10	0.0750	
1.20	0.0875	
1.30	0.1000	
1.50	0.1125	
1.80	0.1250	
2.40	0.1375	
3.50	0.1500	
6.55	0.1625	
9.75	0.1750	
11.65	0.1875	
12.80	0.2000	
13.90	0.2125	
14.30	0.2250	
14.75	0.2375	
14.90	0.2500	
15.00*F	0.2600*F	

TABLE 2 (Continued)

CARDIAC MUSCLE, LEFT VENTRICLE PARALLEL TO THE FIBERS, AVERAGE DYNAMIC RESPONSE

Engineering Stress psi	Axial Extension Ratio	True Stress psi
0.0	1.00	0.0
1.6	1.05	1.7
3.0	1.10	3.3
4.9	1.15	5.6
7.0	1.20	8.4
9.3	1.25	11.6
11.9	1.30	15.5
14.8	1.35	20.0
17.9	1.40	25.1
21.8	1.45	31.6
26.1	1.50	39.2
30.8	1.55	47.7
36.4	1.60	58.2
43.2	1.65	71.3
53.4 F*	1.70*	90.8 F*

CARDIAC MUSCLE, LEFT VENTRICLE ACROSS FIBERS, AVERAGE DYNAMIC RESPONSE

Engineering Stress psi	Axial Extension Ratio	True Stress psi
0.0	1.00	0.0
0.2	1.05	0.2
0.5	1.10	0.6
0.9	1.15	1.0
1.2	1.20	1.4
1.8	1.25	2.3
2.0	1.30	2.6
2.6	1.35	3.5
3.1	1.40	4.3
4.0	1.45	5.8
4.8	1.50	7.2
5.7	1.55	8.8
6.5	1.60	10.4
7.6	1.65	12.5
8.9	1.70	15.1
10.0	1.75	17.5
11.4	1.80	20.5
13.0	1.85	24.1
14.8	1.90	28.1
16.9	1.95	33.0
17.9 F*	1.97 F*	35.3 F*

* Indicates Failure

TABLE 2 (Continued)

AORTA, TRANSVERSE AVERAGE DYNAMIC RESPONSE

Engineering Stress psi	Axial Extension Ratio	True Stress psi
0.0	1.000	0.0
6.0	1.025	6.2
13.0	1.050	13.7
20.0	1.075	21.5
26.0	1.100	28.6
34.0	1.125	38.3
50.0	1.150	57.5
71.0	1.175	83.4
100.0	1.200	120.0
136.0	1.225	167.0
172.0	1.250	215.0
203.0	1.275	259.0
224.0	1.300	291.0
240.0	1.325	318.0
250.0	1.350	338.0
254.0 F*	1.357 F*	345.0 F*

AORTA, LONGITUDINAL AVERAGE DYNAMIC RESPONSE

Engineering Stress psi	Axial Extension Ratio	True Stress psi
0.0	1.000	0.00
0.5	1.025	0.51
1.0	1.050	1.05
2.0	1.075	2.15
3.5	1.100	3.85
4.5	1.125	5.06
7.0	1.150	8.05
10.0	1.175	11.75
15.0	1.200	18.00
21.5	1.225	26.34
30.0	1.250	37.50
39.0	1.275	49.70
50.0	1.300	65.00
64.0	1.325	84.80
82.0	1.350	110.70
102.0	1.375	140.30
122.0	1.400	170.80
145.0	1.425	206.60
166.0	1.450	240.70
190.0	1.475	280.30
214.0	1.500	321.00
235.0	1.525	358.40
254.0	1.550	393.70
265.0 F*	1.562 F*	414.00 F*

* Indicates Failure

TABLE 2 (Continued)

DIAPHRAGM, ACROSS MUSCLE FIBERS, AVERAGE DYNAMIC RESPONSE

Engineering Stress psi	Axial Extension Ratio	True Stress psi
0.0	1.000	0.0
2.0	1.025	2.1
3.0	1.050	3.2
4.0	1.075	4.3
7.5	1.100	8.3
10.0	1.125	11.3
15.0	1.150	17.3
22.0	1.175	25.9
33.0	1.200	39.6
49.0	1.225	60.0
69.0	1.250	86.3
96.5	1.275	123.0
130.0	1.300	169.0
156.0	1.325	207.0
174.0	1.350	235.0
187.0	1.375	257.0
201.0	1.400	281.0
213.0	1.425	304.0
224.0	1.450	325.0
232.0	1.475	342.0
239.0	1.500	359.0
246.0	1.525	375.0
250.0	1.550	388.0
254.0	1.575	400.0
256.0 *F	1.600*F	410.0*F

DIAPHRAGM, PARALLEL TO MUSCLE FIBERS, AVERAGE DYNAMIC RESPONSE

Engineering Stress psi	Axial Extension Ratio	True Stress psi
0.0	1.000	0.00
4.0	1.025	4.10
8.5	1.050	8.92
14.2	1.075	15.27
24.1	1.100	26.51
33.0	1.125	37.12
44.0	1.150	50.60
57.0	1.175	66.98
75.0	1.200	90.00
94.0	1.225	115.15
117.0	1.250	146.25
139.0	1.275	177.23
163.0	1.300	211.90
184.0	1.325	243.80
205.0	1.350	272.65
227.0	1.375	312.13
246.0	1.400	344.40
260.0	1.425	370.50
273.0	1.450	395.85
280.0 *F	1.480 *F	414.40 *F

* Indicates Failure

TABLE 2 (Continued)

PERICARDIUM, AVERAGE DYNAMIC RESPONSE

Engineering Stress psi	Axial Extension Ratio	True Stress psi
0.0	1.000	0.0
5.0	1.025	5.1
12.0	1.050	12.6
30.0	1.075	32.0
52.0	1.100	57.0
88.0	1.125	99.0
146.0	1.150	168.0
270.0	1.175	317.0
448.0	1.200	538.0
542.0	1.225	664.0
596.0	1.250	745.0
628.0	1.275	801.0
640.0 F*	1.290 F*	826.0 F*

ESOPHAGUS, LONGITUDINAL, AVERAGE DYNAMIC RESPONSE

Engineering Stress psi	Axial Extension Ratio	True Stress psi
0.0	1.0	0.0
1.0	1.025	1.0
3.5	1.050	3.7
7.0	1.075	7.5
11.0	1.100	12.1
16.0	1.125	18.0
22.5	1.150	25.9
32.0	1.175	37.6
44.5	1.200	53.4
58.5	1.225	71.7
72.5	1.250	90.6
89.0	1.275	113.5
108.0	1.300	140.4
133.0	1.325	176.2
143.0 F*	1.335 F*	190.9 F*

* Indicates Failure

TABLE 3 TABULAR SUMMARY OF AVERAGE DYNAMIC OF RHESUS MONKEY TISSUES

ESOPHAGUS, TRANSVERSE
AVERAGE DYNAMIC RESPONSE

Engineering Stress psi	Axial Extension Ratio	True Stress psi
0.0	1.00	0
1.8	1.10	2.0
4.5	1.20	5.4
8.0	1.30	10.4
11.5	1.40	16.1
15.0	1.50	22.5
18.5	1.60	29.6
22.5	1.70	38.3
27.2	1.80	49.0
32.2	1.90	61.2
38.0	2.00	76.0
41.0 F*	2.05 F*	84.1 F*

DESCENDING AORTA, TRANSVERSE
AVERAGE DYNAMIC RESPONSE

Engineering Stress psi	Axial Extension Ratio	True Stress psi
0.0	1.00	0
7.5	1.10	8.3
23.0	1.20	27.6
45.0	1.30	58.5
82.0	1.40	114.8
126.0	1.50	189.0
177.0	1.60	283.2
232.0	1.70	394.4
287.0	1.80	516.6
347.0	1.90	659.3
432.0 F*	2.00 F*	864.0 F*

* Indicates Failure

7.0 REFERENCES

REFERENCES

1. Crisp, J. D. C., "Properties of Tendon and Skin," Biomechanics, Its Foundations and Objectives, Prentice-Hall, 1972.

2. Gibson, T., and Kenedi, R. M., "Biomechanical Properties of Skin," Surg. Clin. N. Amer., 47(2) 279-294, 1967.

3. Fung, Y. C. "Stress-Strain-History Relations of Soft Tissues in Simple Elongation," Biomechanics, Its Foundations and Objectives, Prentice Hall, 1972.

4. Green, A. E., and Adkins, J. E., Large Elastic Deformation and Nonlinear Continuum Mechanics, Clarendon Press, Oxford, 1960.

5. Blatz, P. J., Chu, B. M., and Wayland, H., "On the Mechanical Behavior of Elastic Animal Tissue," Trans. Soc. Rheol., Vol. 13, Part 1, 83-102, 1969.

6. Veronda, D. R., Westmann, R. A., "Mechanical Characteristics of Skin-Finite Deformations," J. of Biomechanics, 3(1) 111-124, 1970.

7. Fung, Y. C., "Biorheology of Soft Tissues," Biorheology, Vol. 10, pp. 139-155, 1973.

8. Lanir, Y. and Fung, Y. C., "Two Dimensional Mechanical Properties of Rabbit Skin - II Experimental Results," J. of Biomechanics, Vol. 7, pp. 171-182, 1974.

9. Buchthal, F., and Kaiser, E., "The Rheology of the Cross Striated Muscle Fiber with Particular Reference to Isotonic Conditions," Copenhagen Dan. Biol. Medd.,Vol. 21, No. 7, 318 pp., 1951.

10. Galford, J. E. and McElhaney, J. H., "A Viscoelastic Study of Scalp, Brain and Dura," J. of Biomechanics, 3, 211-221, 1970.

11. Fallenstein, G. Y., Hulce, V. D., and Melvin, J. W., "Dynamic Mechanical Properties of Human Brain Tissue," J. of Biomechanics, Vol. 2, No. 3, 1969.

12. Viidik, A., "Biomechanics and Functional Adaption of Tendons, and Joint Ligaments," Study on the Anatomy and Function of Bone and Joints, Springer-Verlag, New York, pp. 17-39, 1966.

13. Yamada, H., "Strength of Biological Materials," edited by F. Gaynor Evans, The Williams and Wilkins Co., Baltimore, 1970.

14. Vaishnev, Ramesh N., Young, John T., Janecki, Joseph S., and Patel, Dali J., "Nonlinear Anisotropic Elastic Properties of Canine Aorta," Biophys. Journ., Vol. 12, pp. 1008-1026, 1972.

15. Cheung, J. B. and Hsiao, C. C., "Nonlinear Anisotropic Viscoelastic Stresses in Blood Vessels," J. Biomechanics, Vol. 5, pp. 607-619, 1972.

16. Kivity, Y., and Collins, R., "Nonlinear Wave Propagation in Viscoelastic Tubes: Application to Aortic Rupture," J. Biomechanics, Vol. 7, pp. 67-76, 1974.

17. Feng, W. W. and Yang, W. H., "On Axisymmetric Deformation of Nonlinear Membranes," Trans. ASME, Series E - Journal of Applied Mechanics, p. 1002, 1970.

18. Yang, W. H., and Lu, C. H., "General Deformation of Neo-Hookeon Membrane," Trans. ASME Series E - Journal of Applied Mechanics, pp. 7-12, 1973.

19. Wineman, A. S., "Finite Axisymmetric Inflation of a Nonlinear Viscoelastic Membrane," Proceedings of the Fourth Canadian Congress of Applied Mechanics, p. 255, 1973.

20. Lockett, F. J., Nonlinear Viscoelastic Solids, Academic Press, 1972.

21. Smart, J., and Williams, J. G., "A Comparison of Single Integral Non-Linear Viscoelasticity Theories," J. Mech. Phys. Solids, Vol. 20, pp. 313-324, 1972.

22. Lockett, F. J., and Turner, S., "Nonlinear Creep of Plastics," J. Mech. Phys. Solids, Vol. 19, pp. 201-214, 1961.

23. Coleman, B. D., and Noll, W., "Foundations of Linear Viscoelasticity," Rev. Mod. Phys., Vol. 33, pp. 239-249, 1961.

24. Huang, N. C. and Lee, E. H., "Nonlinear Viscoelasticity for Short Time Ranges," J. Appl. Mech., pp. 313-321, June 1966.

25. Lubliner, J., "Short-Time Approximations in Nonlinear Viscoelasticity," Int. J. Solids Structures, Vol. 3, pp. 513-520, 1967.

26. Leigh, D. C., "Asymptotic Constitutive Approximation for Rapid Deformations of Viscoelastic Materials," Acta Mechanica, Vol. 5, pp. 274-288, 1968.

APPENDIX A TEST ANALYSIS

APPENDIX A TEST ANALYSIS

Uniaxial Tension

The analysis of the uniaxial tension tests performed on all tissues used the following approach:

Measured Variables	Calculated Variables
Axial load, P	True axial stress $\sigma_1 = \frac{P}{wh}$
Initial grid length, ℓ_0	Engineering tensile stress =
Current grid length, ℓ	$\frac{P}{w_0 h_0}$
Initial grid width, w_0	Axial stretch ratio $\lambda_1 = \frac{\ell}{\ell_0}$
Current grid width, w	Width stretch ratio $\lambda_2 = \frac{w}{w_0}$
Initial specimen thickness, h_0	
Current specimen thickness, h	Thickness stretch ratio $\lambda_3 = \frac{h}{h_0}$

Biaxial Tension (Inflation of a Circular Membrane)

Appropriate theory, within context of nonlinear elasticity, is outlined in Green and Adkins, [4].

A circular sheet of initial radius a is fixed at its outside edge. The sheet has no prestretch in its plane. Pressure is applied from one side and the sheet deforms into a surface of revolution (as shown in Fig. A-1)

Symbols

λ_1 - stretch ratio ($\frac{\text{final length}}{\text{initial length}}$) of meridional line element

λ_2 - stretch ratio of circumferential line element

$\lambda_1 = \frac{d\xi}{d\rho}$ $\qquad$ $\lambda_2 = \frac{r}{\rho}$

K_1 - principal curvature of meridional line

K_2 - principal curvature of circumferential line

σ_1 - radial stress = force/current area (true stress)

Figure A-1. Inflation of a Circular Membrane (right side before deformation, left side after deformation)

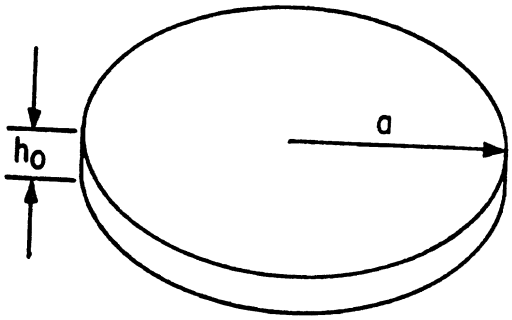
h_0
a

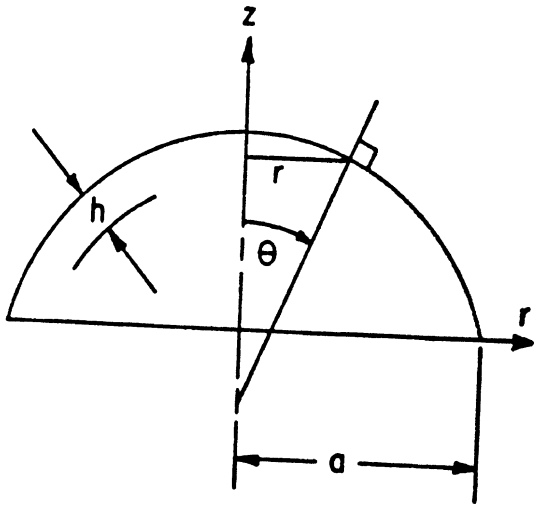
z
r
h
θ
r
a

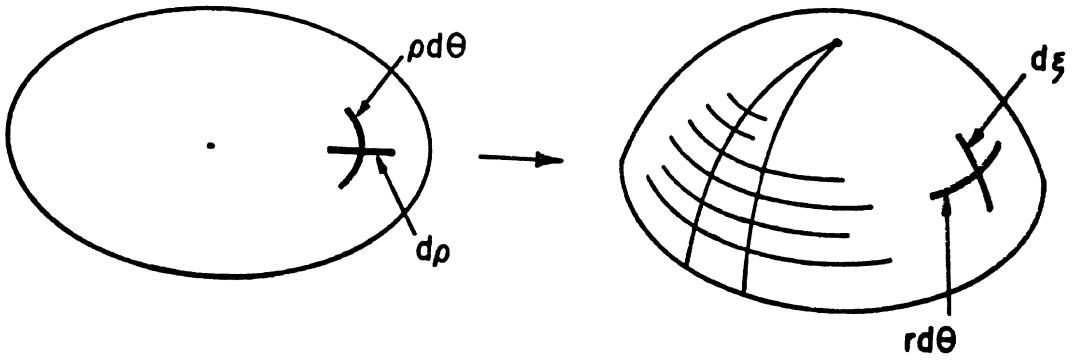
ρdθ
dρ
dξ
rdθ

σ_2 - circumferential stress (true stress)

h_o - initial thickness

h - current thickness

$T_1 = h\sigma_1$ - radial force resultant

$T_2 = h\sigma_2$ - circumferential force resultant

It is shown in Green and Adkins (p 151)

$K_1 = K_2 \qquad \lambda_1 = \lambda_2 \qquad T_1 = T_2$

$P = 2K_1T_1 \qquad p$ = pressure

(also on p. 154)

$$\frac{d\lambda_1}{dr} = \frac{d\lambda_2}{dr} = \frac{dK_1}{dr} = \frac{dK_2}{dr} = 0$$

These results imply that in some region about its axis of symmetry, the deformed surface is spherical. This is true, regardless of material properties.

Based on available theory, the following procedure can be used to establish a biaxial stress-strain relation, i.e. a relation between $\sigma_1 = \sigma_2 = \sigma$ and $\lambda_1 = \lambda_2 = \lambda$, in the following manner.

1. Layout an axially symmetric grid of lines on the surface of the undeformed membrane.

2. Determine the profile of deformed membrane. Measure new radii of each circle.

   Note: λ_2 is the ratio of final radius of a circle to the initial radius. λ_1 is the ratio of the line increments contained between circles. λ_2 can always be measured exactly, but values of λ_1 determined experimentally are always average values. The procedure suggested here requires only determining λ_2.

3. Determine principal circumferential curvature as follows:

For each deformed circle location, draw a normal to the profile of its deformed membrane. Measure angle θ of normal to axis of symmetry. Principal circumferential curvature is

$$K_2 = \frac{\sin\theta}{r}$$

where r is deformed radius of circle.

4. Where deformed membrane surface is spherical, K_2 is constant and equals K_1. Also $\lambda_2 = \lambda_1$, $T_2 = T_1$, $\sigma_2 = \sigma_1$. Determine extent of region where K_2 is constant and determine this constant value.

5. Using the theoretical relation $P = 2K_2T_2$, solve for T_2 using measured value of P and computed K_2. This gives force resultant in equal biaxial test.

6. Measure new thickness h of membrane. In a spherical region, this is constant. Stress in region is determined from relation

$$T = \sigma h$$

7. Now we have one choice of equal biaxial true stress and corresponding stretch ratio λ.

8. Repeat for various values of pressure P to construct complete σ-λ relation.

APPENDIX B CONSTITUTIVE EQUATION DETERMINATION TECHNIQUES

APPENDIX B. CONSTITUTIVE EQUATION DETERMINATION TECHNIQUES

General Considerations

The mathematical theory of nonlinear viscoelasticity has been under development for a number of years, with particular emphasis on the development of useful constitutive equations. The current status of the subject is discussed in a recent book by Lockett [20]. At present, it cannot be said that there is a successful constitutive equation. The earliest nonlinear constitutive equations were represented as sums of single, double and triple integrals over stress or strain histories. Such constitutive equations are regarded as impractical for two reasons. The first is that a complicated and lengthy experimental program is needed to determine relaxation or creep functions [20], p. 82. The second is that numerical methods involving these equations are quite expensive.

This has led to attempts to develop single integral nonlinear constitutive equations, which are easier to handle numerically, analytically, and will hopefully, lead to simple programs for determining material parameters. A number of such models have been developed and are summarized in Lockett's book [20]. The most prominent appear to be:

Finite Linear Viscoelasticity - This is constructed as an approximation for situations in which recent deformations vary slowly relative to the time it takes for past deformations to lose their influence.

Bernstein-Kearsely Zapas Model (BKZ) - This is derived on thermodynamic principles using a generalized concept of entropy.

Modified Superposition Theory - This model is based on the empirical assumption that even though creep and relaxation data may depend nonlinearly on stress or strain level, different creep or relaxation can be superposed in a specific manner.

Shapery Theory - Shapery derived a model from thermodynamic arguments which use creep and relaxation results from linear models.

For each of these approaches, a tensorial three-dimensional constitutive equation can be written down. Although their mathematical details and motivations are different, they are common in one respect. Considering only those forms which express the current value of stress in terms of strain history, they all contain functions of time, current strain and strain history which the model cannot specify. These functions can only be found from experimental data or by derivations from concepts based on the material molecular structure. In most cases, these functions are based on experiment.

For more definiteness, for uniaxial tests, the models reduce to the following form:

$$\sigma(t) = f_1(\varepsilon(t)) + \int_0^t f_2\,(\varepsilon(t),\ \varepsilon(\tau),\ t - \tau)\ d\tau \tag{1}$$

Functions f_1 and f_2 depend on the choice of model. For the modified superposition theory:

$$f_2 = D(t-\tau)\ \frac{d}{d\tau}\ g(\varepsilon(t)),\ \text{or}\ f_2 = R[\varepsilon(\tau),\ t-\tau] \tag{2}$$

For the Shapery model:

$$f_2 = h_1(\varepsilon(t))\ E\ (\rho-\rho')\ \frac{d}{d\tau}\ [h_2(\varepsilon(\tau))\varepsilon(t)$$

$$\rho = \int_0^t \frac{dt'}{a(\varepsilon(t'))} \tag{3}$$

and for the BKZ model

$$f_2 = \left[\left(\frac{\varepsilon(t)}{\varepsilon(\tau)}\right)^2 - \frac{\varepsilon(\tau)}{\varepsilon(t)}\right]\ h\left(\frac{\lambda(t)}{\lambda(\tau)}\ ,\ t - \tau\right) \tag{4}$$

Expressions for $D(t)$, $g(\varepsilon)$, $R(\varepsilon,t)$, $h_1(\varepsilon)$, can only be deduced after a study of experimental data. Different experimenters have tried expressing these functions as various combinations of polynomials, rational functions,

exponentials and logarithms, i.e., in the BZK model, Smart and Williams [21] have tried:

$$h = at^{n_1} + bt^{n_2}\varepsilon + Ct^{n_3}\varepsilon^2, \qquad (5)$$

where A, B, C, n_1, n_2, n_3 are constants found by a nonlinear least squares regression analysis.

The question remains as to which of the above models gives the best results. Smart and Williams [21] used the BKZ, modified superposition and Shapery models to evaluate tests on polypropylene and polyvinyl chloride. For each of these models, the appropriate functions were determined from creep or relaxation tests. The models were then used to predict results of tests involving constant strain rate loading and unloading. The modified superposition model was adequate for lower strain levels.

At this stage in the development of constitutive equations, it is not clear why loading predictions should be better than unloading predictions. Smart and Williams [21], have suggested this may be due to the fact that data is obtained from creep or relaxation tests, in which stress or strain is held constant, while the evaluation tests utilized continuously varying strain or stress histories. A definitive discussion regarding this point has yet to be presented.

Constitutive Equations Determination in Anisotropic Materials - The data generated by experimental procedures which are developed for anisotropic materials must be incorporated into appropriate constitutive equations. Two factors enter into the development of a satisfactory constitutive equation.

1. Constitutive equations for anisotropic materials are much more complex than those for isotropic materials. For an elastic material of unspecified anisotropy, a constitutive equation has the form:

$$\sigma ij = \sum_{\alpha=1}^{n} \phi_\alpha P_{ij}^{(\alpha)}$$

where the scalar-valued functions ϕ_α depend on a set of Q independent scalar-invariant polynomials in the stretch tensor components, and $P_{ij}^{(\alpha)}$ are a set of n independent tensor-valued polynomials in the components of the stretch tensor. For incompressible isotropic materials, where σ_{ij} can be regarded as the deviatoric part of the total stress, $Q = \alpha = 2$. For anisotropic materials, $Q > 2$ and $\alpha > 2$ which implies the necessity of finding a large number of material functions ϕ_α of a large number of arguments. Although there may be more than enough terms for purposes of data fitting, these terms are necessary in order to ensure that the constitutive equations properly represent the kind of anisotropy under consideration. That is, by discarding certain of the arguments of ϕ_α and tensor polynomials $P_{ij}^{(\alpha)}$, the constitutive equations for an orthotropic material could reduce to that for transversely isotropic or even isotropic materials. Similar remarks apply to the more complex constitutive equations for viscoelastic responses.

As part of the data fitting process then, some procedure must be developed for simplifying the constitutive equation, yet maintaining its representation of desired anisotropy. Fung (7), Vaishnev, et. al. (14) and Cheung and Hsaio (15) have discussed some aspects of modeling orthotropy and transverse isotropy which may be of use here.

2. The second factor is the situation discussed in the previous section on general viscoelastic response; i.e. there is no constitutive equation, even for one-dimensional or isotropic behavior, which is totally satisfactory for representing a range of response with reasonable experimental effort and reasonable computational efficiency.

With these remarks in mind, it is felt that the development of a constitutive equation which will be valid for a wide range of loading histories may be impractical, and perhaps unnecessary. In many important situations involving mechanical trauma, the tissue is loaded fairly rapidly. For situations in which the time of loading of a viscoelastic material is short compared to a characteristic relaxation time, approximate constitutive equations have been developed by Huang and Lee (24), Lubliner (25), and Leigh (26). Huang and Lee (24) considered isotropic materials, Lubliner (25) outlined the basic ideas behind the approximation for the one-dimensional case only, and Leigh (26) developed relations without incorporating assumptions about the kind of material symmetry. Thus, approximate constitutive equations for transversely isotropic or orthotropic materials still need to be derived. These constitutive equations, at least in the one-dimensional case, have a well-defined structure allowing for computational efficiency. The material response functions in this simple case can also be determined by a fairly direct experimental procedure (see the following section). It is anticipated that some of the simplifications in measuring properties in the one-dimensional case should be possible in the general case.

Short Time Approximations

Let $\varepsilon(\tau)$ denote the strain at time τ measured from the undeformed state of a viscoelastic material. The general constitutive equations for nonlinear viscoelasticity can be represented in the form:

$$\sigma(t) = \sum_{n-1}^{N} S_n(t),$$

where

$$S_n(t) = \int_{0-}^{t} \int_{0-}^{t} \cdots \int_{0-}^{t} K_n(t-\tau_1, \ldots, t-\tau_n)\ \dot{\varepsilon}(\tau_1) \ldots \dot{\varepsilon}(\tau_n)\, d\tau_1 \ldots d\tau_n$$

and where the lower limit of 0^- denotes inclusion of response to jump discontinuities at time t=0.

Let T_R denote a characteristic relaxation time for the material. Let T_P denote a characteristic time for the duration of a loading. If $T_P/T_R \ll 1$, then the following approximation can be used for the general constitutive equation.

$$\sigma(t) = \sum_n K_n(0,0,\ldots,0)\ \varepsilon^n(t) + \sum_n K_n'(o,0,\ldots,0)\ n\varepsilon(t)^{n-1}\ \varepsilon_1(t)$$

where $K_n(0,0,\ldots,0)$ -- initial value of relaxation function

$K_n'(0,0,\ldots,0)$ -- initial slope of relaxation function.

$$\varepsilon_1(t) = \int_{0-}^{t} (t-\tau)\ \dot{\varepsilon}(\tau)\ d\tau = \int_{0}^{t} \varepsilon(\tau)\ d\tau$$

The error in the above approximation is of $O(t^2)$. The first sum denotes nonlinear elasticity, which is the first approximation for rapid loadings. The second sum denotes correction due to viscoelasticity effects. We regard $K_n(0,0,\ldots,0)$ and $K_n'(0,0,\ldots,0)$ as constants to be determined via testing.

Constant Strain Rate Tests

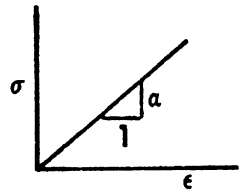

$$\varepsilon(\tau) = \alpha\tau$$

Then $\varepsilon_1(t) = \int_{0-}^{t} (t-\tau)\ \alpha d\tau = \frac{\alpha t^2}{2}$

Then

$$\sigma = \sum(K_n + nK_n' \frac{t}{2})\varepsilon^n$$

$$= \sum(K_n + nK_n' \frac{\dot{\varepsilon}}{2\alpha})\varepsilon^n$$

Note that since K_n' are initial slopes of relaxation functions, $K_n' < 0$. Consider stress-strain graphs. If viscoelastic effects are ignored due to rapidity of loading:

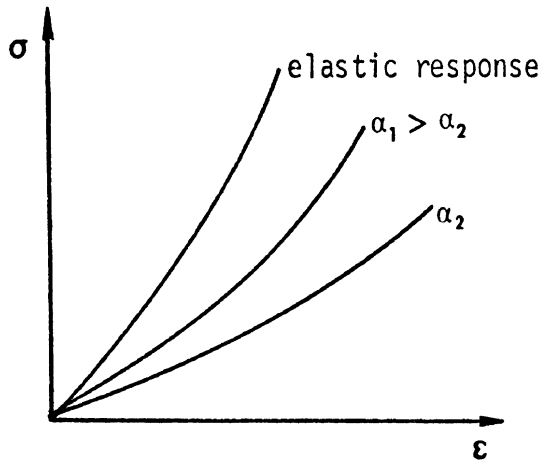

If viscoelasticity effects are considered, the terms $nK_n' \varepsilon/\alpha$ produce a modification to the curve parameters. Since $K_n' < 0$, the curves are probably lowered. The correction is strain dependent and depends especially on α.

Isochrones for Constant Strain Rate

In this case, we hold t fixed, say $t=t_o$. Strain ε is varied by varying α, i.e., $\varepsilon = \alpha t_o$. Then the isochrone is given by:

$$\sigma = \sum_n (K_n + nK_n' \frac{t_o}{2})\varepsilon^n$$

Suppose n has a maximum value of 3, so that the above is a cubic. Suppose cubic expansions in ε can be fitted to isochrones at times t_o and t*. Then we have two sets of coefficients of cubics.

$$C_n^\circ = K_n + nK_n' \frac{t_o}{2} \qquad n = 1,2,3$$

$$C_n^* = K_n + nK_n' \frac{t^*}{2}$$

$$C_n^* - C_n^\circ = \frac{nK_n'}{2}(t^*-t_o) \Rightarrow \text{Knowing } K_n'$$

Substituting back into the expressions for C_n° and C_n^* gives K_n.

More General Strain Variation

Within the duration of validity of the short time approximation, ε may have a general time variation - say quadratic.

$$\varepsilon(t) = \varepsilon_o + \alpha t + \beta\frac{t^2}{2}$$

where ε_o denotes a jump discontinuity at t=0, then:

$$\varepsilon_1 = \int_0^t (t-\tau)\,\dot{\varepsilon}(\tau)\,d\tau = \varepsilon_o t + \frac{\alpha t^2}{2} + \beta\frac{t^3}{6}$$

Then

$$\sigma(t) = \sum[K_n(\varepsilon_o + \alpha t + \beta\frac{t^2}{2}) + nK'_n\,(\varepsilon_o t + \frac{\alpha t^2}{2} + \beta\frac{t^3}{6})]\,\varepsilon^{n-1}$$

No general statements seem meaningful because of the complexity of this expression.

APPENDIX C INDIVIDUAL HUMAN TEST DATA TABLES

HUMAN INTERCOSTAL MUSCLE, PERPENDICULAR TO RIBS

TISSUE SOURCE: 70 Test # 1 AVERAGE SPECIMEN WIDTH: 0.75"

TIME TO FAILURE: 90 sec

LOAD Pounds	AXIAL STRETCH RATIO	LOAD PER UNIT WIDTH LB/IN
0	1.0	0
0.1	1.78	0.13
0.6	2.16	0.8
1.8	2.25	2.4
3.4	2.34	4.5
5.0	2.44	6.7
7.2	2.53	9.6
8.2	2.62	10.9
9.2	2.72	12.3

TISSUE SOURCE: 70 Test # 2 AVERAGE SPECIMEN WIDTH: 0.55"

TIME TO FAILURE: 62 sec

LOAD Pounds	AXIAL STRETCH RATIO	LOAD PER UNIT WIDTH LB/IN
0.0	1.0	0.0
0.05	1.52	0.09
0.08	1.63	0.15
0.23	1.84	0.42
0.8	1.94	1.45
1.7	2.05	3.09
2.8	2.15	5.09
3.72	2.26	6.76
4.0	2.3	7.27

HUMAN INTERCOSTAL MUSCLE, PERPENDICULAR TO RIBS

TISSUE SOURCE: 70 Test # 3 AVERAGE SPECIMEN WIDTH: 0.80"

TIME TO FAILURE: 20 msec

LOAD Pounds	AXIAL STRETCH RATIO	LOAD PER UNIT WIDTH LB/IN
0.0	1.0	0.0
0.2	1.35	0.25
1.6	1.71	1.25
4.4	2.06	5.50
13.0	2.42	16.25

TISSUE SOURCE: 70 Test # 4 AVERAGE SPECIMEN WIDTH: 0.70"

TIME TO FAILURE: 10 msec

LOAD Pounds	AXIAL STRETCH RATIO	LOAD PER UNIT WIDTH LB/IN
0.0	1.0	0.0
0.4	1.27	.57
0.8	1.55	1.14
1.8	1.68	2.57
4.0	1.82	5.71
7.0	1.96	10.0
10.0	2.09	14.3
11.8	2.24	16.9
13.6	2.37	18.4

HUMAN INTERCOSTAL MUSCLE, PERPENDICULAR TO RIBS

TISSUE SOURCE: 70 Test # 5 AVERAGE SPECIMEN WIDTH: 0.75"

TIME TO FAILURE: 44 msec

LOAD Pounds	AXIAL STRETCH RATIO	LOAD PER UNIT WIDTH LB/IN
0.0	1.0	0.0
0.5	1.15	0.67
2.6	1.29	3.47
16.8	1.44	22.4
21.6	1.59	28.8
22.6	1.64	30.1

TISSUE SOURCE: 74 Test # 1 AVERAGE SPECIMEN WIDTH: 0.6"

TIME TO FAILURE: 39 sec

LOAD Pounds	AXIAL STRETCH RATIO	LOAD PER UNIT WIDTH LB/IN
0.0	1.0	0.0
0.04	1.10	0.06
0.2	1.16	0.33
0.74	1.21	1.23
2.0	1.26	3.33
3.66	1.31	6.1
5.24	1.37	8.73
6.24	1.41	10.4

HUMAN INTERCOSTAL MUSCLE, PERPENDICULAR TO RIBS

TISSUE SOURCE: 74 Test # 2 AVERAGE SPECIMEN WIDTH: 0.75"

TIME TO FAILURE: 42 sec

LOAD Pounds	AXIAL STRETCH RATIO	LOAD PER UNIT WIDTH LB/IN
0.0	1.0	0.0
0.08	1.22	0.11
0.32	1.29	0.43
1.0	1.36	1.33
2.32	1.44	3.09
4.08	1.51	5.44
5.84	1.58	7.79
6.32	1.61	8.43

TISSUE SOURCE: 74 Test # 3 AVERAGE SPECIMEN WIDTH: 0.70"

TIME TO FAILURE: 10 msec

LOAD Pounds	AXIAL STRETCH RATIO	LOAD PER UNIT WIDTH LB/IN
0.0	1.0	0.0
0.2	1.08	0.29
1.8	1.16	2.57
4.0	1.24	5.71
7.2	1.32	10.28
10.2	1.4	14.57

HUMAN INTERCOSTAL MUSCLE, PERPENDICULAR TO RIBS

TISSUE SOURCE: 74 Test # 4 AVERAGE SPECIMEN WIDTH: 0.60"

TIME TO FAILURE: 12 msec

LOAD Pounds	AXIAL STRETCH RATIO	LOAD PER UNIT WIDTH LB/IN
0.0	1.0	0.0
0.1	1.09	0.16
0.2	1.18	0.33
1.2	1.28	2.0
3.4	1.37	5.67
6.6	1.46	11.0
9.0	1.56	15.0

TISSUE SOURCE: 74 Test # 5 AVERAGE SPECIMEN WIDTH: 0.60"

TIME TO FAILURE: 4.8 msec

LOAD Pounds	AXIAL STRETCH RATIO	LOAD PER UNIT WIDTH LB/IN
0.0	1.0	0.0
0.6	1.08	1.0
2.2	1.16	3.67
4.6	1.24	7.67
8.7	1.32	14.5
10.0	1.39	16.67

HUMAN INTERCOSTAL MUSCLE, PERPENDICULAR TO RIBS

TISSUE SOURCE: 74 TEST # 6 AVERAGE SPECIMEN WIDTH: 0.70"

TIME TO FAILURE: 38 msec

LOAD Pounds	AXIAL STRETCH RATIO	LOAD PER UNIT WIDTH LB/IN
0.0	1.0	0.0
0.5	1.09	0.7
4.0	1.18	5.7
7.7	1.27	11.0
9.8	1.36	14.0

HUMAN CARDIAC MUSCLE - LEFT VENTRICLE, PARALLEL TO MUSCLE FIBERS

TISSUE SOURCE: 10 Test # 1 SPECIMEN TYPE: 2

TIME TO FAILURE: 65 sec AVERAGE SPECIMEN THICKNESS: 0.066"

LOAD Pounds	AXIAL STRETCH RATIO	WIDTH STRETCH RATIO	THICKNESS STRETCH RATIO	ENGINEERING STRESS PSI
0.0	1.0	1.0	1.0	0.0
0.0	1.131	1.0	.89	0.0
0.02	1.41	1.0	.89	1.2
0.025	1.54	1.0	.87	1.5
0.04	1.68	.95	.81	2.4
0.08	1.72	.93	.78	4.8
0.10	1.97	.87	.76	6.1
0.14	1.94	.86	.76	8.5
0.17	2.07	.81	.74	10.3
0.19	2.29	.74	.71	11.5

TISSUE SOURCE: 74 Test # 2 SPECIMEN TYPE: 2

TIME TO FAILURE: 11 msec AVERAGE SPECIMEN THICKNESS: 0.105"

LOAD Pounds	AXIAL STRETCH RATIO	WIDTH STRETCH RATIO	THICKNESS STRETCH RATIO	ENGINEERING STRESS PSI
0.0	1.0	1.0	1.0	0.0
.04	1.06	.97	.95	2.0
.06	1.19	.94	.90	3.0
.14	1.33	.91	.85	7.1
.26	1.38	.91	.85	13.2
.45	1.40	.89	.85	22.8
.63	1.46	.86	.75	32.0
.69	1.52	.86	.75	35.0

HUMAN CARDIAC MUSCLE - LEFT VENTRICLE, PARALLEL TO MUSCLE FIBERS

TISSUE SOURCE: 74 Test # 3A

SPECIMEN TYPE: 2

TIME TO FAILURE: 17 msec

AVERAGE SPECIMEN THICKNESS: 0.105"

LOAD Pounds	AXIAL STRETCH RATIO	WIDTH STRETCH RATIO	THICKNESS STRETCH RATIO	ENGINEERING STRESS PSI
0.0	1.0	1.0	1.0	0.0
0.04	1.1	1.0	.92	2.0
0.05	1.18	1.0	.83	2.5
0.11	1.27	1.0	.83	5.6
0.26	1.28	0.94	.83	13.2
0.50	1.41	0.94	.79	25.4
0.63	1.43	0.94	.79	32.0
0.87	1.49	0.94	.75	44.2
1.3	1.61	0.91	.75	66.0
1.59	1.61	0.91	.75	80.7

TISSUE SOURCE: 74 Test # 3

SPECIMEN TYPE: 2

TIME TO FAILURE: 90 msec

AVERAGE SPECIMEN THICKNESS: 0.054

LOAD Pounds	AXIAL STRETCH RATIO	WIDTH STRETCH RATIO	THICKNESS STRETCH RATIO	ENGINEERING STRESS PSI
0.0	1.0	1.0	1.0	0.0
0.03	1.09	1.0	1.0	3.0
0.07	1.21	1.0	1.0	7.0
0.16	1.51	1.0	.91	16.0
0.27	1.62	.94	.91	27.0
0.41	1.93	.94	.82	41.0

HUMAN CARDIAC MUSCLE - LEFT VENTRICLE, PARALLEL TO MUSCLE FIBERS

TISSUE SOURCE: 74 Test # 1 SPECIMEN TYPE: 2

TIME TO FAILURE: 7 msec AVERAGE SPECIMEN THICKNESS: 0.045

LOAD Pounds	AXIAL STRETCH RATIO	WIDTH STRETCH RATIO	THICKNESS STRETCH RATIO	ENGINEERING STRESS PSI
0.0	1.0	1.0	1.0	0.0
0.02	1.11	.95	.91	2.4
0.04	1.17	.9	.82	4.7
0.06	1.24	.9	.73	7.1
0.08	1.35	.9	.73	9.5
0.12	1.38	.9	.73	14.2
0.20	1.43	.86	.73	23.7
0.23	1.70	.83	.73	27.2
0.32	1.78	.70	.73	36.7
0.44	1.85	.79	.73	52.0

HUMAN CARDIAC MUSCLE, LEFT VENTRICLE, PERPENDICULAR TO MUSCLE FIBERS

TISSUE SOURCE: 74 Test # 1 SPECIMEN TYPE: 2

TIME TO FAILURE: 9 msec AVERAGE SPECIMEN THICKNESS: 0.074"

LOAD Pounds	AXIAL STRETCH RATIO	WIDTH STRETCH RATIO	THICKNESS STRETCH RATIO	ENGINEERING STRESS PSI
0.0	1.0	1.0	1.0	0.0
0.05	1.19	0.94	1.0	3.6
0.17	1.5	0.82	1.0	12.2
0.25	1.7	0.79	0.93	18.0

TISSUE SOURCE: 74 Test # 2 SPECIMEN TYPE: 2

TIME TO FAILURE: 14 msec AVERAGE SPECIMEN THICKNESS: 0.080"

LOAD Pounds	AXIAL STRETCH RATIO	WIDTH STRETCH RATIO	THICKNESS STRETCH RATIO	ENGINEERING STRESS PSI
0.	1.0	1.0	1.0	0
0.01	1.19	0.95	1.0	0.7
0.02	1.33	0.92	1.0	1.4
0.03	1.38	0.85	.93	2.1
0.06	1.43	0.77	.93	4.2
0.13	1.57	0.77	.93	8.7
0.23	1.64	0.75	.93	15.3
0.33	1.81	0.70	.93	22.0
0.40	2.0	0.67	.93	26.7

HUMAN CARDIAC MUSCLE, LEFT VENTRICLE, PERPENDICULAR TO MUSCLE FIBERS

TISSUE SOURCE: 74 Test # 3 SPECIMEN TYPE: 2

TIME TO FAILURE: 47 msec AVERAGE SPECIMEN THICKNESS: 0.055"

LOAD Pounds	AXIAL STRETCH RATIO	WIDTH STRETCH RATIO	THICKNESS STRETCH RATIO	ENGINEERING STRESS PSI
0.0	1.0	1.0	1.0	0
0.01	1.23	1.0	1.0	0.97
0.04	1.46	.95	1.0	3.88
0.08	1.81	.88	1.0	7.8
0.12	2.38	.85	.90	11.7

HUMAN ASCENDING AORTA, LONGITUDINAL

TISSUE SOURCE: 74 Test # 1 SPECIMEN TYPE: 2

TIME TO FAILURE: 12 msec AVERAGE SPECIMEN THICKNESS: 0.070"

LOAD Pounds	AXIAL STRETCH RATIO	WIDTH STRETCH RATIO	THICKNESS STRETCH RATIO	ENGINEERING STRESS PSI
0.0	1.0	1.0	1.0	0.0
0.02	1.06	1.0	1.0	1.5
0.04	1.15	.92	0.92	3.1
0.06	1.22	.92	0.92	4.6
0.22	1.30	.92	0.92	16.8
0.40	1.35	.9	0.92	30.5
0.62	1.46	.88	0.92	47.3
0.84	1.50	.87	0.85	64.1
1.1	1.56	.85	0.85	84.0
1.68	1.61	.82	0.85	128.2
2.8	1.72	.8	0.85	213.7
3.1	1.74	.8	0.85	236.7
4.05	1.76	.72	0.85	309.2

TISSUE SOURCE: 6 Test No. 1 SPECIMEN TYPE: 1

TIME TO FAILURE: 13 seconds AVERAGE SPECIMEN THICKNESS: 0.11"

LOAD Pounds	AXIAL STRETCH RATIO	WIDTH STRETCH RATIO	THICKNESS STRETCH RATIO	ENGINEERING STRESS PSI
0.0	1.0	1.0	1.0	0.0
1.2	1.17	.96	.86	38.4
2.44	1.23	.93	.77	78.1

HUMAN ASCENDING AORTA, TRANSVERSE

TISSUE SOURCE: 4 Test # 1 SPECIMEN TYPE: 1

TIME TO FAILURE: 7 msec AVERAGE SPECIMEN THICKNESS: 0.065"

LOAD Pounds	AXIAL STRETCH RATIO	WIDTH STRETCH RATIO	THICKNESS STRETCH RATIO	ENGINEERING STRESS PSI
0	1.0	-	-	0
.46	1.1	-	-	32.0
1.28	1.16	-	-	88.1
2.85	1.21	-	-	196.4
3.52	1.22	-	-	243.0

TISSUE SOURCE: 6 Test # 1 SPECIMEN TYPE: 1

TIME TO FAILURE: 13 msec AVERAGE SPECIMEN THICKNESS: 0.077"

LOAD Pounds	AXIAL STRETCH RATIO	WIDTH STRETCH RATIO	THICKNESS STRETCH RATIO	ENGINEERING STRESS PSI
0	1.0	-	-	0
.13	1.17	-	-	6
.26	1.21	-	-	12
.91	1.28	-	-	48
2.1	1.36	-	-	116
3.9	1.4	-	-	208
5.28	1.47	-	-	280
5.43	1.5	-	-	288

HUMAN ASCENDING AORTA, TRANSVERSE

TISSUE SOURCE: 74 TEST No. 1 SPECIMEN TYPE: 2

TIME TO FAILURE: 12 msec AVERAGE SPECIMEN THICKNESS: 0.062"

LOAD Pounds	AXIAL STRETCH RATIO	WIDTH STRETCH RATIO	THICKNESS STRETCH RATIO	ENGINEERING STRESS PSI
0	1.0	1.0	1.0	0
0.06	1.02	1.0	0.95	5.17
0.20	1.11	.95	0.93	17.2
0.34	1.23	.93	0.90	29.3
0.52	1.38	.88	0.90	44.8
0.74	1.47	.88	0.87	63.8
0.85	1.49	.88	0.84	73.3
0.95	1.49	.86	0.80	81.9
1.70	1.50	.83	0.80	146.5
3.46	1.53	.79	0.80	298.3
4.9	1.74	.79	0.80	422.4

HUMAN AORTIC ARCH, LONGITUDINAL

TISSUE SOURCE: 10 Test # 1 SPECIMEN TYPE: 1

TIME TO FAILURE: 105 seconds AVERAGE SPECIMEN THICKNESS: 0.95"

LOAD Pounds	AXIAL STRETCH RATIO	WIDTH STRETCH RATIO	THICKNESS STRETCH RATIO	ENGINEERING STRESS PSI
0.0	1.0	1.0	1.0	0.0
0.25	1.27	.95	1.0	10.2
0.47	1.37	.92	1.0	19.0
0.97	1.43	.89	.92	38.8
1.26	1.45	.82	.84	50.4
1.45	1.47	.82	.84	58.0
2.23	1.49	.82	.80	89.2
2.55	1.45	.82	.80	102.0

TISSUE SOURCE: 70 Test # 2 SPECIMEN TYPE: 2

TIME TO FAILURE: 65 msec AVERAGE SPECIMEN THICKNESS: 0.060"

LOAD Pounds	AXIAL STRETCH RATIO	WIDTH STRETCH RATIO	THICKNESS STRETCH RATIO	ENGINEERING STRESS PSI
0	1.0	1.0	1.0	.0
.04	1.04	.93	1.0	3.6
.11	1.22	.83	0.92	9.8
.80	1.28	.74	0.92	71.1
2.00	1.43	.74	0.92	177.8
2.6	1.56	.64	0.92	231.1

HUMAN AORTIC ARCH, LONGITUDINAL

TISSUE SOURCE: 70 Test # 1 SPECIMEN TYPE: 2

TIME TO FAILURE: 10 msec AVERAGE SPECIMEN THICKNESS: 0.062"

LOAD Pounds	AXIAL STRETCH RATIO	WIDTH STRETCH RATIO	THICKNESS STRETCH RATIO	ENGINEERING STRESS PSI
0.0	1.0	1.0	1.0	0.0
0.06	1.07	1.0	.93	5.2
0.14	1.09	0.97	.93	12.1
0.32	1.13	0.97	.86	27.6
0.62	1.17	0.92	.86	53.4
1.06	1.23	0.92	.86	91.4
1.52	1.27	0.87	.86	131.0
1.92	1.3	0.87	.86	165.5
2.12	1.35	0.82	.86	182.8

TISSUE SOURCE: 56 Test # 1 SPECIMEN TYPE: 2

TIME TO FAILURE: 54 sec AVERAGE SPECIMEN THICKNESS: 0.072"

LOAD Pounds	AXIAL STRETCH RATIO	WIDTH STRETCH RATIO	THICKNESS STRETCH RATIO	ENGINEERING STRESS PSI
0.0	1.0	1.0	1.0	0.0
.02	1.18	.90	.9	1.5
.06	1.30	.85	.85	4.4
.54	1.48	.79	.85	40.0
.96	1.53	.76	.85	71.1
1.4	1.62	.65	.85	103.7

HUMAN AORTIC ARCH, TRANSVERSE

TISSUE SOURCE: 56 Test # 5 SPECIMEN TYPE: 2

TIME TO FAILURE: 6 msec AVERAGE SPECIMEN THICKNESS: 0.068"

LOAD Pounds	AXIAL STRETCH RATIO	WIDTH STRETCH RATIO	THICKNESS STRETCH RATIO	ENGINEERING STRESS PSI
0	1.0	1.0	1.0	0
0.04	1.1	0.91	0.83	7.7
0.1	1.18	0.91	0.83	15.4
0.33	1.33	0.89	0.79	215.4
2.5	1.42	0.86	0.79	192.3

TISSUE SOURCE: 70 Test # 2 SPECIMEN TYPE: 2

TIME TO FAILURE: 41 msec AVERAGE SPECIMEN THICKNESS: 0.070"

LOAD Pounds	AXIAL STRETCH RATIO	WIDTH STRETCH RATIO	THICKNESS STRETCH RATIO	ENGINEERING STRESS PSI
0	1.0	1.0	1.0	0
0.02	1.03	1.0	1.0	1.53
0.14	1.1	0.92	1.0	10.7
1.1	1.18	0.92	1.0	84.0
2.3	1.24	0.92	0.92	175.6
2.82	1.4	0.87	0.83	215.3

HUMAN AORTIC ARCH, TRANSVERSE

TISSUE SOURCE: 70 Test # 1 SPECIMEN TYPE: 2

TIME TO FAILURE: 7 msec AVERAGE SPECIMEN THICKNESS: 0.085"

LOAD Pounds	AXIAL STRETCH RATIO	WIDTH STRETCH RATIO	THICKNESS STRETCH RATIO	ENGINEERING STRESS PSI
0	1.0	1.0	1.0	0
0.12	1.06	1.0	.94	7.55
0.28	1.14	.98	.89	17.6
0.80	1.23	.93	.86	50.3
2.0	1.26	.91	.84	125.8
2.72	1.28	.91	.83	176.1
3.52	1.28	.89	.83	221.4

TISSUE SOURCE: 56 Test # 1 SPECIMEN TYPE: 2

TIME TO FAILURE: 49 sec AVERAGE SPECIMEN THICKNESS: 0.076"

LOAD Pounds	AXIAL STRETCH RATIO	WIDTH STRETCH RATIO	THICKNESS STRETCH RATIO	ENGINEERING STRESS PSI
0	1.0	1.0	1.0	0
0.4	1.18	1.0	1.0	28.6
0.9	1.25	.96	.95	64.3
1.5	1.28	.91	.9	107.1
2.06	1.3	.86	.89	147.1
2.5	1.31	.86	.89	178.6
2.9	1.32	.84	.84	207.1
3.0	1.32	.84	.84	214.3

HUMAN DESCENDING AORTA (THORACIC), LONGITUDINAL

TISSUE SOURCE: 4 Test # 1 SPECIMEN TYPE: 1

TIME TO FAILURE: 6 msec AVERAGE SPECIMEN THICKNESS: 0.060"

LOAD Pounds	AXIAL STRETCH RATIO	WIDTH STRETCH RATIO	THICKNESS STRETCH RATIO	ENGINEERING STRESS PSI
0	1.0	1.0	-	0
0.27	1.1	1.0	-	18.2
0.9	1.2	0.96	-	60.0
2.1	1.4	0.92	-	140.0
2.2	1.48	0.82	-	146.7

TISSUE SOURCE: 70 Test # 1 SPECIMEN TYPE: 1

TIME TO FAILURE: 14 msec AVERAGE SPECIMEN THICKNESS: 0.070"

LOAD Pounds	AXIAL STRETCH RATIO	WIDTH STRETCH RATIO	THICKNESS STRETCH RATIO	ENGINEERING STRESS PSI
0.0	1.0	1.0	1.0	0
0.05	1.13	0.96	1.0	1.9
0.16	1.24	0.91	1.0	10.0
0.5	1.24	0.85	1.0	31.2
1.72	1.27	0.74	1.0	107.5
3.72	1.47	0.72	1.0	232.5
5.72	1.59	0.7	1.0	357.5
7.00	1.7	0.7	1.0	437.5
9.00	1.75	0.7	0.86	562.5

HUMAN DESCENDING AORTA (THORACIC), LONGITUDINAL

TISSUE SOURCE: 70 Test # 3 SPECIMEN TYPE: 2

TIME TO FAILURE: 110 msec AVERAGE SPECIMEN THICKNESS: 0.059"

LOAD Pounds	AXIAL STRETCH RATIO	WIDTH STRETCH RATIO	THICKNESS STRETCH RATIO	ENGINEERING STRESS PSI
0	1.0	1.0	1.0	0
0.01	1.03	1.0	1.0	0.7
0.02	1.07	0.96	0.93	1.4
0.04	1.14	0.94	0.93	2.8
0.06	1.19	0.92	0.86	4.1
0.20	1.28	0.85	0.86	13.8
1.48	1.4	0.79	0.86	102.1
2.88	1.42	0.69	0.86	198.6
3.8	1.45	0.62	0.86	262.1

TISSUE SOURCE: 8 Test # 1 SPECIMEN TYPE: 1

TIME TO FAILURE: 12.6 sec AVERAGE SPECIMEN THICKNESS: 0.065"

LOAD Pounds	AXIAL STRETCH RATIO	WIDTH STRETCH RATIO	THICKNESS STRETCH RATIO	ENGINEERING STRESS PSI
0	1.0	1.0	1.0	0
.81	1.03	.94	.96	53.1
1.85	1.11	.93	.92	121.3
2.1	1.2	.86	.89	137.7

HUMAN DESCENDING AORTA (THORACIC), LONGITUDINAL

TISSUE SOURCE: 8 Test # 2 SPECIMEN TYPE: 1

TIME TO FAILURE: 18.0 sec AVERAGE SPECIMEN THICKNESS: 0.073"

LOAD Pounds	AXIAL STRETCH RATIO	WIDTH STRETCH RATIO	THICKNESS STRETCH RATIO	ENGINEERING STRESS PSI
0	1.0	1.0	1.0	0
.4	1.12	.97	.97	22.2
.54	1.2	.93	.96	30.0
1.04	1.27	.91	.96	57.8
1.2	1.47	.87	.88	66.7

TISSUE SOURCE: 56 Test # 2 SPECIMEN TYPE: 1

TIME TO FAILURE: 83 sec AVERAGE SPECIMEN THICKNESS: 0.075"

LOAD Pounds	AXIAL STRETCH RATIO	WIDTH STRETCH RATIO	THICKNESS STRETCH RATIO	ENGINEERING STRESS PSI
0	1.0	1.0	1.0	0
.12	1.07	.96	.96	6.4
.72	1.27	.88	.86	38.3
.88	1.28	.88	.86	46.8
1.6	1.46	.81	.86	85.1

HUMAN DESCENDING AORTA (THORACIC), TRANSVERSE

TISSUE SOURCE: 70 Test # 1 SPECIMEN TYPE: 2

TIME TO FAILURE: 8 msec AVERAGE SPECIMEN THICKNESS: 0.065"

LOAD Pounds	AXIAL STRETCH RATIO	WIDTH STRETCH RATIO	THICKNESS STRETCH RATIO	ENGINEERING STRESS PSI
0	1.0	1.0	1.0	0
0.2	1.17	1.0	1.0	16.4
0.28	1.22	.97	.82	23.0
0.54	1.37	.97	.82	44.3
0.86	1.39	.91	.82	70.5
2.2	1.43	.91	.82	180.3
3.9	1.72	.91	.82	319.7

TISSUE SOURCE: 56 Test # 5 SPECIMEN TYPE: 1

TIME TO FAILURE: 18 msec AVERAGE SPECIMEN THICKNESS: 0.068"

LOAD Pounds	AXIAL STRETCH RATIO	WIDTH STRETCH RATIO	THICKNESS STRETCH RATIO	ENGINEERING STRESS PSI
0	1.0	1.0	1.0	0
0.03	1.02	1.0	1.0	1.2
0.05	1.04	.91	1.0	3.1
0.10	1.14	.86	1.0	6.2
0.29	1.30	.86	.82	18.1
0.61	1.41	.77	.82	38.3
1.7	1.52	.68	.82	106.3
3.3	1.64	.68	.82	206.3
4.07	1.74	.68	.82	251.3

HUMAN DESCENDING AORTA (THORACIC), TRANSVERSE

TISSUE SOURCE: 6 Test # 1 SPECIMEN TYPE: 1

TIME TO FAILURE: 12 sec AVERAGE SPECIMEN THICKNESS: 0.14"

LOAD Pounds	AXIAL STRETCH RATIO	WIDTH STRETCH RATIO	THICKNESS STRETCH RATIO	ENGINEERING STRESS PSI
0	1.0	1.0	1.0	0
.22	1.10	.97	.95	9.78
.86	1.18	.96	.92	38.2
1.92	1.18	.9	.92	85.3
2.76	1.25	.9	.92	122.7

TISSUE SOURCE: 8 Test # 1 SPECIMEN TYPE: 1

TIME TO FAILURE: 12 sec AVERAGE SPECIMEN THICKNESS: 0.077"

LOAD Pounds	AXIAL STRETCH RATIO	WIDTH STRETCH RATIO	THICKNESS STRETCH RATIO	ENGINEERING STRESS PSI
0	1.0	1.0	1.0	0
.04	1.07	1.0	.92	2.1
.06	1.1	.98	.9	3.2
.22	1.17	.95	.9	11.7
.80	1.23	,89	.89	42.7
1.6	1.28	.82	.89	85.3

HUMAN DESCENDING AORTA (THORACIC), TRANSVERSE

TISSUE SOURCE: 56 Test # 1 SPECIMEN TYPE: 1

TIME TO FAILURE: 92 sec AVERAGE SPECIMEN THICKNESS: 0.070"

LOAD Pounds	AXIAL STRETCH RATIO	WIDTH STRETCH RATIO	THICKNESS STRETCH RATIO	ENGINEERING STRESS PSI
0	1.0	1.0	-	0
0.06	1.22	.91	-	3.3
0.48	1.39	.81	-	26.7
1.0	1.42	.78	-	55.6
1.46	1.45	.75	-	81.1
2.0	1.48	-	-	111.1
2.5	1.51	-	-	138.9

HUMAN DESCENDING AORTA (THORACIC), TRANSVERSE

TISSUE SOURCE: 8 Test # 2 SPECIMEN TYPE: 1

TIME TO FAILURE: 18 sec AVERAGE SPECIMEN THICKNESS: 0.060"

LOAD Pounds	AXIAL STRETCH RATIO	WIDTH STRETCH RATIO	THICKNESS STRETCH RATIO	ENGINEERING STRESS PSI
0	1.0	1.0	-	0
1.85	1.28	.92	-	105
2.6	1.32	-	-	148

TISSUE SOURCE: 57 Test # 1 SPECIMEN TYPE: 1

TIME TO FAILURE: 62 sec AVERAGE SPECIMEN THICKNESS: 0.069"

LOAD Pounds	AXIAL STRETCH RATIO	WIDTH STRETCH RATIO	THICKNESS STRETCH RATIO	ENGINEERING STRESS PSI
0	1.0	1.0	1.0	0
.22	1.1	.96	.95	13.5
.73	1.4	.84	.85	45.1
1.2	1.44	.77	.85	74.0
1.79	1.47	.75	.85	110.0
2.35	1.49	.74	.80	145.0

HUMAN DIAPHRAGM, PARALLEL TO MUSCLE FIBERS

TISSUE SOURCE: 70 Test # 2 SPECIMEN TYPE: 1

TIME TO FAILURE: 14 msec AVERAGE SPECIMEN THICKNESS: 0.094"

LOAD Pounds	AXIAL STRETCH RATIO	WIDTH STRETCH RATIO	THICKNESS STRETCH RATIO	ENGINEERING STRESS PSI
0	1.0	1.0	1.0	0
0.35	1.044	.93	1.0	16
3.4	1.22	.92	.86	151
4.5	1.28	.92	.86	200
5.1	1.38	.92	.86	227

TISSUE SOURCE: 70 Test # 1 SPECIMEN TYPE: 1

TIME TO FAILURE: 17 msec AVERAGE SPECIMEN THICKNESS: 0.077"

LOAD Pounds	AXIAL STRETCH RATIO	WIDTH STRETCH RATIO	THICKNESS STRETCH RATIO	ENGINEERING STRESS PSI
0.0	1.0	1.0	1.0	0
0.3	1.01	0.95	0.92	17.1
0.76	1.08	0.95	0.92	43.4
2.0	1.18	0.95	0.84	120.0
4.7	1.32	0.95	0.84	268
6.9	1.53	0.92	0.80	394
7.3	1.57	0.85	0.80	417

HUMAN DIAPHRAGM, PARALLEL TO MUSCLE FIBERS

TISSUE SOURCE: 74 Test # 1 SPECIMEN TYPE: 1

TIME TO FAILURE: 23 msec AVERAGE SPECIMEN THICKNESS: 0.095"

LOAD Pounds	AXIAL STRETCH RATIO	WIDTH STRETCH RATIO	THICKNESS STRETCH RATIO	ENGINEERING STRESS PSI
0	1.0	1.0	1.0	0
0.3	1.11	1.0	.96	13.3
0.7	1.24	1.0	.96	31.1
1.6	1.33	1.0	.96	71.1
3.4	1.37	0.94	.92	151.1
4.4	1.47	0.94	.88	195.1
4.52	1.52	0.91	.88	200.9

TISSUE SOURCE: 74 Test # 2 SPECIMEN TYPE: 1

TIME TO FAILURE: 120 msec AVERAGE SPECIMEN THICKNESS: 0.085"

LOAD Pounds	AXIAL STRETCH RATIO	WIDTH STRETCH RATIO	THICKNESS STRETCH RATIO	ENGINEERING STRESS PSI
0	1.0	1.0	1.0	0
0.3	1.1	.95	1.0	16.5
0.8	1.18	.95	.9	44.0
1.1	1.2	.95	.9	60.5
3.4	1.34	.90	.9	187.0
4.4	1.4	.85	.9	242.0

HUMAN DIAPHRAGM, PARALLEL TO MUSCLE FIBERS

TISSUE SOURCE: 6 Test # 1 SPECIMEN TYPE: 1

TIME TO FAILURE: 10 sec AVERAGE SPECIMEN THICKNESS: 0.042"

LOAD Pounds	AXIAL STRETCH RATIO	WIDTH STRETCH RATIO	THICKNESS STRETCH RATIO	ENGINEERING STRESS PSI
0	1.0	1	1	0
0.5	1.078	.933	.949	44.4
2.3	1.15	.804	.951	204

TISSUE SOURCE: 8 Test # 1 SPECIMEN TYPE: 1

TIME TO FAILURE: 15 sec AVERAGE SPECIMEN THICKNESS: 0.063"

LOAD Pounds	AXIAL STRETCH RATIO	WIDTH STRETCH RATIO	THICKNESS STRETCH RATIO	ENGINEERING STRESS PSI
0	1.0	1.0	1.0	0
0.4	1.03	1.0	.97	24.6
1.9	1.05	1.0	.97	117.0
3.75	1.09	1.0	.93	231.0

HUMAN DIAPHRAGM, PARALLEL TO MUSCLE FIBERS

TISSUE SOURCE: 8 TEST # 2 SPECIMEN TYPE: 1

TIME TO FAILURE: 150 sec AVERAGE SPECIMEN THICKNESS: 0.052"

LOAD Pounds	AXIAL STRETCH RATIO	WIDTH STRETCH RATIO	THICKNESS STRETCH RATIO	ENGINEERING STRESS PSI
0	1.0	1	1	0
0.39	1.13	.94	1	28.4
1.5	1.16	.87	1	109.0
2.3	1.18	.79	1	167.3
2.75	1.2	.78	1	200.0

TISSUE SOURCE: 9 Test # 3 SPECIMEN TYPE: 2

TIME TO FAILURE: 34 sec AVERAGE SPECIMEN THICKNESS: 0.085"

LOAD Pounds	AXIAL STRETCH RATIO	WIDTH STRETCH RATIO	THICKNESS STRETCH RATIO	ENGINEERING STRESS PSI
0	1.0	1.0	1.0	0
0.1	1.21	1.0	0.84	6.3
0.35	1.35	1.0	0.8	22.0
1.0	1.38	1.0	0.76	62.7
1.42	1.38	.95	0.76	89.1
1.95	1.54	.95	0.76	122.3
2.1	1.6	.95	0.7	131.8

HUMAN DIAPHRAGM, PARALLEL TO MUSCLE FIBERS

TISSUE SOURCE: 9 Test # 2 SPECIMEN TYPE: 1

TIME TO FAILURE: 60 sec AVERAGE SPECIMEN THICKNESS: 0.083"

LOAD Pounds	AXIAL STRETCH RATIO	WIDTH STRETCH RATIO	THICKNESS STRETCH RATIO	ENGINEERING STRESS PSI
0	1.0	1.0	1.0	0
0.1	1.08	.97	.92	4.7
0.5	1.16	.97	.92	23.5
0.8	1.19	.97	.92	37.7
1.15	1.23	.95	.92	54.2
1.55	1.26	.93	.9	73.1
1.95	1.30	.93	.88	91.9
2.1	1.43	.92	.88	101.1

TISSUE SOURCE: 57 Test # 2 SPECIMEN TYPE: 1

TIME TO FAILURE: 78 sec AVERAGE SPECIMEN THICKNESS: 0.075"

LOAD Pounds	AXIAL STRETCH RATIO	WIDTH STRETCH RATIO	THICKNESS STRETCH RATIO	ENGINEERING STRESS PSI
0	1.0	1.0	1.0	0
0.12	1.04	1.0	.925	6.4
1.04	1.08	1.0	.925	56
1.8	1.13	1.0	.925	95
2.9	1.14	.913	.925	154
3.61	1.22	.869	.925	191
3.76	1.29	.869	.92	199

HUMAN DIAPHRAGM, PERPENDICULAR TO MUSCLE FIBERS

TISSUE SOURCE: 8 Test No. 2 SPECIMEN TYPE: 1

TIME TO FAILURE: 30 sec AVERAGE SPECIMEN THICKNESS: 0.072"

LOAD Pounds	AXIAL STRETCH RATIO	WIDTH STRETCH RATIO	THICKNESS STRETCH RATIO	ENGINEERING STRESS PSI
0	1	1	1	0
.85	1.21	.921	1	44.7
1.25	1.25	.913	.92	65.8
1.55	1.27	.878	.92	81.6

TISSUE SOURCE: 9 Test # 1 SPECIMEN TYPE: 1

TIME TO FAILURE: 64 sec AVERAGE SPECIMEN THICKNESS: 0.085"

LOAD Pounds	AXIAL STRETCH RATIO	WIDTH STRETCH RATIO	THICKNESS STRETCH RATIO	ENGINEERING STRESS PSI
0	1	1	1	0
0.5	1.28	.96	.89	23
0.9	1.3	.93	.89	42
1.25	1.31	.93	.82	58.8
1.85	1.32	.90	.82	87.0
2.35	1.33	.90	.82	110.5
2.8	1.34	.87	.81	131.7
3.2	1.37	.87	.81	150.5

HUMAN DIAPHRAGM, PERPENDICULAR TO MUSCLE FIBERS

TISSUE SOURCE: 9 Test # 2 SPECIMEN TYPE: 1

TIME TO FAILURE: 70 sec AVERAGE SPECIMEN THICKNESS: 0.087"

LOAD Pounds	AXIAL STRETCH RATIO	WIDTH STRETCH RATIO	THICKNESS STRETCH RATIO	ENGINEERING STRESS PSI
0	1	1	1.0	0
0.5	1.16	.99	.93	22
0.98	1.18	.96	.93	43
1.5	1.22	.91	.92	65
2.5	1.23	.86	.89	108
3.6	1.23	.86	.87	157
4.5	1.23	.86	.87	194
5.0	1.27	.86	.87	217
5.2	1.28	.85	.80	226
5.3	1.32	.85	.85	230

HUMAN DIAPHRAGM, PERPENDICULAR TO MUSCLE FIBERS

TISSUE SOURCE: 57 Test No. 1 SPECIMEN TYPE: 1

TIME TO FAILURE: 44 sec AVERAGE SPECIMEN THICKNESS: 0.074"

LOAD Pounds	AXIAL STRETCH RATIO	WIDTH STRETCH RATIO	THICKNESS STRETCH RATIO	ENGINEERING STRESS PSI
0	1	1	1	0
0.42	1.01	1	1	22
0.96	1.06	.92	1	53
1.54	1.07	.92	.98	81
1.55	1.08	.92	.9	82

TISSUE SOURCE: 57 Test No. 2 SPECIMEN TIME: 1

TIME TO FAILURE: 50 sec AVERAGE SPECIMEN THICKNESS: 0.093"

LOAD Pounds	AXIAL STRETCH RATIO	WIDTH STRETCH RATIO	THICKNESS STRETCH RATIO	ENGINEERING STRESS PSI
0	1	1	1	0
0.5	1.12	1	.89	21
3.4	1.31	.978	.86	145

TISSUE SOURCE: 6 Test # 2 SPECIMEN TYPE: 1

TIME TO FAILURE: 13 sec AVERAGE SPECIMEN THICKNESS: 0.072"

LOAD Pounds	AXIAL STRETCH RATIO	WIDTH STRETCH RATIO	THICKNESS STRETCH RATIO	ENGINEERING STRESS PSI
0	1	1	1	1
1.95	1.125	.967	.908	156

HUMAN DIAPHRAGM, PERPENDICULAR TO MUSCLE FIBERS

TISSUE SOURCE: 58 Test # 2 SPECIMEN TYPE: 1

TIME TO FAILURE: 65 sec AVERAGE SPECIMEN THICKNESS: 0.078"

LOAD Pounds	AXIAL STRETCH RATIO	WIDTH STRETCH RATIO	THICKNESS STRETCH RATIO	ENGINEERING STRESS PSI
0	1	1	1	0
0.2	1.09	1	.97	1
0.37	1.09	1	.97	19.7
0.6	1.11	1	.97	32
0.87	1.12	1	.95	46.4
1.1	1.13	1	.89	59.2
1.36	1.13	0.95	.83	72.5
1.87	1.13	0.95	.83	99.7
2.38	1.14	0.95	.83	126.9
2.62	1.15	0.91	.83	139.7
2.87	1.18	0.88	.83	153
2.87	1.18	0.88	.81	153

TISSUE SOURCE: 6 Test # 1 SPECIMEN TYPE: 1

TIME TO FAILURE: 17 sec AVERAGE SPECIMEN THICKNESS: 0.046"

LOAD Pounds	AXIAL STRETCH RATIO	WIDTH STRETCH RATIO	THICKNESS STRETCH RATIO	ENGINEERING STRESS PSI
0	1	1	1	0
.1	1.12	.96	.91	8.9
.9	1.2	.91	.9	80.0
2.78	1.28	.76	.82	247

HUMAN DIAPHRAGM, PERPENDICULAR TO MUSCLE FIBERS

TISSUE SOURCE: 74 Test # 1

SPECIMEN TYPE: 1

TIME TO FAILURE: 15 msec

AVERAGE SPECIMEN THICKNESS: 0.090"

LOAD Pounds	AXIAL STRETCH RATIO	WIDTH STRETCH RATIO	THICKNESS STRETCH RATIO	ENGINEERING STRESS PSI
0	1	1	1	0
1.6	1.17	1	1	75.6
4.5	1.3	1	1	216
5.6	1.35	.95	.98	263
6.0	1.41	.9	1	276
6.3	1.5	.86	1	296
6.3	1.6	.86	1	296

TISSUE SOURCE: 74 Test # 3

SPECIMEN TYPE: 1

TIME TO FAILURE: 90 msec

AVERAGE SPECIMEN THICKNESS 0.082"

LOAD Pounds	AXIAL STRETCH RATIO	WIDTH STRETCH RATIO	THICKNESS STRETCH RATIO	ENGINEERING STRESS PSI
0	1	1	1	0
0.3	1.07	1	1	16.5
1.2	1.08	1	.9	59.0
2.0	1.11	.95	.9	102.5
2.6	1.18	.92	.83	132
2.7	1.19	.92	.83	139

HUMAN DIAPHRAGM, PERPENDICULAR TO MUSCLE FIBERS

TISSUE SOURCE: 74 Test No. 2 SPECIMEN TYPE: 1

TIME TO FAILURE: 140 msec AVERAGE SPECIMEN THICKNESS: 0.093"

LOAD Pounds	AXIAL STRETCH RATIO	WIDTH STRETCH RATIO	THICKNESS STRETCH RATIO	ENGINEERING STRESS PSI
0	1.0	1	1	0
0.1	1.125	.96	1	4.0
0.35	1.22	.91	.92	15.0
1.95	1.28	.91	.92	83.9
4.1	1.35	.91	.91	176.3
5.5	1.42	.91	.84	236.5
5.7	1.45	.91	.84	245

TISSUE SOURCE: 3 Test # 1 SPECIMEN TYPE: 1

TIME TO FAILURE: 8 msec AVERAGE SPECIMEN THICKNESS 0.075"

LOAD Pounds	AXIAL STRETCH RATIO	WIDTH STRETCH RATIO	THICKNESS STRETCH RATIO	ENGINEERING STRESS PSI
0	1	1	-	0
.05	1.05	1	-	2.7
0.1	1.13	1	-	5.3
0.2	1.15	1	-	10.6
0.3	1.18	1	-	15.9
0.6	1.28	.81	-	31.8
1.2	1.33	.8	-	63.6
2.0	1.36	.8	-	100.7
2.7	1.41	.75	-	144.0
3.5	1.5	.7	-	186.7
4.0	1.6	.7	-	213.4

HUMAN PERICARDIUM

TISSUE SOURCE: 58 Test # 1 SPECIMEN TYPE: 2

TIME TO FAILURE: 43 sec AVERAGE SPECIMEN THICKNESS: 0.03"

LOAD Pounds	AXIAL STRETCH RATIO	WIDTH STRETCH RATIO	THICKNESS STRETCH RATIO	ENGINEERING STRESS PSI
0.0	1.0	1.0	1.0	0
0.03	1.03	1.0	1.0	5.4
0.22	1.13	1.0	1.0	39.3
0.6	1.13	.96	1.0	107.1
1.02	1.17	.96	1.0	182.0
2.42	1.26	.96	1.0	432.0

TISSUE SOURCE: 58 Test # 5 SPECIMEN TYPE: 1

TIME TO FAILURE: 14 msec AVERAGE SPECIMEN THICKNESS: 0.02"

LOAD Pounds	AXIAL STRETCH RATIO	WIDTH STRETCH RATIO	THICKNESS STRETCH RATIO	ENGINEERING STRESS PSI
0.0	1.0	-	-	0
0.16	1.09	-	-	33
0.42	1.12	-	-	84
0.85	1.16	-	-	120
1.85	1.19	-	-	370
2.65	1.21	-	-	530
3.0	1.24	-	-	600
3.16	1.28	-	-	632

HUMAN ESOPHAGUS, LONGITUDINAL

TISSUE SOURCE: 70 Test # 1 SPECIMEN TYPE: 1

TIME TO FAILURE: 12 msec AVERAGE SPECIMEN THICKNESS: 0.061"

LOAD Pounds	AXIAL STRETCH RATIO	WIDTH STRETCH RATIO	THICKNESS STRETCH RATIO	ENGINEERING STRESS PSI
0.0	1.0	1.0	1.0	0
0.02	1.01	0.95	0.94	1.3
0.12	1.07	0.88	0.94	7.5
0.36	1.11	0.88	0.94	22.5
0.9	1.14	0.825	0.94	56.3
3.0	1.31	0.78	0.94	187.5

HUMAN ESOPHAGUS, LONGITUDINAL

TISSUE SOURCE: 56 Test # 1 SPECIMEN TYPE: 1

TIME TO FAILURE: 82 seconds AVERAGE SPECIMEN THICKNESS: 0.11"

LOAD Pounds	AXIAL STRETCH RATIO	WIDTH STRETCH RATIO	THICKNESS STRETCH RATIO	ENGINEERING STRESS PSI
0.0	1.0	1.0	1.0	0.0
0.52	1.07	1.0	.92	18.6
0.96	1.15	0.98	.92	34.0
1.26	1.16	0.97	.84	45.0

TISSUE SOURCE: 56 Test # 5 SPECIMEN TYPE: 1

TIME TO FAILURE: 14 msec AVERAGE SPECIMEN THICKNESS: 0.10"

LOAD Pounds	AXIAL STRETCH RATIO	WIDTH STRETCH RATIO	THICKNESS STRETCH RATIO	ENGINEERING STRESS PSI
0.0	1.0	1.0	1.0	0
0.1	1.06	.94	.83	4.0
0.17	1.08	.88	.81	6.8
0.29	1.11	.87	-	11.6
0.46	1.17	-	-	18.4
0.86	1.18	-	-	34.4
1.53	1.24	-	-	61.2
2.14	1.25	-	-	85.6
2.45	1.35	-	-	98.0

HUMAN BRONCHUS, LONGITUDINAL

TISSUE SOURCE: 76 Test # 1 SPECIMEN TYPE: 2

TIME TO FAILURE: 39 sec AVERAGE SPECIMEN THICKNESS: 0.062"

LOAD Pounds	AXIAL STRETCH RATIO	ENGINEERING STRESS PSI
0.0	1.0	0.0
0.16	1.12	13.3
0.54	1.22	45.0
0.93	1.27	77.5
1.45	1.32	120.8

TISSUE SOURCE: 76 Test # 2 SPECIMEN TYPE: 2

TIME TO FAILURE: 40 sec AVERAGE SPECIMEN THICKNESS: 0.065"

LOAD Pounds	AXIAL STRETCH RATIO	ENGINEERING STRESS PSI
0.0	1.0	0.0
0.0	1.09	0.0
0.16	1.24	13.3
0.54	1.36	45.0
0.93	1.39	57.5
1.26	1.45	105.0
1.53	1.48	127.5

HUMAN TRACHEA, LONGITUDINAL

TISSUE SOURCE: 76 Test # 1 SPECIMEN TYPE: 1

TIME TO FAILURE: 81 sec AVERAGE SPECIMEN THICKNESS: 0.080"

Load Pounds	AXIAL STRETCH RATIO	ENGINEERING STRESS PSI
0.0	1.0	0.0
0.01	1.07	0.5
0.21	1.16	10.5
0.67	1.20	33.5
1.41	1.23	70.5
1.86	1.24	93.0
2.16	1.24	108.0

TISSUE SOURCE: 76 Test # 2 SPECIMEN TYPE: 2

TIME TO FAILURE: 52 sec AVERAGE SPECIMEN THICKNESS: 0.085"

LOAD Pounds	AXIAL STRETCH RATIO	ENGINEERING STRESS PSI
0.0	1.0	0.0
0.14	1.2	8.8
0.52	1.25	32.7
1.00	1.27	62.9
1.50	1.27	94.3
2.18	1.28	137.0
2.24	1.29	141.0

HUMAN TRACHEA, LONGITUDINAL

TISSUE SOURCE: 76 Test # 3 SPECIMEN TYPE: 2

TIME TO FAILURE 29 sec AVERAGE SPECIMEN THICKNESS: 0.080"

LOAD Pounds	AXIAL STRETCH RATIO	ENGINEERING STRESS PSI
0.0	1.0	0.0
0.0	1.11	0.0
0.16	1.20	10.7
0.94	1.24	62.7
1.49	1.28	99.3
1.96	1.28	130.7

TISSUE SOURCE: 76 Test # 4 SPECIMEN TYPE: 2

TIME TO FAILURE: 32 sec AVERAGE SPECIMEN THICKNESS: 0.065"

LOAD Pounds	AXIAL STRETCH RATIO	ENGINEERING STRESS PSI
0.0	1.0	0.0
0.16	1.11	13.3
0.61	1.24	50.8
1.33	1.24	110.8
1.93	1.31	160.8

APPENDIX D INDIVIDUAL RHESUS MONKEY TEST DATA TABLES

RHESUS MONKEY ASCENDING AORTA, TRANSVERSE

TISSUE SOURCE: R 1 Test # 1 SPECIMEN TYPE: Ring

TIME TO FAILURE: 68 sec AVERAGE SPECIMEN THICKNESS: 0.040"

LOAD Pounds	AXIAL STRETCH RATIO	ENGINEERING STRESS PSI
0.0	1.00	0.0
0.8	1.56	11.4
0.14	1.72	20.0
0.28	1.88	40.6
0.67	2.04	96.2
0.97	2.05	138.9

RHESUS MONKEY DESCENDING AORTA, LONGITUDINAL

TISSUE SOURCE: R 1 Test # 1 SPECIMEN TYPE: 2

TIME TO FAILURE: 71 sec AVERAGE SPECIMEN THICKNESS: .033

LOAD Pounds	AXIAL STRETCH RATIO	WIDTH STRETCH RATIO	THICKNESS STRETCH RATIO	ENGINEERING STRESS PSI
0.0	1.0	1.0	1.0	0.0
0.02	1.32	0.89	0.67	3.3
0.18	1.55	0.83	0.67	30.0
0.52	1.66	0.66	0.67	66.7
0.78	1.72	0.60	0.67	130.0
0.83	1.77	0.57	0.67	138.3

TISSUE SOURCE: R 1 Test # 2 SPECIMEN TYPE: 2

TIME TO FAILURE: 88 sec AVERAGE SPECIMEN THICKNESS: .030"

LOAD Pounds	AXIAL STRETCH RATIO	WIDTH STRETCH RATIO	THICKNESS STRETCH RATIO	ENGINEERING STRESS PSI
0.0	1.0	1.0	1.0	0.0
0.0	1.3	0.91	0.9	0.0
0.02	1.48	0.94	0.85	3.2
0.06	1.52	0.89	0.85	9.7
0.13	1.63	0.83	0.85	21.0
0.2	1.76	0.77	0.85	32.3
0.35	1.85	0.77	0.85	56.4
0.53	1.89	0.77	0.76	85.5
0.55	2.11	0.62	0.76	88.7

RHESUS MONKEY DESCENDING AORTA, TRANSVERSE

TISSUE SOURCE: R 1 Test # 3 SPECIMEN TYPE: Ring

TIME TO FAILURE: 43 sec AVERAGE SPECIMEN THICKNESS: 0.040"

LOAD Pounds	AXIAL STRETCH RATIO	ENGINEERING STRESS PSI
0.0	1.00	0
0.04	1.37	5.3
0.07	1.59	9.2
0.43	1.92	56.6
1.5	2.21	197.4

TISSUE SOURCE: R 1 Test # 2 SPECIMEN TYPE: Ring

TIME TO FAILURE: 55 sec AVERAGE SPECIMEN THICKNESS: .035"

LOAD Pounds	AXIAL STRETCH RATIO	ENGINEERING STRESS PSI
0.0	1.00	0.0
0.07	1.63	11.4
0.12	1.90	19.6
0.28	2.09	45.7
0.58	2.23	94.7
1.1	2.37	179.6

RHESUS MONKEY DESCENDING AORTA, TRANSVERSE

TISSUE SOURCE: R 1 Test # 1 SPECIMEN TYPE: Ring

TIME TO FAILURE: 53 sec AVERAGE SPECIMEN THICKNESS: 0.038"

LOAD Pounds	AXIAL STRETCH RATIO	ENGINEERING STRESS PSI
0.0	1.00	0.0
0.07	1.54	10.5
0.16	1.77	24.1
0.29	1.86	43.6
0.67	2.00	100.8
1.37	2.17	206.0

RHESUS MONKEY DESCENDING AORTA, TRANSVERSE

TISSUE SOURCE: R 2 - DAT - 1 SPECIMEN TYPE: Ring

TIME TO FAILURE: 4 msec AVERAGE SPECIMEN THICKNESS: 0.020"

LOAD Pounds	AXIAL STRETCH RATIO	ENGINEERING STRESS PSI
0.0	1.00	0.0
0.075	1.31	21.4
0.67	1.72	191.4
1.59	1.86	454.2

TISSUE SOURCE: R 2 - DAT - 2 SPECIMEN TYPE: Ring

TIME TO FAILURE: 3 msec AVERAGE SPECIMENT THICKNESS: 0.020

LOAD Pounds	AXIAL STRETCH RATIO	ENGINEERING STRESS PSI
0.0	1.00	0.0
0.075	1.24	19.2
0.60	1.55	153.8
1.375	2.03	352.6

RHESUS MONKEY DESCENDING AORTA, TRANSVERSE

TISSUE SOURCE: R 2 - DAT - 3 SPECIMEN TYPE: Ring

TIME TO FAILURE: 3.5 msec AVERAGE SPECIMEN THICKNESS: 0.019"

LOAD Pounds	AXIAL STRETCH RATIO	ENGINEERING STRESS PSI
0.0	1.00	0.
0.115	1.24	184.9
0.82	1.59	221.3
1.8	2.10	485.8

RHESUS MONKEY DIAPHRAGM, PARALLEL TO MUSCLE FIBERS

TISSUE SOURCE: R 1 Test # 1 SPECIMEN TYPE: 2

TIME TO FAILURE: 57 sec AVERAGE SPECIMEN THICKNESS: 0.040"

LOAD Pounds	AXIAL STRETCH RATIO	ENGINEERING STRESS PSI
0.0	1.0	0.0
0.07	1.2	9.8
0.28	1.24	37.3
0.58	1.27	77.3
0.86	1.32	114.7
1.05	1.36	140.0
1.16	1.39	154.7
1.17	1.42	156.0

RHESUS MONKEY DIAPHRAGM, PERPENDICULAR TO MUSCLE FIBERS

TISSUE SOURCE: R 1 Test # 1 SPECIMEN TYPE: 2

TIME TO FAILURE: 38 sec AVERAGE SPECIMEN THICKNESS: 0.040"

LOAD Pounds	AXIAL STRETCH RATIO	WIDTH STRETCH RATIO	THICKNESS STRETCH RATIO	ENGINEERING STRESS PSI
0.0	1.0	1.0	1.0	0.0
0.13	1.08	1.0	0.89	16.3
0.32	1.15	1.0	0.89	40.0
0.39	1.17	1.0	0.79	48.0
0.59	1.25	1.0	0.79	73.8

RHESUS MONKEY ESOPHAGUS, LONGITUDINAL

TISSUE SOURCE: R 1 Test # 1 SPECIMEN TYPE: Tubular

TIME TO FAILURE: 160 sec AVERAGE SPECIMEN THICKNESS: .075"

LOAD Pounds	AXIAL STRETCH RATIO	ENGINEERING STRESS PSI
0.0	1.0	0.0
0.25	1.4	3.2
1.1	1.93	14.0
1.8	2.33	22.9
2.35	2.6	29.8
3.5	3.0	44.5
3.8	3.2	48.7

RHESUS MONKEY ESOPHAGUS, TRANSVERSE

TISSUE SOURCE: R 1 Test #1 SPECIMEN TYPE: Ring

TIME TO FAILURE: 102 sec AVERAGE SPECIMEN THICKNESS: .070"

LOAD Pounds	AXIAL STRETCH RATIO	ENGINEERING STRESS PSI
0.0	1.0	0.0
0.05	1.74	4.9
0.14	2.41	13.8
0.22	2.62	21.7
0.35	2.84	34.5
0.44	3.18	43.3

TISSUE SOURCE: R 1 Test # 2 SPECIMEN TYPE: Ring

TIME TO FAILURE: 78 sec AVERAGE SPECIMEN THICKNESS: 0.065"

LOAD Pounds	AXIAL STRETCH RATIO	ENGINEERING STRESS PSI
0.0	1.0	0.0
0.07	1.59	7.2
0.14	2.03	14.4
0.18	2.45	18.4
0.19	2.67	19.4

RHESUS MONKEY ESOPHAGUS, TRANSVERSE

TISSUE SOURCE: R 1 Test # 4 SPECIMEN TYPE: Ring

TIME TO FAILURE: 98 sec AVERAGE SPECIMEN THICKNESS: .075"

LOAD Pounds	AXIAL STRETCH RATIO	ENGINEERING STRESS PSI
0.0	1.0	0.0
0.08	2.11	7.1
0.11	2.62	10.5
0.18	3.12	16.7
0.19	3.47	18.0

TISSUE SOURCE: R 1 Test # 3 SPECIMEN TYPE: Ring

TIME TO FAILURE: 93 sec AVERAGE SPECIMEN THICKNESS: 0.075

LOAD Pounds	AXIAL STRETCH RATIO	ENGINEERING STRESS PSI
0.0	1.0	0.0
0.05	1.66	4.2
0.11	2.40	9.2
0.18	2.88	15.0
0.22	3.28	18.3

RHESUS MONKEY ESOPHAGUS, TRANSVERSE

TISSUE SOURCE: R 2 - ET - 2 SPECIMEN TYPE: Ring

TIME TO FAILURE: 5 msec AVERAGE SPECIMEN THICKNESS: 0.07"

LOAD Pounds	AXIAL STRETCH RATIO	ENGINEERING STRESS PSI
0.0	1.0	0
0.01	1.24	0.8
0.11	1.50	9.82
0.235	1.82	21.0
0.36	2.12	32.1

TISSUE SOURCE: R 2 - ET- 4 SPECIMEN TYPE: Ring

TIME TO FAILURE: 6 msec AVERAGE SPECIMEN THICKNESS: 0.06"

LOAD Pounds	AXIAL STRETCH RATIO	ENGINEERING STRESS PSI
0.0	1.0	0.0
0.0775	1.24	8.1
0.25	1.65	26
0.5425	2.03	56.5

RHESUS MONKEY ESOPHAGUS, TRANSVERSE

TISSUE SOURCE: R 2 Test #3 SPECIMEN TYPE: Ring

TIME TO FAILURE: 5.6 msec AVERAGE SPECIMEN THICKNESS: .07

LOAD Pounds	AXIAL STRETCH RATIO	ENGINEERING STRESS PSI
0.0	1	0
.16	1.36	11.4
.325	1.58	23.2
.565	1.83	40.34

TISSUE SOURCE: R 2 Test #1 SPECIMEN TYPE: Ring

TIME TO FAILURE: 6.5 msec AVERAGE SPECIMEN THICKNESS: .07

LOAD Pounds	AXIAL STRETCH RATIO	ENGINEERING STRESS PSI
0	1	0
.205	1.37	7.3
.445	1.71	15.9
.995	2.13	35.5